Dissertation

Submitted to the
Combined Faculties of Natural Sciences - Mathematics
of the
Ruprecht-Karl University of Heidelberg, Germany
for the degree of
Doctor of Natural Sciences

presented by
Olga M. Shatnyeva, Biol. MSc.
Born in Kharkiv, Ukraine
Oral-examination:

The Role of CD95 Glycosylation in CD95 Signaling

Referees:

Prof Dr. Walter Nickel
Faculty for Biosciences, University of Heidelberg

Prof Dr. Peter H. Krammer
German Cancer Research Center

To my family, my wonderful friend Anna and my god-daughter Maria.

DECLARATION

This thesis is based on research conducted in the Division of Immunogenetics at the German Cancer Research Center, under supervision of Prof. Dr. Peter H. Krammer and direct supervision of Dr. Inna Lavrik in the period from March, 2006 to March, 2010

Herewith, I declare that I wrote this thesis independently under supervision and no other sources and aids than those indicated in the manuscript were used.

Heidelberg,
Olga M. Shatnyeva

CONTENT

ABBREVIATIONS

Å - Ångstrom

aa - amino acid

AIF - apoptosis inducing factor

AICD - activation-induced cell death

AIDS - acquired immune deficiency syndrome

Apaf-1 - apoptosis activating factor-1

APS - ammonium persulphate

ATP - adenosine triphosphate

BCA - bicinchoninic acid

BSA - bovine serum albumin

bp (kb) - base pair (kilo base pair)

C8 - caspase 8

CAD - caspase-activated DNAse

CARD - caspase recruitment domains

Caspase- cysteine-aspartic protease

CBS - Center for Biological Sequence Analysis

CD - cluster of differentiation

CRD - cystein-rich domain

cDNA - complementary DNA

DAPI - 4',6-diamidino-2-phenylindole

DD - death domain

DcRs - decoy receptors

DED - death effector domain

DISC - death-inducing signaling complex

DMM - 1-deoxymannojirimycin

DMSO - dimethyl sulphoxide

DNA - deoxyribonucleic acid

dNTP - deoxyribonucleotide triphosphate

DMEM - Dulbecco's Modified Eagle Medium

Dol-P-P - dolichol pyrophosphate

DTT - dithiothreitol

DR - death receptor

EDTA - ethylenediaminetetraacetic acid

ELISA - Enzyme-linked immunosorbent assay

ER - endoplasmic reticulum

EtBr - ethidium bromide

EtOH - ethanol

FADD - Fas–associated death domain

FACS - fluorescence-activated cell sorter

FBS - fetal bovine serum

FSC - forward scatter

FLICE - FADD-like ICE (interleukin 1β-converting enzyme)

FLIP - FLICE-inhibitory protein

FRET - fluorescence resonance energy transfer

GalNac - N-acetyl-D-galactosamine

GFP- green fluorescent protein

GT - glycosyltransferases

GH - glycosyl hydrolases/glycosidaes

GPI - glycosylphosphatidylinositol

HRP - horseradish peroxidase

hiDISC - high molecular weight DISC

HIV-1 - human immunodeficiency virus (type 1)

IAP - inhibitor of apoptosis

ICAD - inhibitor of CAD

ICE - Interleukin-1β-convertin

IgG - Immunoglobulin G

IgG_H - Immunoglobulin G heavy chain

IgG_L - Immunoglobulin G light chain

IL - interleukin

IP - immunoprecipitation

kDa - kilo Dalton

MeOH - methanol

MFI - mean fluorescence intensity

MMP7 - Matrix metalloprotease 7

NF-AT - nuclear factor of activated T cells

NF-κB - nuclear factor

OD - optical density

PAGE - polyacrylamide gel electrophoresis

PBS - phosphate buffered saline

PBS-T - phosphate buffered saline

PCR - polymerase chain reaction

PHA - phytohaemagglutinin

PI - propidium iodide

PFA - paraformaldehyde

PKC - protein kinase C

PLAD - Pre-Ligand Assembly Domain

PMSF - phenyl-methanesulphonylfluoride

PYD - pyrin domains

RNA - ribonucleic acid

rpm - rotations per minute

RPMI - Roswell Park Memorial Institute

RT - reverse transcription

RT - room temperature

SDS - sodium dodecyl sulfate

siRNA - small interfering RNA

Smac/DIABLO - second mitochondria-derived activator of caspases / direct IAP binding protein with low isoelectric point

SSC - side scatter

TCR - T cell receptor

TEMED - N,N,N',N' - tetramethyl-ethylenediamine

TRAIL - TNF-related apoptosis-inducing ligand

TNF - tumor necrosis factor

Tris - tris-[hydroxymethyl]amino-methane

Tuni - tunicamycin

U - Unit

VCN - *Vibrio cholerae* neuraminidase

WT - wild type

SUMMARY

The CD95 (APO-1/Fas)-mediated apoptotic pathway is one of the well-studied death receptor pathways. CD95 is a highly glycosylated type I transmembrane protein and has a molecular mass of 37.5 kDa. The N-terminal domain of CD95 contains two putative N-linked glycosylation sites at N118 and N136 and posttranslational glycosylation leads to an increase of molecular mass of CD95 to 45–52 kDa. Upon stimulation of CD95, either with its natural ligand CD95L or with agonistic antibodies such as anti-APO-1, a Death-Inducing Signaling Complex (DISC) is formed. The DISC consists of oligomerized, most probably trimerized, CD95, the DD-containing adaptor molecule *Fas associated death domain containing protein* (FADD), procaspase-8, procaspase-10 and *cellular FLICE inhibitory protein* (c-FLIP). The interactions between the molecules in the DISC are based on homophilic contacts. The *death domain (*DD) of CD95 interacts with the DD of FADD while the death effector domain (DED) of FADD interacts with the N-terminal tandem DED of procaspase-8. Binding of procaspase-8 to the DISC results in its autocatalytic cleavage with the formation of the mature caspase-8 which is released into the cytosol to propagate the apoptotic signal.

The data presented here show that N-glycosylation of CD95 influences death-inducing signaling complex (DISC) formation and procaspase-8 activation at the CD95 DISC. Treatment with the chemical inhibitors of N-glycosylation tunicamycin and Deoxymannojirimycin (DMM), neuraminidase from *Vibrio cholerae* and generation of CD95 glycosylation mutants at N136 and N118 show that N-deglycosylation of CD95 results in the reduction of caspase-8 processing at the DISC. Modelling of the core CD95 DISC structure and the structure of the CD95 DISC network on the membrane indicated that the glycan attached to N118 could be important for the contacts between neighboring DISCs forming a network. A glycan moiety attached to N136 of CD95 could be important for the complex formation and/or stability as it is located in close proximity to one of the CD95L molecules.

The present study shows that the CD95 glycostructure can contribute to the amount of generated caspase-8, which defines cell death initiation. This regulation might be important for cancer cells when a subtle difference in the amount of activated caspase-8 regulates life or death of the cell.

ZUSAMMENFASSUNG

Apoptose ausgelöst durch CD95 (APO-1/Fas) gehört zu den bestuntersuchtesten Signalwegen. CD95 ist ein hochglykosyliertes Typ I Transmembranprotein und hat eine molekulare Masse von ca. 37,5 kDa. Die N-terminale Domäne von CD95 enthält zwei mögliche stickstoffverbundene Glykosylierungsstellen an Position N118 und N136. Die posttranslationale Glykosylierung führt zu einer Erhöhung der molekularen Masse von CD95 auf 45–52 kDa. Nach Stimulierung von CD95 mit seinem natürlichen Liganden CD95L oder mit dem agonistischen Antikörper anti-APO-1, bildet sich der Death-Inducing Signaling Complex (DISC).

Der DISC besteht aus oligomerisiertem, wahrscheinlich trimerisiertem CD95 und dem Adaptermolekül *Fas associated death domain containing protein* (FADD), Procaspase-8, Procaspase-10 und *cellular FLICE inhibitory protein* (c-FLIP). Alle Interaktionen am DISC basieren auf homophilen Proteinbindungen. Mittels seiner Todesdomäne wird FADD an CD95 rekrutiert und *via* seiner Todeseffektordomänen kommt es zur Rekrutierung von Procaspase-8 an den DISC. Die Rekrutierung von Procaspase-8 an den DISC führt zur autokatalytischen Spaltung und Bildung der aktiven Caspase-8. Diese wird ins Zytosol freigesetzt und initiiert Apoptose.

In dieser Arbeit konnte gezeigt werden, dass die CD95 N-Glykosylierung die Formierung des DISC und die damit verbundene Aktivierung der Procaspase-8 am CD95-DISC beeinflusst. Mittels Inhibitorstudien und der Herstellung von Glykosylierungsmutanten (N118Q and N136Q), sowie der Untersuchung von deglycosyliertem CD95 (durch Neuraminidase-Behandlung) konnte demonstriert werden, dass die N-Deglykosylierung von CD95 in einer verminderten Prozessierung von Procaspase-8 resultiert.

Die Modellierung der CD95 DISC-Struktur und der Vernetzung mehrerer CD95-DISCs an einer Membran hat gezeigt, dass das Glykan, welches an N118 angeheftet ist, für den Kontakt zwischen benachbarten DISCs eine Rolle spielen kann. Auch an N136 befestigte Glykanreste könnten wichtig für die Komplexbildung und/oder die Stabilität von CD95 sein, da sie in der direkten Umgebung der CD95L Moleküle liegt.

Diese Untersuchungen demonstrieren, dass die Glykosylierung von CD95 Einfluss auf die Bildung aktiver Caspase-8 hat, welche die Initierung des Zelltods bestimmt. Dies kann Bedeutung für die Entstehung von Krebszellen haben, da geringe

Mengenunterschiede an aktiver Caspase-8 Überleben oder Tod der Zelle beeinflussen.

1. INTRODUCTION

1.1. Apoptosis

1.1.1. Types of cell death

Cell death is an essential and highly orchestrated process in multicellular organisms. It plays an important role during development, for homeostasis of tissue in mature organisms and for elimination of infectious pathogens (Krammer 2000; Strasser et al. 2009). Defective regulation of cell death leads to a spectrum of diseases such as diabetes, degenerative disorders and cancer.

There are three major types of cell death: apoptosis, necrosis and autophagy which can be distinguished by morphology (Fig. 1).

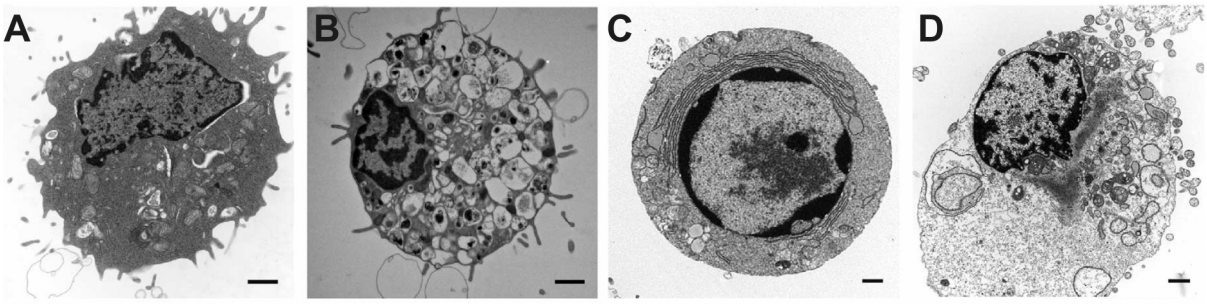

Figure 1. Morphological features of autophagic, apoptotic and necrotic cells. A. Viable cell. **B**. Autophagic cell. **C**. Apoptotic cell. **D**. Necrotic cell. (Edinger et al. 2004).

Apoptosis - programmed cell death - is a highly regulated physiological process of cell death that is conserved among all multicellular organisms. The term is derived from ancient Greek (apo = off, ptosis = falling, dropping), meaning the ‘‘falling off of petals from a flower’’ or ‘‘of leaves from a tree in autumn’’. It was first introduced by John Kerr in 1972 and refers to the morphological feature of formation of “apoptotic bodies” from a cell during the course of apoptosis (Kerr et al. 1972). The phenomenon was discovered in 1842 by the German scientist Carl Christoph Vogt who showed that in the course of development of the midwife toad tadpole (*Alytes obstetricians*), cells undergo programmed cell death.

Apoptotic cells are usually rounding up, retract pseudopodes, reduce cellular and nuclear volume and show nuclear fragmentation and plasma membrane blebbing (Fig. 1C). Usually, they are quickly engulfed by resident phagocytes (Kroemer et al. 2009).

Necrosis (from the Greek νεκρός, "dead") is the death by injury of cells and living tissue (Syntichaki et al. 2003). Typically it is caused by external factors, such as

infection, toxins or trauma. It can be characterized by cytoplasmic swelling, rupture of the plasma membrane, swelling of cytoplasmic organelles and a moderate chromatin condensation (Fig. 1D).

During autophagic cell death, the cell's own components are degraded by the lysosomal machinery (Kundu et al. 2008). Autophagy can be characterized by a lack of chromatin condensation, massive vacuolization of the cytoplasm and accumulation of autophagic vacuoles. Furthermore, autophagic cells are rarely taken up by phagocytic cells *in vivo* (Fig. 1B).

1.1.3. Apoptosis in the immune system

Apoptosis plays an essential role in the immune system during the development of lymphocytes and the regulation of the immune response. Aberrations in genes encoding pro- or anti-apoptotic proteins have been implicated in the initiation of diseases such as immunodeficiency, autoimmunity and cancer (Krammer 2000).

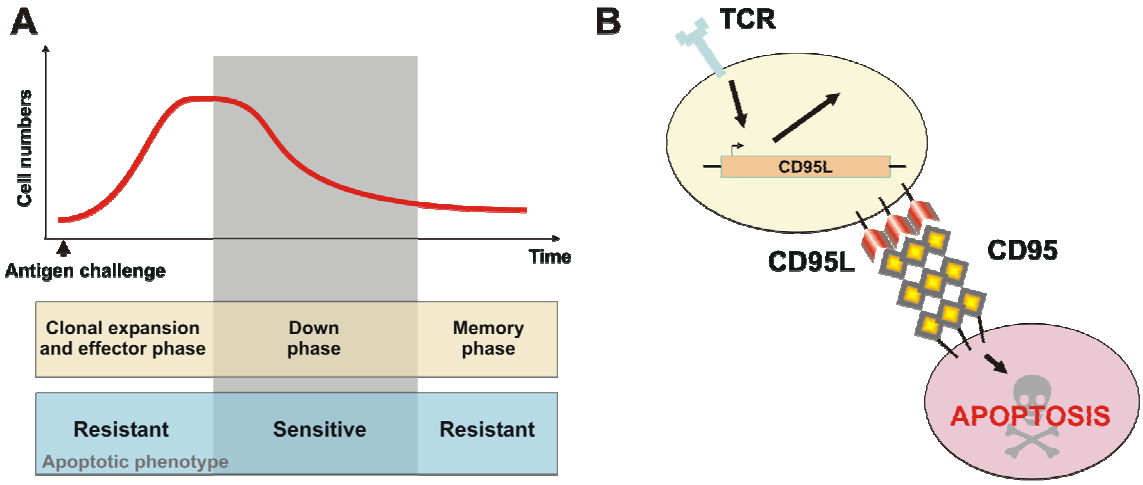

Figure 2. The course of a T cell immune response and Activation-Induced Cell Death (AICD). A. The T cell immune response comprises a clonal expansion and effector phase, a "down" or "retraction" phase, and a memory phase. During the clonal expansion and effector phase, proliferating T cells are resistant to apoptosis. In the down phase T cells become sensitive to apoptosis. By contrast, in the memory phase T cells become again resistant to apoptosis. **B**. The CD95/CD95L system plays an important role in AICD. Naive T cells do not express CD95L. Upon TCR triggering T cells start to express CD95L and become sensitive to CD95-mediated apoptosis. Adapted from Krammer 2000.

The survival of lymphocytes is regulated at several points in their lifespan (Strasser 1995). During lymphocyte development, survival depends on signaling through their antigen receptors. The selection is highly stringent, resulting in the

elimination of most lymphocytes. Early survival of B or T cells requires a functional B cell - (BCR) or T cell receptor (TCR), respectively (Krammer 2000). Cells whose receptors do not recognize antigen are eliminated by apoptosis. Lymphocytes expressing functional antigen receptors are then tested to determine whether they are autoreactive and dangerous. Antigen receptors that react strongly with a self-antigen undergo cell death during negative selection (Krammer 2000). In contrast, cells that express functional receptors which do not react strongly with self-antigen differentiate into mature lymphocytes.

Apoptosis also plays an important role during the regulation of T cell immune responses *via* Activation-Induced Cell Death (AICD) (Fig. 2). Typically, the immune response consists of several steps: in the clonal expansion/effector phase of the immune response, T cells are activated upon antigen recognition, proliferate and differentiate into effector cells. In this phase, they are resistant towards apoptosis. In the down phase of the immune response, T cells become sensitive to apoptosis and die by AICD. Memory T cells are resistant towards apoptosis and survive. The CD95/CD95L system plays an important role in AICD. Naive T cells do not express CD95L. Upon TCR triggering T cells start to produce CD95L and become sensitive to CD95-mediated apoptosis (Fig. 2B) (Krammer 2000). This was strongly supported by the phenotype of lpr and gld (CD95 and CD95L mutant) mice, which suffer from lymphoproliferation and autoimmunity due to lack of AICD (Martin et al. 1999). Mutations in the CD95/CD95L system are also responsible for most cases of the human autoimmune lymphoproliferative syndrome (ALPS) (Rieux-Laucat et al. 1995; Siegel et al. 2000).

1.1.4. Apoptosis-associated disorders

The diseases caused by a dysfunctional apoptotic cellular machinery can be divided into two groups characterized by "too little" apoptosis and "too much" apoptosis (Thompson 1995).

The first group comprises neoplastic and autoimmune diseases associated with severe apoptosis inhibition (Kim et al. 2006; de Bruin et al. 2008). These diseases are distinguished by an excessive accumulation of cells such as cancer or autoimmune diseases. Neoplastic diseases are characterized by mutations in the cell cycle-regulating genes p53, ras or c-myc. Deregulation of genes leads to malignant degeneration and blockade of multiple apoptotic pathways (Chamond et al. 1999).

Deregulation of apoptotic pathways contributes to almost all stages of tumor development (Hanahan et al. 2000). Autoimmune diseases, such as systemic lupus erythematosus, may be associated with mutations in genes rendering the lymphocytes resistant to apoptosis (Thompson 1995).

The second group of diseases is associated with "too much" apoptosis. A large group of neurodegenerative diseases, among them Alzheimer's disease, Parkinson's disease, amyotrophic lateral sclerosis and retinitis pigmentosa, are associated with increased susceptibility to apoptosis of neurons (Gschwind et al. 1995; Walkinshaw et al. 1995).

During ischemia, *e.g.* myocardial infarction, ischemic renal damage or cerebrovascular accidents cell death is generally considered to occur through necrosis. However, cells surrounding the ischemic zone die through apoptosis (Vexler et al. 1997; Zhang et al. 2004; Hong et al. 2008). Apoptosis is thought to happen as a consequence of the alterations in the biochemical metabolism accompanying the ischemic process.

The acquired immunodeficiency syndrome (AIDS), which is caused by infection with the human immunodeficiency virus (HIV), is characterized by an imbalance between the number of $CD4^+$ lymphocytes and the ability of the bone marrow to generate new mature cells (Badley et al. 2000). The $CD4^+$ cells of the patients die through apoptosis when stimulated *in vitro*. Apoptosis is supposed to be involved in the gradual $CD4^+$ T cell depletion in the course of HIV infection (Ameisen 2001; Arthos et al. 2002; Herbeuval et al. 2005).

1.1.5. Apoptotic signaling pathways

A cell is responding to death signals by two major apoptotic pathways: the intrinsic pathway, which is triggered *via* mitochondria, and the extrinsic pathway, which is induced by death receptor stimulation.

1.1.5.1. The intrinsic mitochondrial pathway

Apoptosis can be initiated by intrinsic signals that are produced in response to cellular stress (Fulda et al. 2006). Cellular stress can result from exposure to UV, γ-irradiation, DNA damage and by TCR stimulation. It might also be a consequence of growth factor deprivation or oxidative stress caused by free radicals. These intrinsic signals initiate apoptosis *via* the mitochondria.

The regulation of the mitochondrial pathway is associated with the balance between proapoptotic and antiapoptotic members of the Bcl-2 family (Letai 2005). Intracellular stress is first sensored by the so called "BH3-only subfamily" proteins bearing only one of the BH3 domains, *e.g.* Bid, Bim, Harikari, Noxa, and Puma (Cory et al. 2002). These proapoptotic Bcl-2 family members transmit the stress signal *via* yet not completely known mechanisms to multidomain Bcl-2 family members: Bax, Bcl-xS, Nbk (also called Bik), Bak and Bad. This may lead to oligomerization of Bax and Bak and their insertion into the mitochondrial membrane. This association results in mitochondrial outer membrane permeabilisation (MOMP) and a breakdown of the mitochondrial membrane potential. Antiapoptotic members of the family such as Bcl-2, Bcl-xL, Bfl-1/A1 and Mcl-1 block apoptosis by preventing the mitochondrial release of the intermembrane proteins from mitochondria, including cytochrome c (Bouillet et al. 2002).

After MOMP cytochrome c is released from the mitochondria into the cytoplasm (Green et al. 1998). Release of cytochrome c from mitochondria leads to association with Apaf-1 (apoptosis protease-activating factor 1) in an ATP-dependent way. Apaf-1 is recruited and interacts *via* its CARD domain with the CARD domain of procaspase-9. These events lead to formation of a complex called apoptosome (Korsmeyer et al. 2000). The apoptosome consists of procaspase-9, Apaf-1 and cytochrome c molecules (Srinivasula et al. 1998).

Formation of the apoptosome leads to the activation of procaspase-9 that belongs to the caspase (cysteinyl aspartate proteinases) family (Salvesen 2002). Caspases are key enzymes of apoptotic signal transduction. They are synthesized as proenzymes containing an N-terminal prodomain, as well as p20 and p10 domains that form the active enzyme. Active caspase is a tetramer of two p20/p10 heterodimers containing two active sites (Lavrik et al. 2005). Because cleavage sites of the p10 and p20 subunits contain critical aspartate residues and, hence, potential caspase substrate sequences, other active caspases can clip the prodomain from inactive caspases (Salvesen 2002). According to the length of their prodomain and their function, caspases are classified into initiator and effector caspases (Zou et al. 1999; Acehan et al. 2002). Initiator apoptotic caspases comprise procaspase-9, procaspase-8, procaspase-10, and procaspase-2. Effector caspases comprise caspase-3, -6 and -7. Activation of initiator caspases leads to the activation of effector caspases and ultimately to apoptosis. Procaspase-9 is proteolytically

activated at the apoptosome, and subsequently cleaves and activates effector caspase-3, -6 and -7 (Rodriguez et al. 1999).

Caspase activation can be blocked by inhibitor of apoptosis family (IAPs) members consisting of eight mammalian proteins, including XIAP, C-IAP1 and -2, and MLIAP/livin (Siegelin et al. 2005). The activity of IAPs can be modulated by Smac/Diablo (second mitochondria-derived activator of caspase/direct IAP binding protein with low isoelectric point) (Shiozaki et al. 2004) and a mitochondria-located serine protease Omi/HtrA2, which are released from mitochondria (Faccio et al. 2000).

1.1.5.2. The extrinsic pathway

The extrinsic apoptotic pathway is initiated by the binding of death-inducing ligands to cell surface receptors called death receptors (DR) (Wajant 2003). The detailed structure and function of DRs as well as the signal transduction of the extrinsic apoptotic pathway is described in the next chapter.

1.2. Death receptors

The DR family (Fig. 3) is a subfamily of the tumor necrosis factor receptor (TNFR) superfamily which includes tumor necrosis factor receptor 1 (TNFR1), also known as DR1, CD120a, p55 and p60; CD95 also known as Fas, APO-1 and DR2; DR3 also known as APO-3, LARD, TRAMP and WSL1; TNF-related apoptosis-inducing ligand receptor 1 (TRAILR1), also known as DR4 and APO-2; TRAILR2 also known as DR5, KILLER and TRICK2; DR6 (TNFRSF21), ectodysplasin A receptor (EDAR) and nerve growth factor receptor (NGFR) (French et al. 2003; Wajant 2003). All members of the DR subfamily have a cytoplasmic region of about 80 residues called death domain (DD), which plays an important role in signal transduction. DRs can activate apoptotic and non-apoptotic pathways *via* formation of the corresponding receptor complexes (Fig. 3).

Two types of DR signaling complexes are known so far. The first group comprises the death-inducing signaling complexes (DISCs) that are formed by CD95, TRAILR1 or TRAILR2 (Peter et al. 1999; Lavrik et al. 2005) (Fig. 3).

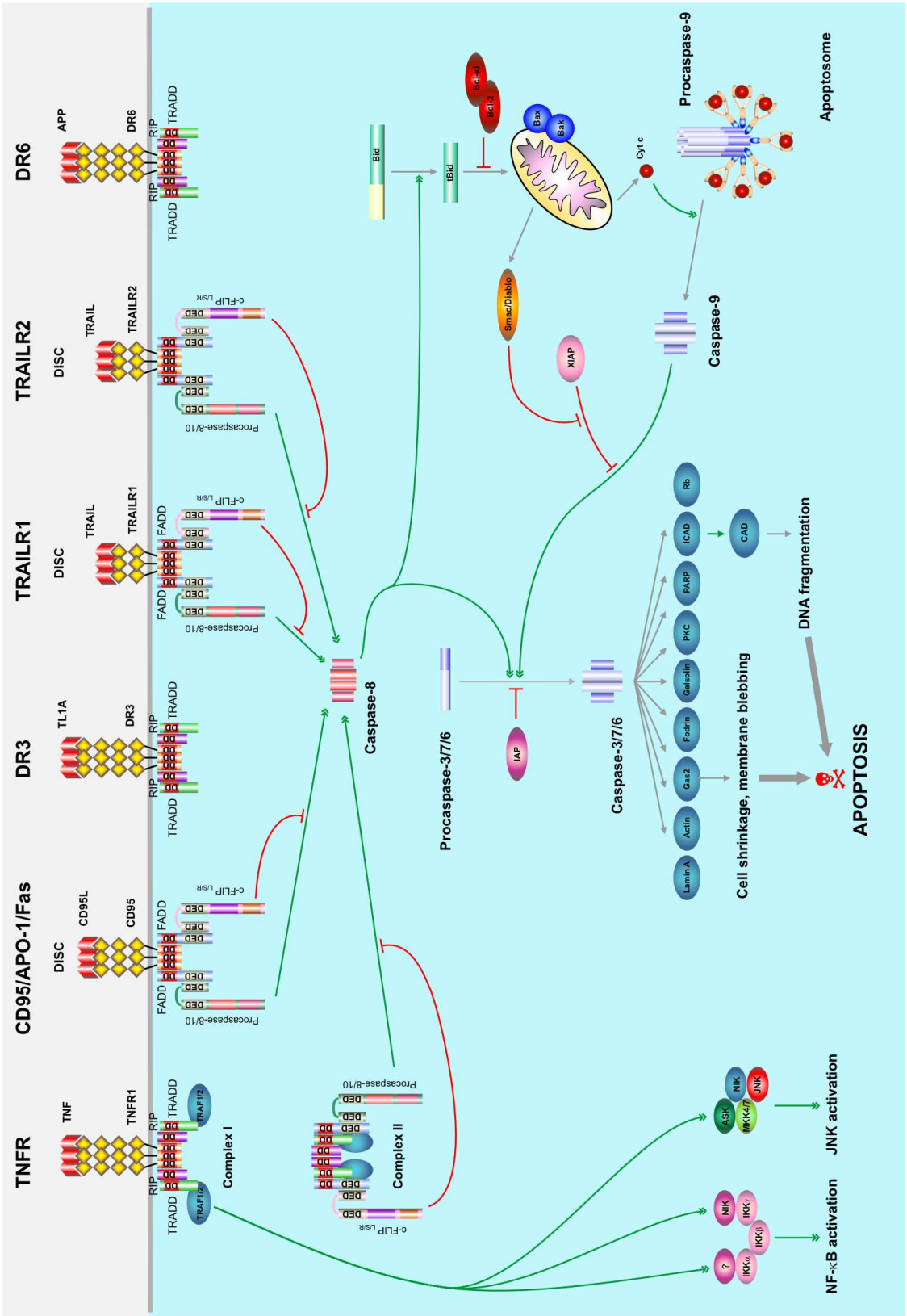

Figure 3. Death receptor (DR) signaling pathways. Induction of apoptotic and non-apoptotic pathways *via* formation of DR complexes: death-inducing signaling complex (DISC), complex I and complex II are shown. DRs are shown in yellow, death ligands are shown in red. Death Domains (DD) are shown in red, Death Effector Domain (DED) in green. Adapted from (Lavrik et al. 2005).

All three receptors form DISCs with a similar composition. DISC formation results in the activation of procaspase-8, which plays a central role in the transduction of the

apoptotic signal (Fig. 3). The second group comprises the TNFR1, DR3, DR6 and EDAR. These recruit a different set of molecules that could transduce both apoptotic and survival signals.

Death ligands also interact with decoy receptors (DcRs) that do not possess DDs and therefore can not form signaling complexes. To date, four decoy receptors have been characterized: TRAILR3 also known as DcR1, TRAILR4 also known as DcR2, DcR3 and osteoprotegrin (OPG) (Lavrik et al. 2005).

1.2.1. Signal transduction by death receptors

1.2.1.1. CD95/Fas/APO-1 signaling

The CD95-mediated apoptotic pathway is one of the most-studied DR pathways. The human CD95 is constitutively expressed in a wide range of hematopoetic and nonhematopoetic cells, and with particular abundance in thymus, liver and kidney (Leithauser et al. 1993).

The human CD95 gene is a single copy gene comprising nine exons and eight introns (Behrmann et al. 1994). The promoter sequence contains consensus binding sites for transcription factors Sp1, AP-1, AP-2, Ets, GF-1, EBP20, c-myb, CREB, GAF, NF-κB, NF-AT, NY-Y and NF-IL6 (Cheng et al. 1995). Regulation of CD95 expression has been described for a wide range of stimuli (Kontny et al. 2005).

The classical view of DR function is typified by CD95 (Fas/APO-1) (Oehm et al. 1992; Peter et al. 1998; Lavrik et al. 2005). Interactions of CD95 with its ligand, CD95L (CD178/FasL/TNSF6), play a pivotal role in the regulation of peripheral tolerance and lymphoid homeostasis. Natural mutations within CD95 and CD95L in humans and mice are associated with the development of autoimmune lymphoproliferative syndromes (Nagata 1999).

1.2.1.1.1. CD95 DISC

CD95 is expressed on the surface of cells possibly as preassociated homotrimers. Upon CD95L binding, CD95 likely undergoes a conformational change to reveal its cytoplasmic death domain (DD) to favor homotypic interactions with other DD containing proteins (Itoh et al. 1993; Boldin et al. 1995; Chinnaiyan et al. 1995). Binding of CD95L within seconds results in formation of the death-inducing signaling complex (DISC) (Peter et al. 2003) (Fig. 4). DISC formation starts with recruitment of the CD95-adaptor protein FADD (Fas-associated DD) through its C-terminal DD. The

N-terminal part of FADD contains a death effector domain (DED) that recruits procaspase-8/10 or its enzymatically inactive homolog c-FLIP$_{L/S/R}$ (Fig. 4).

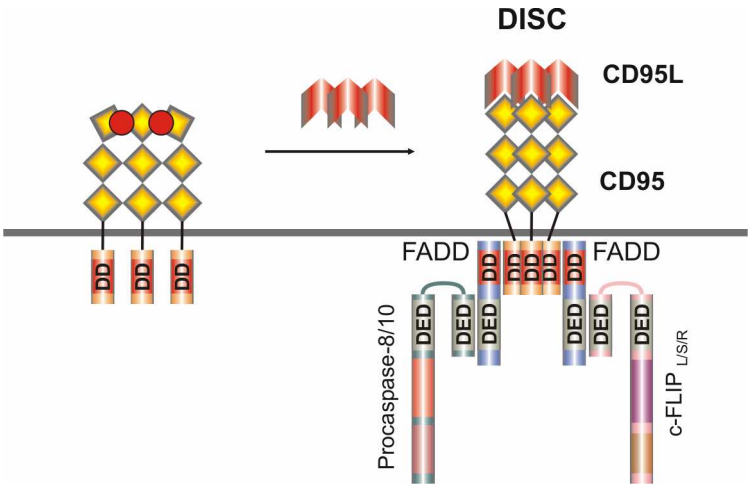

Figure 4. **Formation of CD95 DISC upon CD95L stimulation.** The DISC consists of CD95, (depicted in yellow), FAS-associated death domain, FADD, (depicted in light blue), procaspase-8/procaspase-10, (depicted in green), and cellular FLICE-inhibitory proteins, c-FLIP, (depicted in purple). The interactions between the molecules at the DISC are based on homotypic contacts. The death domain (DD) of CD95 interacts with the DD of FADD while the death effector domain (DED) of FADD interacts with the N-terminal tandem DEDs of procaspase-8, procaspase-10 and c-FLIP. DD are shown in red; DED are shown in light yellow.

It has also been reported that RIP (Stanger et al. 1995), FAF1 (Chu et al. 1995), UBC-FAP (UBC9) (Wright et al. 1996), FAP-1 (Sato et al. 1995), Sentrin (Okura et al. 1996), FLASH (Imai et al. 1999), Ezrin (Parlato et al. 2000), Btk (Jackson et al. 1999), TRAF-1/2 (Kataoka et al. 2000) and Raf-1 are recruited to the DISC. The role of these proteins in the modulation of apoptotic signaling is still illusive.

1.2.1.1.2. Proteins associated with the CD95 DISC

1.2.1.1.2.1. FADD

FADD is an essential protein for CD95 signaling, which acts by recruiting apoptosis-initiating procaspases-8 and -10 to the DISC. FADD has no enzymatic activity and consists of an N-terminal DD and a C-terminal DED (Fig. 5). FADD-deficient MEFs and Jurkat T cells are completely resistant to apoptosis mediated by anti-CD95 agonistic antibodies, CD95L, TNFα, or TRAIL.

Apart from its apoptotic function, it has been shown that FADD is crucially involved in development. FADD-deficient embryos die of heart defects at day 10 of gestation

(Varfolomeev et al. 1998; Yeh et al. 1998). It also appears to play a role in T and B lymphocyte development (Kabra et al. 2001; Zhang et al. 2001).

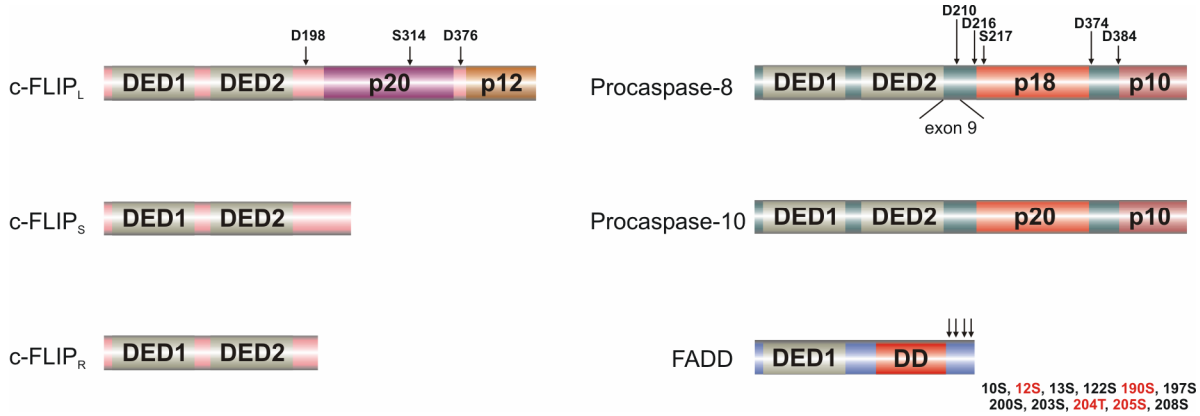

Figure 5. **DED-proteins of the DISC: c-FLIP$_{L/S/R}$, procaspase-8, procaspase-10 and FADD.** c-FLIP isoforms contain two death effector domains (DEDs) (depicted in grey). c-FLIP$_L$ contains caspase-like domains p20 and p12 (depicted in purple and brown). Aspartate residues which are needed proteolytic cleavage are shown with black arrows (D198, D376). Procaspase-8/10 contains two DEDs (depicted in grey), the large catalytic subunit p18/p20, respectively, (depicted in red) and the small catalytic subunit p10 (depicted in bordeux). Aspartate residues which are needed for caspase-8 proteolytic cleavage activation are shown with black arrows (D374, D384, D210 and D216). FADD contains a C-terminal DD (depicted in red) and an N-terminal DED (depicted in grey). Phosphorylation sites of FADD and procaspase-8 are shown with black arrows.

Mice lacking FADD or expressing a dominant-negative FADD show reduced thymic cellularity and inhibition of T cell development. These mice also have defects in T cell receptor (TCR) activation-induced proliferation of T cells due to impaired G1→S transition (Walsh et al. 1998). FADD was shown to be selectively phosphorylated at Ser194 (Scaffidi et al. 2000). Highly phosphorylated FADD was found in cells in G2/M, whereas FADD phosphorylation was low in G1. The ability of FADD to promote cell cycle progression of T cells was found to depend on the phosphorylation of this site (Hua et al. 2003).

1.2.1.1.2.2. Procaspase-8

Caspase-8 has been identified as enzymatically active component of the CD95 DISC (Kischkel et al. 1995). It was initially named CAP4 and later it got several other names such as FLICE (FADD-like Interleukin-1ß-converting enzyme), MACH (Boldin

et al. 1996) and MCH5 (Fernandes-Alnemri et al. 1996). Caspase-8 has a preferred substrate specificity for I/L/V/E-X-D, where X is any amino acid (Lavrik et al. 2005).

The human gene is located at the locus 2q33-34. The murine homologue has been found in the chromosomal region 1B-proximal C (Kischkel et al. 1998). Procaspase-8 is expressed in a wide range of the cells. Procaspase-8 knockout mice are prenatally lethal. Mutant MEFs are resistant to receptor-mediated apoptosis (Varfolomeev et al. 1998; Kang et al. 2004).

Eleven forms of procaspase-8 were described at the mRNA level, but only 5 isoforms have been characterized so far at the protein level - caspase-8a, caspase-8b, caspase-8i, caspase-8k and caspase-8l (Eckhart et al. 2001; Himeji et al. 2002). Both procaspase-8a and -8b play a key role in apoptotic signaling as initiator caspases of the extrinsic apoptotic pathway. In addition, procaspase-8a and -8b are implicated in migration, adhesion, NF-κB activation, proliferation and differentiation (Fulda 2009). Caspase-8l has been shown to play an inhibitory role because it lacks a catalytic domain (Himeji et al. 2002). Caspase-8l expression has been reported to be regulated by alternative splicing in leukemia and neuroblastoma (Mohr et al. 2005).

Procaspase-8a/b is a 55/53 kDa protein of 496/479 amino acids. It contains two DEDs in its N-terminal prodomain and two C-terminal catalytic protease domains: p18 and p10 (Fig. 5). The DEDs function as a platform for protein-protein interactions (Kischkel et al. 1995). Upon proteolytic activation at the DISC, active caspase-8 is generated as a heterotetramer consisting of two large (p18) and two small subunits (p10) (Lavrik et al. 2003). Besides its proteolysis at the DISC, procaspase-8 can also be activated downstream of mitochondria upon initiation of the intrinsic apoptosis pathway*, e.g. via* caspase-6 (Fulda 2009).

The mechanism of procaspase-8 activation at the DISC includes oligomerization and, consequently, two-step autoproteolytic cleavage (Medema et al. 1997; Muzio et al. 1998). The cleavage occurs at defined aspartate residues: the first cleavage step at Asp374 separates the p12 subunit from the remaining p43 and p41 (for procaspase-8a or -8b, respectively). The second cleavage step occurs at Asp384 and Asp210/Asp216, which leads to the generation of p10, p18 and the prodomain p24/p26. The active heterotetramer $p18_2$-$p10_2$ can still be detected at the DISC indicating that the heterotetramer is produced directly at the DISC and then released into the cytosol (Lavrik et al. 2003). Recently it also has been reported that the fully

active caspase-8 heteroteramer $p41_2$-$p10_2$ cleaves procaspase-3 and Bid and thereby might also drive CD95-induced apoptosis without processing to the $p18_2$-$p10_2$ form (Hughes et al. 2009). In addition, recently the alternative way of caspase-8 activation has been reported by our group, which involves an alternative C-terminal cleavage product of procaspase-8, p30, generated by cleavage at Asp210 (Hoffmann et al., 2009).

It was reported that c-$FLIP_L$ plays an important role in procaspase-8 activation by heterodimerisation of the protease-like domain of c-$FLIP_L$ with the protease domain of procaspase-8 and 10, leading to their allosterical activation (Micheau et al. 2002; Chang et al. 2003; Yu et al. 2009). This heterooligomerisation between c-$FLIP_L$ and caspase-8 catalytic domains occurs more efficiently than homodimerisation of caspase-8 catalytic domains. This leads to an increase of procaspase-8 proteolytic activity by c-$FLIP_L$.

The activity of caspase-8 can be also regulated by posttranslational modifications (Fig. 5). Several studies have shown that phosphorylation at Y380 of procaspase-8 inhibits CD95-induced caspase-8 activation (Cursi et al. 2006; Senft et al. 2007). For the TRAILR1 and CD95 DISC it has been reported that the full activation of procaspase-8 requires CUL3-RBX1-dependent polyubiquitination. Polyubiquitination of procaspase-8 at the DISC is followed by its translocation from the DISC into an ubiquitin complex, called aggresome (Jin et al. 2009).

1.2.1.1.2.3. Procaspase-10

Caspase-10 shares homologous DEDs with caspase-8 (Fig. 5). Caspase-10 is recruited to the DISC *via* DED interactions with FADD. Caspase-8 and caspase-10 may regulate each other by competing for the binding to FADD DED at the DISC (Wang et al. 2001). Procaspase-10 is proteolytically activated at the DISC, however, whether caspase-10 can initiate apoptosis in the absence of caspase-8 is still elusive (Sprick et al. 2002). It has been shown that caspase-10 is also located at other DR-signaling complexes formed in response to DR stimulation. Interestingly, the substrate specificity of caspase-10 is different from that of caspase-8 (Wang et al. 2007).

Various autoimmune lymphoproliferative syndromes are associated with decreased caspase-10 function and thereby defective DR signaling. Procaspase-10 is expressed at high levels in primary cells derived from the immune system but it is

present at low level or absent in many transformed cell lines. It was shown that mice and rats do not have the *CASP-10* gene (Reed et al. 2003).

1.2.1.1.2.4. c-FLIP$_{L/S/R}$

DR-mediated apoptosis can be regulated at the DISC by c-FLIP (also known as FLAME-1, I-FLICE, Casper, CASH, MRIT, CLARP or usurpin), which was originally found in the family of herpes viruses. Several splice variants of c-FLIP were found to exist on the mRNA level, but so far only three c-FLIP proteins have been identified: c-FLIP$_S$, c-FLIP$_R$ and c-FLIP$_L$ (Irmler et al. 1997; Scaffidi et al. 1999; Golks et al. 2005) (Fig. 5). All c-FLIP variants have two DEDs and function in a dominant-negative way to block the recruitment to the DISC and the activation of procaspase-8 (Krueger et al. 2001). c-FLIP$_S$ has a similar structure as viral FLIP (v-FLIP), except that the two DEDs of the c-FLIP$_S$ are followed by a short C-terminal extension of around 20 amino acids that seems to be crucial for its ubiquitylation and therefore its proteasomal degradation. c-FLIP$_R$ also contains two DEDs but lacks the additional C-terminal amino acids. c-FLIP$_L$ contains a longer C-terminal extension with a caspase-like region that is similar to procaspase-8 and procaspase-10 (Fig. 5). However, the C-terminal part of c-FLIP$_L$ lacks caspase enzymatic activity due to the substitution of several amino acids, such as the cysteine residue required for catalytic activity (Goltsev et al. 1997; Inohara et al. 1997).

1.2.1.1.3. Two CD95 signaling pathways

Cell death can be initiated by CD95 activation in two different ways (Scaffidi et al. 1998; Barnhart et al. 2003). Type I cells release large amounts of active caspase-8 from the DISC. This is sufficient to directly cleave and activate procaspase-3, -6, and -7. Effector caspases-3, -6, -7 cleave various cellular components as nuclear lamins, cytoskeleton proteins fodrin and gelsolin, and inhibitor of caspase-activated DNase (ICAD), thus activating caspase-mediated DNA degradation by DNase (Scaffidi et al. 1998; Lavrik et al. 2005; Fulda 2009).

Type II cells, by contrast, produce a very low amount of active caspase-8 at the DISC. This, however, is sufficient to cleave the proapoptotic BH3 domain only containing Bcl-2 family member Bid to tBID (truncated Bid) (Li et al. 1998; Luo et al. 1998). tBid translocates to the mitochondria where it induces the release of cytochrome c.

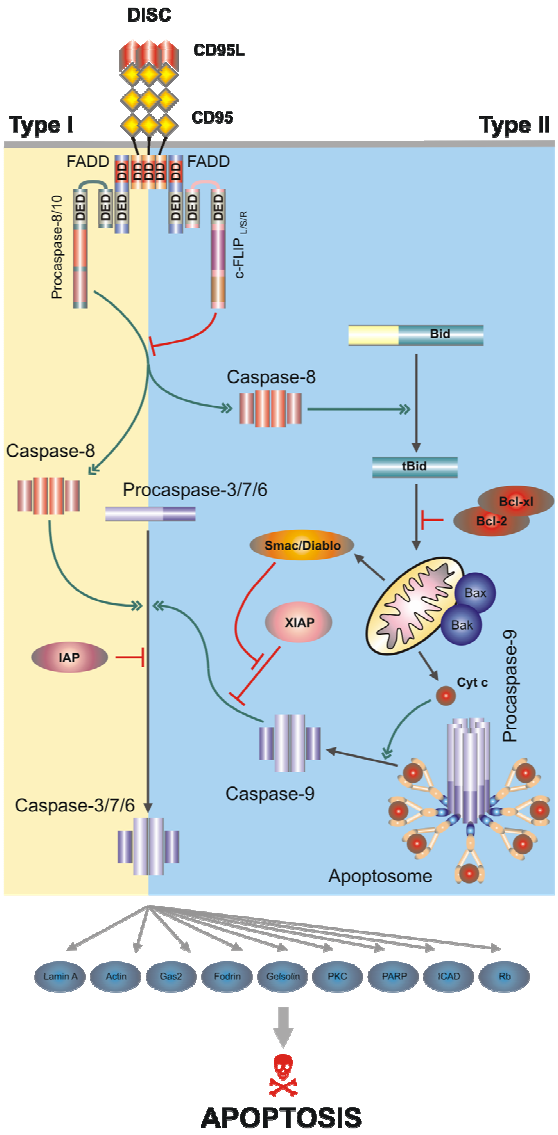

Figure 6. **Two CD95 signaling pathways.** Type I cells form high amounts of the DISC and active caspase-8 (left side). Type II cells form the DISC and active caspase-8 in lower amounts and require amplification of the apoptotic signal *via* mitochondria. Apoptosis in Type II cells can be blocked by Bcl-2 family members (right side) (adapted from (Krammer 2000)).

This results in apoptosome formation and activation of procaspase-9. In a next step activation of effector caspases-3, -6 and -7 occurs (Fig. 6). Apoptosis in Type I cells can be induced independently of mitochondria. Deletion or overexpression of Type II pathway proteins (procaspase-9, Apaf-1) confirm a physiological role for the two pathway model (Scaffidi et al. 1998). Knockout studies in mice provide evidence that thymocytes are Type I and liver cells are Type II cells (Strasser 1995; Lacronique et al. 1996; Rodriguez et al. 1999).

Recently, it has been reported that XIAP is a regulator of Type I and Type II cells. It was shown using XIAP knockout mice and double BID-XIAP knockout mice that

XIAP can convert cell death from Type II to Type I (Jost et al. 2009). However, this hypothesis has not been really brought in line with the original Type I/Type II definition (Scaffidi et al. 1998), which classifies CD95 signaling as Type I or Type II based on the amount of DISC formation.

A number of CD95 signaling events in Type I and Type II cells have been described, which are controversially discussed. Upon initiation of signaling CD95 has been reported to form SDS- and β-mercaptoethanol-stable aggregates (Kischkel et al. 1995; Kamitani et al. 1997; Papoff et al. 1999) (Henkler et al. 2005) CD95 has been reported to be translocated to membrane rafts in Type I but not in Type II cells (Hueber et al. 2002; Eramo et al. 2004; Muppidi et al. 2004; Legembre et al. 2006). Another controversially discussed finding is that CD95 is internalized in Type I cells, which amplifies apoptosis induction (Algeciras-Schimnich et al. 2002).

1.2.1.2. DR3 signaling

DR3 shows close sequence similarity to TNFR1 (Chinnaiyan et al. 1996; Kitson et al. 1996; Marsters et al. 1996; Bodmer et al. 1997; Screaton et al. 1997). Upon overexpression, DR3 triggers responses that resemble those of TNFR1, namely, NF-κB activation and apoptosis. Like TNFR1, DR3 activates NF-κB through TRADD, TRAF2, and RIP and apoptosis through TRADD, FADD, and caspase-8. DR3 binds to Apo3L, which is related most closely to TNF (Marsters et al. 1998; Kabra et al. 2001).

1.2.1.3. TRAILR1 and TRAILR2 signaling

TRAIL binds to TRAILR1 (DR4) and TRAILR2 (DR5). Both receptors are often co-expressed in one cell type. Nonetheless, TRAILR2 seems to play a more important role than TRAILR1 in triggering apoptosis in cells expressing both receptors (Pan et al. 1997; Pan et al. 1997). Upon activation, TRAILR1 and TRAILR2 recruit FADD, procaspase-8 and procaspase-10 to their respective DISCs. Followed by the initiation of a caspase cascade which resembles the CD95 signaling pathway (Fig. 3) (Kuang et al. 2000; Sprick et al. 2000; Merino et al. 2006).

A posttranslational modification, O-glycosylation of TRAIL receptors has been reported to increase TRAIL sensitivity by promoting ligand-induced receptor clustering and consequently procaspase-8 activation. Expression of O-glycosyltransferases correlates with sensitivity to TRAIL-mediated apoptosis in a

large number of tumor cell lines and represents a potential new biomarker for screening cancer patients for TRAIL-based clinical trials (Wagner et al. 2007).

TRAIL has also been reported to promote activation of prosurvival proteins such as NF-κB, protein kinase B (PBK)/Akt, and MAP kinases through distinct, independent pathways (Secchiero et al. 2004). TRAILR1, TRAILR2, and TRAILR4 have been shown to activate NF-κB *via* a TRAF-2-NIK-IKK complex (IκB kinase complex)-dependent signaling cascade, whereas TRAILR1 induces JNK/SAPK activation *via* a TRAF-2-MEKK1-MKK4 dependent pathway (Falschlehner et al. 2007).

1.2.1.4. TNFR1 signaling

The TNFα/TNF-receptor signaling system consists of two distinct receptors, TNFR1 and TNFR2 (p75/CD120b). Three ligands are known: the membrane-bound TNFα (mTNFα), the soluble TNF-α (sTNFα), and the soluble lymphocyte-derived cytokine (LTα/TNFβ) (Wallach et al. 1999).

While TNFR1 is considered to be a canonical DR, TNFR2 does not contain an intracellular death domain. To a great extent TNFR1 appears to be responsible for TNF signaling in most cell types. Studies of TNFR1-deficient mice have shown that TNFR1 is essential for TNF-induced apoptosis of pathogen-infected cells (Pfeffer et al. 1993; Zhao et al. 2000). TNFα plays a key role in inflammation and immunity, as well as in proliferation and differentiation (Wajant et al. 2003). It is mainly produced by mononuclear phagocytes and T cells in response to infection and inflammatory conditions, but also by other cell types, such as B cells, fibroblasts, and hepatocytes. Soluble and membrane-bound TNFα are biologically active, and while the soluble form acts as an effector molecule at a distance from the producer cell, the membrane-bound form likely has a specific role in localized TNFα responses.

TNFR1 is primarily involved in mediating inflammation and not cell death. Engagement of TNFR1 by TNFα induces recruitment of RIP1, TRAF2, and c-IAP1/2 to the receptor to form the membrane-bound complex I (Micheau et al. 2003). The presence of TRADD in this complex is controversial (Schneider-Brachert et al. 2004). It has been reported that complex I requires translocation of TNFR1 to lipid rafts, where several proteins in the complex undergo posttranslational modifications (Legler et al. 2003). In particular, RIP1 is polyubiquitinated at Lys377 by cIAP1 and cIAP2, which act as E3 ligase, a step required for the activation of NF-κB (Li et al. 2006).

These lysine 63-linked polyubiquitin chains of RIP1 are essential for the recruitment of TAK1 and IKK complexes to the TNF receptor complex (Ea et al. 2006).

Two distinct pathways originate from the association of RIP1 and TRAF-2 to the receptor, whose balance determines the ultimate fate of the cell in response to TNFα (Wajant et al. 2001). The first pathway promotes NF-κB activation and signals through binding of the protein kinase TAK1 *via* interaction of the TAK1 complex, consisting of the TAK1 kinase and its associated TAK1-binding proteins 1/2/3 (TAB1, TAB2, and TAB3) with RIP1 lysine 63-linked polyubiquitin chains, resulting in TAK1 kinase phosphorylation and activation. TAK1 proceeds to activate the catalytic IKK complex, comprising the three proteins IKKα (IKK1), IKKβ (IKK2), and IKKγ (NEMO), leading to phosphorylation of the NF-κB inhibitory protein IκBα. Phosphorylated IκBα is then degraded upon ubiquitination *via* the proteasome; allowing NF-κB to be translocated into the nucleus and initiate transcription of antiapoptotic genes such as c-FLIP, cIAP1, cIAP2, TRAF1, and TRAF2. Thus, ubiqutination of RIP1 dictates its survival signaling cascade. It has recently been published that cIAP1 and cIAP2 directly ubiquitinate RIP1 and induce constitutive RIP1 polyubiquitination in cancer cells, thereby sustaining cancer cell proliferation (Ea et al. 2006).

The second pathway originating from the association of RIP1 and TRAF-2 with the receptor leads to activation of JNK *via* the sequential activation of MEKK-1 and JNKK (JNK kinase). JNK phosphorylates and activates c-Jun, a component of the transcription factor complex termed activator protein-1 (AP-1). Transient JNK pro-death stimuli are normally inhibited by NF-κB regulated genes, such as xiap, which encodes the endogenous inhibitor of apoptosis, XIAP, and promotes cell survival (Tang et al. 2001). However, JNK-sustained activation mediates phosphorylation and activation of the E3 ubiquitin ligase Itch, which specifically ubiquitinates c-FLIP and promotes its proteasomal degradation, resulting in enhanced procaspase-8 activation and apoptosis (Chang et al. 2006).

Activation of procaspase-8 and apoptosis initiation upon TNF stimulation has been explained by two different mechanisms, but both of them are still questioned. According to Micheau et al., activation of procaspase-8/10 occurs in Complex II which contains TRADD, TRAF2, RIP1, FADD, and procaspase 8/10. Complex II dissociates from complex I directly to the cytosol (Micheau et al. 2003). Alternatively, it was suggested that following the transient formation of complex I, the receptor is

probably internalized by endocytosis (Schneider-Brachert et al. 2006). It has been suggested that RIP1, TRAF2, and perhaps TRADD dissociates from TNFR1 during endocytosis, allowing the DD of RIP1 to interact with the DD of FADD, which, in turn, recruites procaspase-8 and -10.

1.2.1.5. DR6 signaling

DR6 is broadly expressed by developing neurons and required for normal cell death and axonal pruning *in vivo*. It also plays a role in lymphocyte development (Schmidt et al. 2003). APP was shown to be the ligand for DR6. APP-DR6 signaling leads to neurodegenration possibly *via* caspase-6 activation and contributes to the pathophysiology of Alzheimer's disease (Nikolaev et al. 2009).

1.2.2. Structures of CD95 and other death receptors

Structural information about DRs is based on the structures of the TNFR1-TNFα complex (Banner et al. 1993), TNFR1 ectodomain (ECD) (Naismith et al. 1996) and intracelular domain (Sukits et al. 2001), herpes virus entry mediator (HVEM), Apo2L/TRAIL-TRAILR2 complex (Hymowitz et al. 1999; Mongkolsapaya et al. 1999; Cha et al. 2000), complex of FADD-CD95 DDs (Scott et al. 2009) and CD95 DD (Huang et al. 1996). These structures show that the ECD of DRs as well as that of other TNFR family members contain several cysteine-rich domains (CRD) which form elongated structures composed of loops tethered together by disulfide bridges (Fig. 7A). These receptors bind at the monomer-monomer interfaces of their trimeric ligands to form a complex consisting of three copies of the receptor and one trimeric ligand (Fig. 7B).

The ligands of TNFRs are members of the TNF family. The ligands have been structurally characterized more thoroughly than the receptors. Initially the structure of TNF has been determined and so far supplemented by the structures of several other family members. These structures show that TNFs are homotrimeric globular proteins with distant structural homology to viral capsid proteins as well as to the complement protein C1q and to the NCI domain of collagen X (Jones et al. 1989; Shapiro et al. 1998; Bogin et al. 2002).

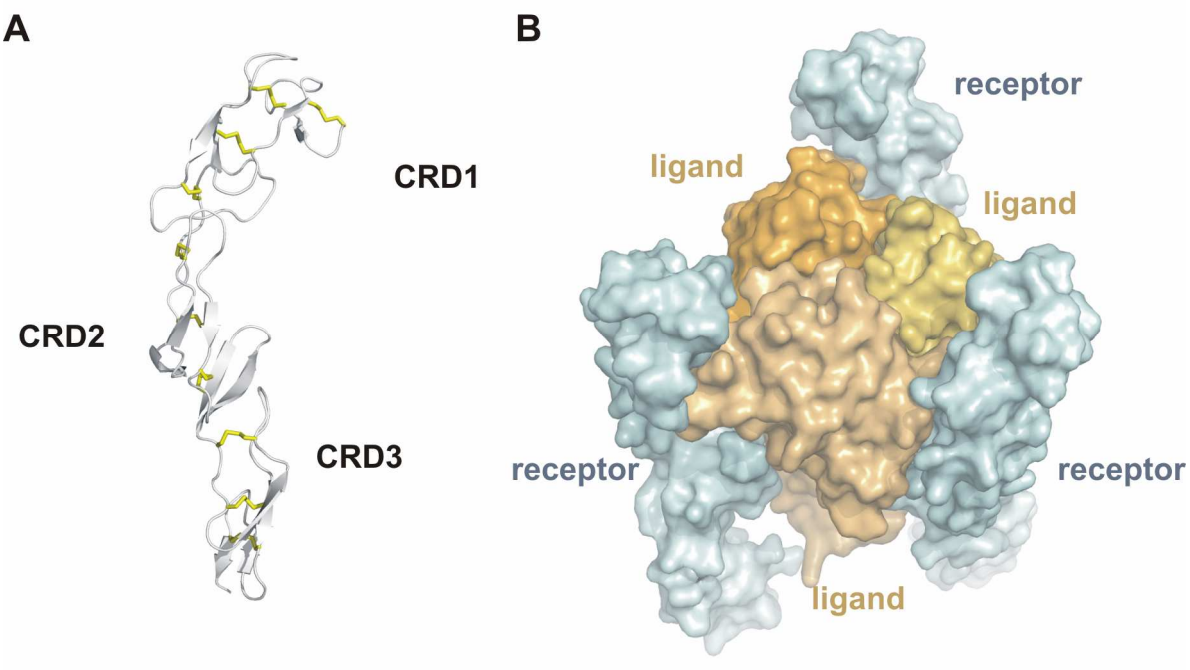

Figure 7. Structural properties of Death Receptors (DR). A. Cartoon representation of TNFR1 extracellular domain with three cystein-rich domains (CRD) and disulfide bonds shown as yellow sticks (PDB ID 1tnr chain) **B.** Example of trimeric DR-ligand extracellular domains complex based on TNFR1-TNFα complex (PDB ID 1tnr).

Most of the TNFRs are type I transmembrane proteins with the N-terminal signal sequence followed by the CRDs, a transmembrane helix and a C-terminal intracellular domain. Some of the family members are type III transmembrane proteins without a signal sequence. TNFRs are very divergent and have very low pairwise sequence identity. This divergence is a consequence of a nonglobular fold composed of cysteine-rich pseudorepeats. A typical CRD contains approx 40 residues with 6 cysteins connected in a 1-2, 3-5, 4-6 pattern of disulfide linkages (Fig. 7A).

Several TNFR family members have been determined to be preoligomerized by FRET, coimmunoprecipitation and FACS analysis (Siegel et al. 2000). This seems to be dependent on the N-terminal part of the first CRD, called PLAD. However, further biophysical characterization of the PLAD is necessary to understand its role in TNFR regulation.

1.2.2.1. TNFR1 and TRAILR2 complexes

Formation of TNFR-TNFα complexes has been largely derived from the structure of the LTα homotrimer bound to the ECD of TNFR1. Determination of the structure of

Apo2/TRAIL bound to DR5 by several groups confirmed that this binding mode (Fig. 9) is conserved for other multidomain TNFRs and showed that the structurally equivalent loops in other TNFRs are similar.

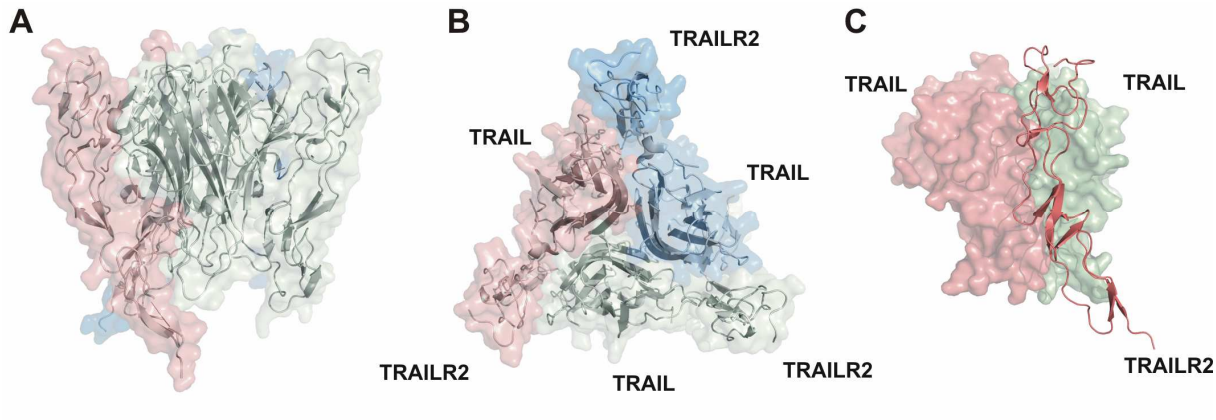

Figure 8. **Crystal structure of extracellular domain complex of TRAILR2-TRAIL (PDB ID 1d0g)**. Corresponding TRAILR2-TRAIL monomers are shown in the same color. **A.** Side view of the complex (cartoon-surface representation). **B.** View on the complex from the first CRD of TRAILR2 (cartoon-surface representation). **C.** One receptor (cartoon representation) interacts with two ligands (surface representation).

CRD2 and the first loop of CRD3 mediate most of the contacts to the ligand in both TNFR1-TNFα and TRALR2-Apo2L/TRAIL complexes. This is consistent with the observation that CRD2 is the most conserved region in TNFR1, HveA and TRAILR2.

In both the TNFR1-TNFα and TRALR2-Apo2L/TRAIL complexes, the spacing of the C-termini of the receptors as they enter the cell form an almost equilateral triangle with sides of approximately 50 Å. This similarity in geometry suggests that this spacing is likely physiologically relevant and may be required for signaling.

Modelling studies of other receptor-ligand complexes including CD95 (Bajorath 1999; Bajorath 1999) and CD40 (Bajorath et al. 1995; Bajorath 1998) suggest that these receptors also interact with their ligands in a similar manner.

1.2.2.2. CD95/Fas/APO-1

DD complexes are key protein arrangements in the regulation of various cellular signaling events. The 'Death domain superfamily' includes DD, DED, CARD and pyrin domain (PYD). All of these domains are typically globular protein units that exhibit a characteristic six helix fold and are known to undergo homotypical

interactions with other death domains of the same family (Boldin et al. 1995; Chinnaiyan et al. 1995; Kischkel et al. 1995; Muzio et al. 1996; Tibbetts et al. 2003).

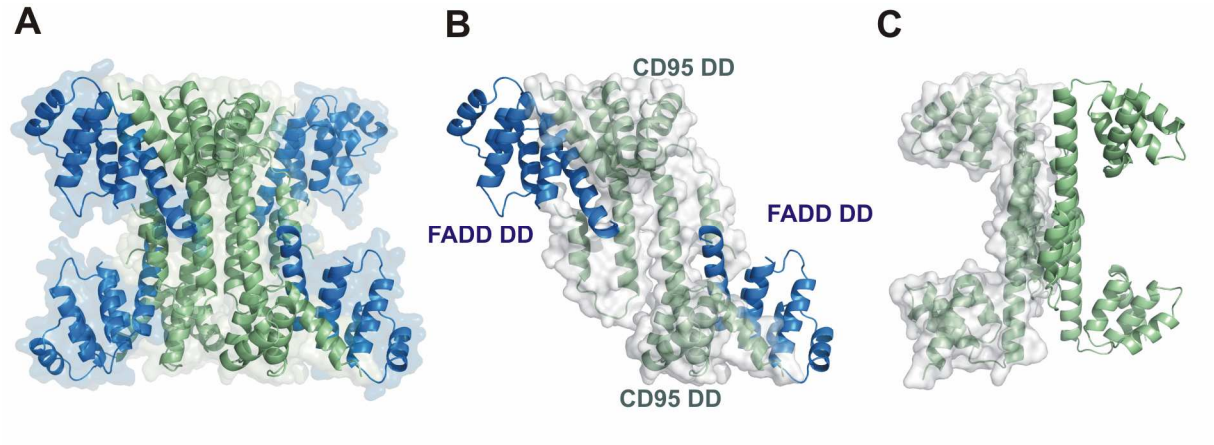

Figure 9. **Crystal structure of death domains complex of CD95 (green) and FADD (blue) (PDB ID 3ezq). A.** Heterooctamer structure found in the crystal consisting of four molecules of CD95 DD and four molecules of FADD DD. **B.** Complex is formed *via* interactions of two extended helixes of CD95 DD. One FADD DD molecule interacts with only one CD95 DD in the region which was occupied by an extended helix of the CD95 DD. **C.** Octamer is formed by interaction of extended helixes of the CD95 DD.

In the case of the CD95/FADD/procaspase-8 DISC the 'death domain network' is built by an interaction of the DD of CD95 with the DD of FADD, which also contains a DED to recruit procaspase-8 through homotypical DED interactions (Fig. 9).

The structure of the CD95/FADD DD complex, which represents the first known structure of a 'death domain network', has been reported recently. The complex has been obtained *in vitro* by combining bacterial lysates of the overexpressed DDs. To solve the structure of the CD95/FADD DD complex a broad crystallization effort was undertaken. The key observation was that the CD95 DD had undergone a significant opening transition in the CD95/FADD complex. This opening creates binding sites for the FADD DD that are absent in the closed form of CD95. The predominant CD95-CD95 association has also been observed in the structure. It is formed by stem helices and C-helices of the two CD95 DDs (Fig. 9C). Opening of CD95 provides the basis for both FADD DD binding and the formation of a regulatory bridge between CD95 molecules (Scott et al. 2009).

The availability of crystal structures of several TNF family members facilitates the construction of homology models for the whole family. These models can be very useful for determining potential residues to mutate in order to identify the receptor

binding sites, for understanding tertiary structure and for the analysis of posttranslational modifications.

1.2.3. Different forms and posttranslational modifications of CD95

A number of reports on CD95 have suggested the presence of several forms of CD95, which have different molecular mass (Oehm et al. 1992; Peter et al. 1995). The presence of these forms can be explained by alternative splicing or by posttranslational modifications.

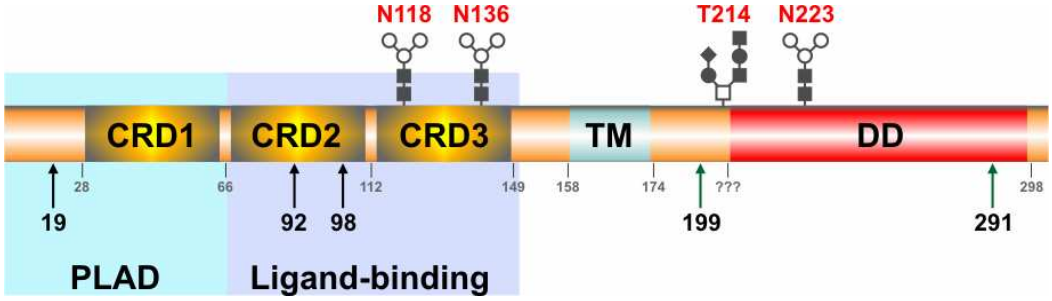

Figure 10. **Schematic representation of the domain organization of CD95.** The CRD are shown in yellow, the transmembrane domain (TM) in blue, the DD in red. Potential glycosylation sites are depicted as schematic oligosaccharides, phosphorylation sites as black arrows, palmitoylation sites as green arrows.

1.2.2.2.1. CD95 splice variants

Alternative splicing of CD95 primarily results in the translation of soluble CD95 protein or peptides (sCD95). There are six reported sCD95 isoforms. All of them lack the transmembrane region encoded in exon 6 of the CD95 gene. These sCD95 variants are secreted and appear to have a dominant negative effect on CD95 activation by interacting with CD95L. These splice variants are associated with different types of cancer (Cascino et al. 1995; Cascino et al. 1998).

1.2.2.2.2. CD95 phosphorylation

CD95 has been reported to be phosphorylated at Thr, Tyr and Ser in the PLAD and cystein-rich extracellular regions (Lautrette et al. 2006) (Fig. 10). In addition, CD95 is phosphorylated intracellulary at the area comprising amino acids 191-275 (Fig. 10). The potential intracellular phosphorylation sites are Tyr232, Tyr291, as well as four Thr and two Ser located between amino acids 229 and 275. All of them lie in

the DD of CD95 and might influence apoptotic signaling *via* modulation of the binding of adaptor proteins.

It has also been reported that CD95 might be phosphorylated by extracellular protein kinase C (PKC) (Lautrette et al. 2006). There are three potential sites for PKC in the extracellular region. The first one is located in PLAD. Therefore, phosphorylation of this site by ecto-PKC may directly modulate CD95L-independent oligomerisation of CD95 receptors and apoptosis signaling by blocking preassociation of the receptors. Two others are located in the ligand-binding region. Phosphorylation at this area might modulate CD95L binding to the receptor (Fig.10).

1.2.2.2.3. CD95 S-palmitoylation

Another possible modification of CD95 which has been reported is palmitoylation (Feig et al. 2007). Formation of CD95 SDS-stable aggregates has been shown to be regulated by palmitoylation of CD95 at cysteine 199. These aggregates were called hiDISC - high molecular weight DISC. In hiDISC procaspase-8 and FADD are suggested to be recruited to the CD95 DISC leading to caspase-8 activation.

1.2.2.2.4. CD95 glycosylation

CD95 is a 36 kDa membrane glycoprotein (Oehm et al. 1992). CD95 glycosylation has not been studied in detail so far. However, it is known that the apparent mass of CD95 increases from 36 to 45-54 KDa due to addition of variable oligosaccharide chains. CD95 contains three potential sites for N-linked glycosylation and one potential site for O-glycosylation. Glycosylation of CD95 has been demonstrated to comprise a high degree of sialylation (Peter, 1995). It has been shown that CD95 is present at least as 12 differently sialylated forms in different subclones of the B lymphoblastoid cell line BJAB and in the T leukemia cell line Jurkat. Removal of sialic acid residues from the surface of these cell lines increased their sensitivity to CD95-mediated death (Peter et al. 1995; Keppler et al. 1999).

Another interesting observation is that treatment with IFNγ increases the amount of N-glycosylated forms of CD95 in different cell lines, which results in higher expression of CD95 on the cell surface and consequently increases sensitivity to CD95-induced apoptosis. In another study, inhibition of enzymes of the glycosylation machinery and enzymatic removal of the glycans did not influence surface localization of CD95 (Dorrie et al. 2002).

1.3. Glycosylation

Glycosylation plays an important role in many processes in an organism, from fertilization to ontogenesis and development. The main players of the glycosylation process are enzymes (glycosyltransferases and glycosidases) which ensure addition and removal of carbohydrates, respectively.

Cell surface carbohydrates are major components of the outer surface of mammalian cells. Carbohydrate structures change drastically during mammalian development. Specific sets of carbohydrates are expressed at different stages of differentiation. In many instances these carbohydrates can be recognized as differentiation antigens by specific antibodies. In mature organisms, production of distinct carbohydrates is eventually restricted to specific cell types which results in cell type-specific carbohydrates. Aberrations in these cell surface carbohydrates are associated with various pathological conditions, including malignant transformation (Parodi 2000).

1.3.1. The nature of carbohydrate diversity

Carbohydrates are unique in their structural complexity. In contrast to nucleic acids and proteins, carbohydrates are linked in many different ways. One sugar residue could bind another sugar at three or four different positions of hydroxyl groups having either α- or β-isoconformations. These multiple binding abilities allow carbohydrates to have branches, unlike all other biological macromolecules, which contain almost exclusively linear structures. Because of this complexity, carbohydrate structures are very variable (Yarema et al. 2001).

1.3.2. Different types of glycosylation and glycoproteins

There are six classes of glycans (Fig. 11): 1) N-linked glycans attached to the amide nitrogen of Asn side chains; 2) O-linked glycans attached to the hydroxyl group of serine and Thr residues; 3) glycosaminoglycans attached to the hydroxyl group of serine; 4) glycolipids in which the glycans are attached to ceramide; 5) hyaluronan which is unattached to either protein or lipid; and 6) GPI anchors which link proteins to lipids through glycan linkages (Lowe et al. 2003).

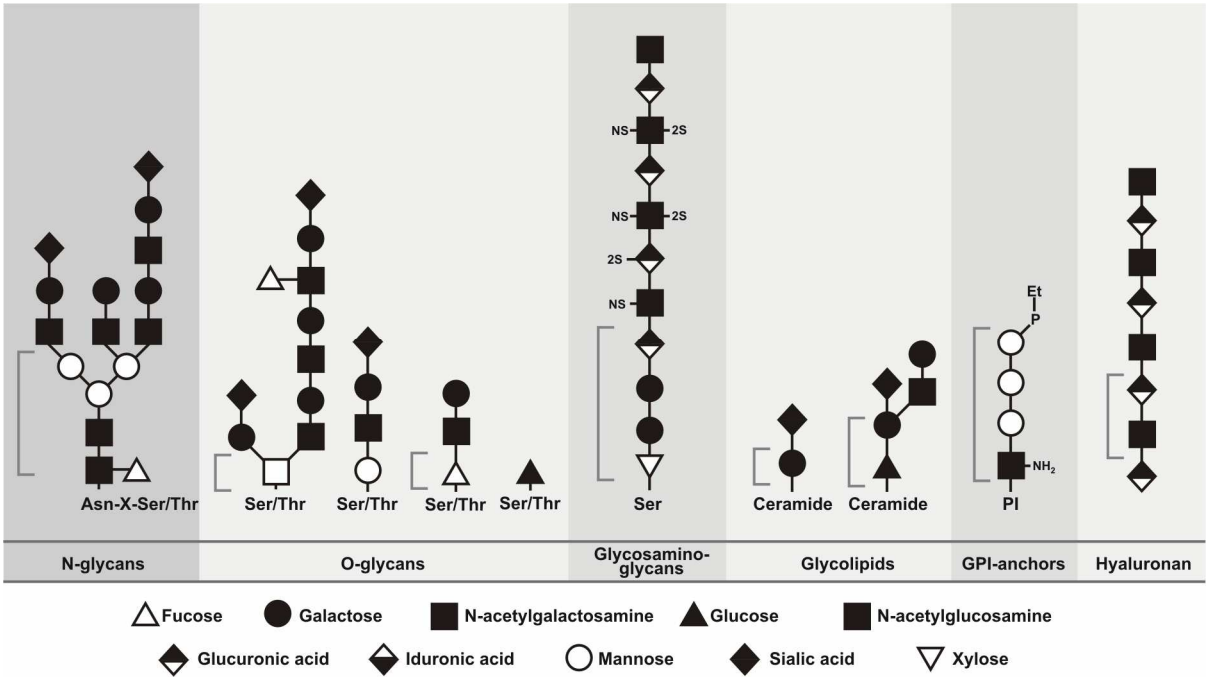

Figure 11. **Six classes of glycans.** Representative examples of each distinct class of mammalian glycans are depicted schematically. The symbols used to denote each component monosaccharide within each glycan are described in the legend. Adapted from (Lowe et al. 2003).

There are two types of protein-attached carbohydrates – O- and N-glycans (Fig. 11). In O-glycans, saccharides are attached to the hydroxyl groups of amino acids. In N-glycans, terminal N-acetylglucosamine is linked to the amide group of asparagine, forming an aspartylglucosamine linkage. Since the hydroxyl group originally attached to C-1 of the N-acetylglucosamine residue is removed during formation of this linkage, the amino group is directly attached to C-1.

N-glycans can be classified into three different groups according to their structures: high mannose, hybrid and complex (Fig. 12). All three types contain a common structure “core”. This core portion is composed of di-N-acetylchitobiose and three mannose residues, in which the latter form branches. In high mannose oligosaccharides two to six more mannose residues are attached to this core (Fig. 12) (Parodi 2000).

Complex oligosaccharides always contain three mannose residues. The outer two α-mannose residues are linked to N-acetyllactoseamine (Fig. 12). This is followed by sialic acid residues or additional N-acetyllactosamine residues. Hybrid N-glycans contain more than three mannose residues, but also contain an N-acetyllactoseamine side chain which is attached to α1-3-linked mannose. This type of oligosaccharide is

formed when the high mannose oligosaccharide is partially processed and additional sugars are attached.

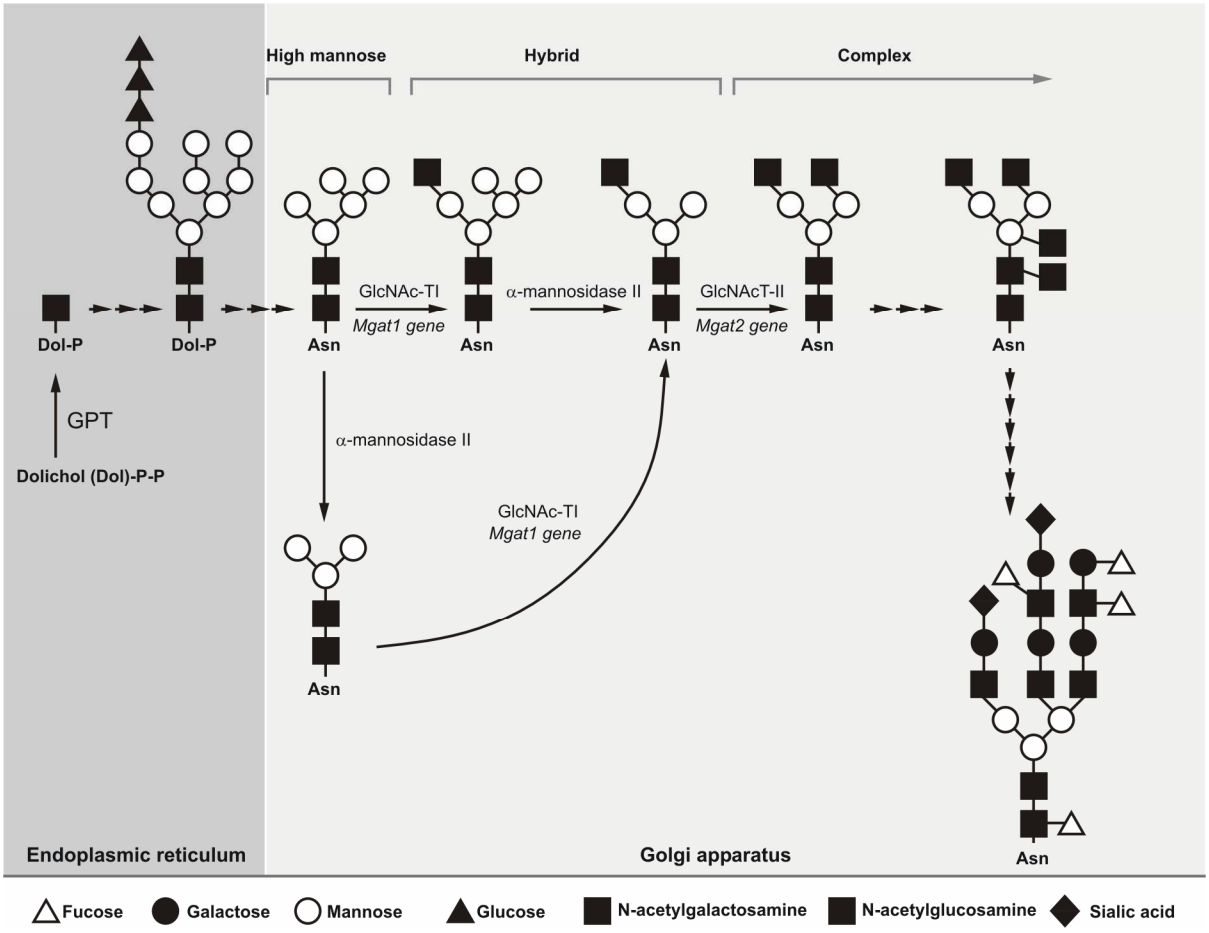

Figure 12. **Mammalian N-glycan synthesis.** The synthesis starts with dolichol pyrophosphate (Dol-P-P) and ends with final multiantennary structure. Potential branching patterns are made possible by the actions of several distinct glycosylttransferases (represented by multiple arrows without labels). The general category of each class of N-glycan is identified at top. The subcellular location where the steps of the synthesis occur is identified at the bottom. Symbols used to denote each component monosaccharide are identified at the legend the bottom. Adapted from (Lowe et al. 2003).

Complex, high mannose and hybrid types of N-glycan share a common core structure because all three types are synthesized from a common precursor. The biosynthesis of N-glycans is initiated by the addition of a precursor sugar which is attached to dolichol. This lipid-linked oligosaccharide is composed of nine mannoses, three glucoses and two N-acetylglucosamine residues. This dolichol-linked intermediate is then transferred as a block to an asparagine residue of a polypeptide. This step also occurs in the synthesis of complex N-glycans. The conversion of a

high mannose oligosaccharide to a complex one requires multiple steps, involving trimming and then addition of monosaccharides.

The processing of N-glycans is initiated by removal of three glucose residues in the endoplasmic reticulum (ER). After that, one α-2 linked mannose is removed and the glycoprotein is transported to the cis-Golgi. If the first step does not take place properly, a chaperone that recognizes malformed structures either forces the glycoprotein back into ER or subjects it to proteolytic digestion. After proper trimming the oligosaccharide is processed by α-mannosidase I to remove three more α1-2-linked mannose residues. The resultant oligosaccharide can now be an acceptor for N-acetylglucoseaminyltransferase I (Parodi 2002).

1.3.3. Enzymes associated with glycosylation

There are two types of enzymes associated with glycosylation – glycosyltransferases (GT) and glycosyl hydrolases/glycosidaes (GH). GT catalyze glycosidic bond formation using sugar donors containing a nucleoside phosphate or a lipid phosphate leaving group. Nowadays for *H. sapiens* 250 GT genes and around 250 GH genes are discovered.

The known GT from all species can be classified in 91 families and all GH can be classified in 115 families (Cantarel et al. 2009). GT plays an important role during embryogenesis and ontogenesis. This has been shown for many GT using knockout mice. Deficiency for many GT is associated with embryonic lethality and different disorders. Correspondingly, many human genetic defects in glycan formation are associated with diseases. These diseases were in some cases the result of the deficiency on GTs or they were associated with defects in glycan structure (Coutinho et al. 2003).

Biochemical and structural studies indicate that glycosyltransferases are partially segregated into distinct compartments within the secretory pathway. Most information relevant for the retention of glycosyltransferases within specific Golgi compartments is derived from experiments done with α2–6 sialyltransferase (ST6Gal-I), a β1-4 galactosyltransferase (GalT-I), and an N-acetylglucosaminyltransferase (GlcNAcT-I). Two models have been proposed to account for retention of specific glycosyltransferases to specific Golgi subcompartments. The first of these, termed the kin-recognition model, suggests that members of a set of glycosyltransferases have evolved to localize to a specific compartment will aggregate with themselves in

a multimeric complex, after arriving at the proper Golgi compartment. This hypothetical process would involve homo- and hetero-oligomerization through interactions between the stem regions and/or transmembrane segments of the glycosyltransferases in the aggregate (Colley 1997).

A second model proposes that each glycosyltransferase sorts itself into the proper Golgi location by virtue of the length of its transmembrane segment, which will retain the enzyme once it reaches the proper compartment during the enzyme's transit through the secretory pathway. This model was formulated largely on the basis of experiments involving ST6Gal-I, where the length of the membrane-spanning domain appears to play an important role in Golgi retention.

GHs are classified into families according to their amino acid similarities (Vocadlo et al. 2008). These enzymes also play an important role in N-glycoprotein synthesis, but they are not considered as important as GTs. However, deficiencies of GHs are associated with serious disorders in humans. Hereditary erythroblastic multinuclearity with a positive acidified-serum lysis test (HEMPAS) is an autosomal recessive disorder of glycosylation. HEMPAS is characterized by the lysis of red cell progenitors, hyperplasia of erythroid precursors, multinucleated erythroblasts and anemia. Red cells from HEMPAS patients contain defective glycoproteins. Using knockout mice it has been shown that deficiency on GHs such as α-mannosidase II and α-mannosidase IIx are associated with autoimmune diseases, dyserythropoiesis, spermatogenic failure and male sterility (Chui et al. 1997; Akama et al. 2002).

1.4. The aim of the study

The CD95 (APO-1/Fas)-mediated apoptotic pathway is one of the best-studied DR pathway. Significant progress has been achieved in the understanding of CD95-mediated events: DISC formation, caspase activation and Type I/Type II signaling. However, the role of CD95 modifications in signaling is still poorly understood. The aim of this study was to unravel the molecular mechanism how glycosylation of CD95 influences DISC formation and apoptosis induction. In particular, the question was which step of CD95 DISC formation is dependent on the proper glycostructure of CD95: the trimerization of CD95, the binding of the ligand or the maintenance of the fine structure of the CD95 DISC complex. Furthermore, another challenging question was whether CD95 glycosylation might be a reason for the differences in Type I and Type II signaling. Finally, based on previous reports on the degree of CD95 sialylation, which is a crucial factor for sensitivity and resistance of BJAB cells towards CD95-induced apoptosis, our goal also was to understand if this finding can be applied to a wide panel of cancer cell lines and to understand the exact molecular mechanism of this phenomenon.

2. MATERIALS AND METHODS

2.1. Materials

2.1.1. Chemicals

All chemicals for which the producer is not specified were purchased from the following companies: Fluka (Neu-Ulm, Germany), Merck (Darmstadt, Germany), Roth (Karlsruhe, Germany), Sigma-Aldrich (Steinheim, Germany) or Serva (Heidelberg, Germany).

2.1.2. Buffers and solutions

Name	Final concentration	Content
Triton X-100 Lysis buffer:	20 mM 137 mM 1% (v/v) 2 mM 1 mM 1 tablet	1.5 M Tris-HCl pH 7.4 NaCl Triton X-100 EDTA PMSF Protease inhibitor cocktail (Roche (Mannheim, Germany))
PBS:	137 mM 8.1 mM 2.7 mM 1.5 mM	NaCl Na_2HPO_4 KCl KH_2PO_4 pH 7.4
TBE (10x):	0.45 M 0.45 M 10 mM	Tris-Base Boric acid (“ice cold”) EDTA pH 8.3
Reducing sample buffer (2x):	20% (v/v) 3% (w/v) 20 mM 10% (v/v) 0.10 mg/ml	Glycerin SDS TrisHCl pH 6.8 β-Mercapto EtOH Bromophenol blue
Running buffer (SDS PAGE):	25 mM 0.19 M 1% (w/v)	Tris-Base Glycine SDS
Western blot transfer buffer:	25 mM 0.19 M 20% (v/v)	Tris Glycine MeOH
Western-blot strip buffer	62.5 mM 100 mM 2% (w/v)	Tris-HCl pH 8.0 β-Mercapto EtOH SDS
PBS-T solution	0.1% (v/v)	Tween 20 in PBS
ACK buffer (pH 7.2)	1 mM 0.5 mM 155 mM	$KHCO_3$ EDTA NH_4Cl
SSC buffer	3 M 0.3 M	NaCl Na_3-citrate
10 x HBS (pH 6.5)	1.4 M 100 mM 500 mM	NaCl KCl HEPES

	20 mM 22.2 mM	Na_2HPO_4 Glucose
ELISA Coating buffer (pH 9.6)	100 mM	Na_2CO_3
ELISA Washing buffer:	0.05 % (v/v)	Tween 20 in PBS
FACS buffer:	10 % (v/v)	FBS in PBS

2.1.3. Commercial kits

Name	Experimental purpose	Producer
BCA Assay	Protein content measurement	Pierce (Bonn, Germany)
Pro-Q Diamond Phosphoprotein Gel Stain	Selective staining of phosphoproteins in polyacrylamide gels	Invitrogen (Karlsruhe, Germany)
Reverse transriprion system	Synthesis of single-stranded cDNA from total or poly(A)+ isolated RNA	Promega (Mannheim, Germany)
High Fidelity PCR Kit	PCR	Roche (Mannheim, Germany)
Gel Extracton Kit	DNA fragments purification ready for direct use in all applications	Qiagen (Hilden, Germany)
Plasmid Maxi Kit	Preparative scale plasmid isolation	Qiagen (Hilden, Germany)
RNeasy Protect Mini Kit	Total RNA isolation	Qiagen (Hilden, Germany)
Trypsin EDTA solution	Detachment of the adherent cells/ cell culture	Gibco BRL (Karlsruhe, Germany) BRL
Western Lightning™ Chemiluminescence Kit	Enhancement of the chemiluminescence	Perkin Elmer (Jügesheim, Germany)
QuikChangeIIXL Site-Directed Mutagenesis Kit	Generation of the mutants	Stratagene (La Jolla, USA)

2.1.4. Biological materials

2.1.4.1. Bacterial strains and vectors

E. coli strains	Plasmid/ Resistance	Experimental purpose
XL10- Gold (Stratagene (La Jolla, USA))	pIRES-CD95/ ampicilin, pKEX-CD95/ ampicillin	Mammalian host protein expression vector containing an IRES element and - cDNA of human CD95. Generation of the CD95 glycomutants
DH5α	pKEX-CD95/ ampicillin pEGFP/ ampicillin, pIRES-CD95 and CD95 glycomutants.	Amplification of the plasmids

2.1.4.2. Eukaryotic cell lines

Cell line	Characteristics
Jurkat16 (Schneider et al. 1977)	Human T-cell leukaemia line
Jurkat A3	Human T-cell leukaemia line
CEM (Foley et al. 1965)	Human T-cell leukaemia line
SKW6. 4 (Ralph et al. 1983)	Human B lymphoblastoid line
Hut 78 (J Exp Med 1981;154:1403)	Human T cell lymphoma/ Derived from patient with Sezary syndrome
BJAB	EBV-negative Burkitt-similar lymphoblastoid human cell line
HeLa (Scherer et al. 1953)	Human cervix epitheloid carcinoma

2.1.5. Cell culture media

2.1.5.1.Media for bacteria

Medium type	Content
LB (Luria-Bertani)	10 g/l casein hydrolysate 5 g/l yeast extract 10 g/l NaCl pH = 7.2; adjusted with 1N NaOH Medium was supplemented with 30 µg/ml ampicillin for selection pressure
SOC medium (100ml)	2 ml of filter-sterilized 20% (w/v) glucose 98 ml of SOB medium
SOB Medium	20.0 g/l tryptone 5.0 g/l yeast extract 0.5 g/l of NaCl 10 ml/l of filter-sterilized 1 M $MgCl_2$ 10 ml/l of filter-sterilized 1 M $MgSO_4$

2.1.5.2. Cell culture media

Cell type	Culture medium
Peripheral blood human T cells	RPMI-1640 medium supplemented with 25 U/ml of IL-2
Jurkat16, Jurkat A3, CEM, SKW6. 4, Hut 78, BJAB	RPMI-1640 medium
HeLa	DMEM

Media were supplemented with 10% (v/v) FBS and 0.5% penicillin-streptomycin. All media and supplementary products were purchased from Gibco BRL (Karlsruhe, Germany).

2.1.6. Antibodies

2.1.6.1. Primary antibodies

Name (catalogue number)	Antigen	Serum / Isotype	Producer, Reference
Anti-GM130 (371-990) (CB1008)	GM130	Rabbit polyclonal IgG	Calbiochem (La Jolla, CA, USA)
Calreticulin (PA3-900)	Calreticulin	Rabbit polyclonal IgG	Affinity Bioreagents (Dublin, OH, USA)
Anti-α-Tubulin	α-Tubulin	Mouse monoclonal IgG1	Sigma-Aldrich (Steinheim, Germany)
Anti-CD95 (C20)	CD95	Rabbit polyclonal	Santa Cruz Biotechnology (Heidelberg, Germany)
Anti-APO-1	CD95	Mouse monoclonal IgG3	(Trauth et al. 1989)
Anti-CD95	CD95	Rabbit polyclonal	Santa Cruz Biotechnology (Heidelberg, Germany)
Anti-Caspase-8 (C15)	Caspase-8	Mouse monoclonal, IgG2b	(Scaffidi et al. 1997)
Anti- FADD (1C4)	FADD	Mouse monoclonal, IgG1	(Scaffidi et al. 2000)
Anti-cFLIP (NF6)	c-FLIP	Mouse monoclonal, IgG1	(Scaffidi et al. 1999)
Anti-Bid (44-433)	Bid p15	Rabbit polyclonal	Biosource (Invitrogen) (Karlsruhe, Germany)
Anti-Caspase-3	Caspase-3	Rabbit polyclonal	Cell Signaling (Danvers, MA, USA) (Danvers, MA, USA) Technology
Anti-ERK (MK12)	ERK	Rabbit polyclonal	BD Transduction Laboratories (Heidelberg, Germany)
Anti-Actin	Actin	Mouse monoclonal, IgG2a	Sigma-Aldrich (Steinheim, Germany)
Anti-JNK	JNK1	Rabbit polyclonal	Santa Cruz Biotechnology (Heidelberg, Germany)

2.1.6.2. Secondary antibodies

Name	Antigen	Producer
Secondary HRP-conjugated	Goat polyclonal IgG anti-rabbit IgG	Santa Cruz Biotechnology (Heidelberg, Germany)
Secondary HRP-conjugated	Donkey polyclonal IgG anti-goat IgG	Santa Cruz Biotechnology (Heidelberg, Germany)
Secondary HRP-conjugated	Goat polyclonal IgG anti-mouse IgG	Santa Cruz Biotechnology (Heidelberg, Germany)
Secondary HRP-conjugated	Goat polyclonal IgG anti-mouse IgG	Santa Cruz Biotechnology (Heidelberg, Germany)
Alexa-594	Goat polyclonal anti-mouse IgG	Molecular Probes (Invitrogen) (Karlsruhe, Germany)
Alexa 488	Sheep polyclonal anti-rabbit IgG	Molecular Probes (Invitrogen) (Karlsruhe, Germany)

2.1.7. Chemical reagents and antibodies used for cell treatment

Name and abbreviation	Final oncentration range	Stock solution	Producer
Sodium azide (Az)	1-100 µg/ml	1 mg/ml in H_2O	Sigma-Aldrich (Steinheim, Germany)
Tunicamycin	2 µg/ml	200 µg/ml	Calbiochem (La Jolla, CA, USA)
DMM	2 mM	In H_2O	Calbiochem (La Jolla, CA, USA)
N-glycosidase F	10 U	In H_2O	Roche (Mannheim, Germany)
VCN	100 mU	In PBS	Sigma-Aldrich (Steinheim, Germany)
Staurosporine	1 µM	1 mM in DMSO	Sigma-Aldrich (Steinheim, Germany)
Puromycin	1 µg/ml	10 mg/ml in H_2O	Sigma-Aldrich (Steinheim, Germany)

2.1.8. Fluorescent probes

Name and abbreviation	Usage	Final concentration	Stock solution	Producer
Propidium iodide (PI)	Plasma membrane permeability indicator	5 µM	2 mM in PBS	Sigma-Aldrich (Steinheim, Germany)
DAPI	Detection of single nucleic acid molecules	0.125 µg/ml in 2x SSC	0.25 mg/ml in H_2Odd	Sigma-Aldrich (Steinheim, Germany)

Generally all stock solutions were stored as aliquots at –20 ^{o}C. PI stock solution was stored at 4 ^{o}C.

2.1.9. Molecular biological materials

2.1.9.1. Primers

Name	Primer sequence (5'- 3')
N118QF	GACATGGCTTAGAAGTGGAAATACAGTGCACCCGGACC
N118QR	CTGTACCGAATCTTCACCTTTATGTCACGTGGGCCTGG
N136QF	ACCAAGTGCAGATGTAAACCAAACTTTTTTTGTCAGTCTACTGTATGTGAACA
N136QR	TGTTCACATACAGTAGACTGACAAAAAAAGTTTGGTTTACATCTGCACTTGGT'
T214QF	GAAAACCAAGGTTCTCATGAATCTCCACAGTTAAATCCTGAAACAGTGGCAATAAAT
T214QR	ATTTATTGCCACTGTTTCAGGATTTAACTGTGGAGATTCATGAGAACCTTGGTTTTC
N223QF	TTAAATCCTGAAACAGTGGCAATACAGTTATCTGATGTTGACTTGAGTAAAT
N223QR	ATTTACTCAAGTCAACATCAGATAACTGTATTGCCACTGTTTCAGGATTTAA
FasIF	ATGCTGGGCATCTGGACCCT
FasIR	GCCATGTCCTTCATCACACAA
FasIIF	CATGGCTTAGAAGTGGAAAT
FasIIR	ATTTATTGCCACTGTTTCAG
FasIIIF	AAATTTATCTGATGTTGACT
FasIIIR	TCTAGACCAAGCTTTGGATTTC

All FasXXX primers are taken from (Cascino et al. 1995).

2.1.10. Instruments

Name	Producer
Semi-Dry blotting system: - Power supply, Consort E865 600V-500mA - Semi-dry transfer cell Trans-Blot SD	Bio-Rad (München, Germany)
Laminar chambers SG600	Baker Company (Maine, USA)
Flow cytometers: FACScan, FACSCalibur and FACSCantoII	BD Transduction Laboratories (Heidelberg, Germany)
Agarose gel electrophoresis apparatus	Gibco BRL (Karlsruhe, Germany) BRL
Water baths	Kotterman, B. Braun
Thermostated hot-block 5320	Eppendorf (Wesseling-Berzdorf, Germany)
Thermomixer Compact	Eppendorf (Wesseling-Berzdorf, Germany)
Thermocycler DNA Engine DYAD	MJ Research (Ramsey, Minnesota, USA)
Light microscope ID 02	Zeiss (Göttingen, Germany)
Fluorescence microscope	Leica (Wetzlar, Germany)
Confocal microscope	Leica (Wetzlar, Germany)
CO_2-cell culture incubator	Forma Scientific (Thermo) (Dreieich, Germany)
Microwave oven HMG 730B	Bosch (München, Germany)

Polyacrylamide gel electrophoresis apparatus PROTEAN II Cell	Bio-Rad (München, Germany)
Electrophoresis power supply PS 500	Renner (Dannstadt - Schauernheim, Germany)
Bacteria culture incubator/shaker CH-403	Infors AG (Bottmingen, Switzerland)
Spectrophotometer, BioPhotometer	Eppendorf (Wesseling-Berzdorf, Germany)
Quartz cuvettes Suprasil	Hellma (Müllheim, Germany)
Developing system for Roentgen films Curix 160	Agfa (Mortsel, Belgium)
Gel documentation system	Bio-Rad (München, Germany)
Analytical and precision balances	Sartorius (Göttingen, Germany)
Neubauer cell-counting chamber	Brand (Wertheim Germany)
Centrifuges: - Biofuge Fresco 17 - Biofuge A - Megafuge 3. 0R - Sorvall Evolution RC	 Heraeus (Hanau, Germany) Heraeus (Hanau, Germany) Heraeus (Hanau, Germany) Kendro (Langenselbold, Germany)

2.1.11. Software

The following software was used: Microsoft Office, Adobe Photoshop 9.0, CellQuestPro4.0, BioEdit 5.0.9, CSS-Palm2, NetPhos 2.0, NetPhosK 1.0, NetCGlyc 1.0, CSS-Palm 2.0, NetNGlyc 1.0, NetOGlyc 3.1.

2.2. Methods

2.2.1. Standard procedures for eukaryotic cell cultures

2.2.1.1. Cell culture

All cell lines were propagated at 37^{o}C in an incubator with a humidified 5% CO_2 atmosphere. Cells were grown as suspension culture and maintained by addition or replacement of fresh medium (every 2-3 days). Cell density was adjusted to 1.0-2.5 x 10^5 cells/ml and monitored with the use of a Neubauer cell counting chamber. Cells were cultured in the type of medium specified before (2.1.5.2.).

2.2.1.2. Maintenance of cell culture stocks

To maintain genetically unchanged stocks of cell lines, the cells were stored in liquid nitrogen (-196^{o}C). The aliquots were thawn according to need.

2.2.1.2.1. Freezing cells

Cells (1-2 x 10^6 cells/ml) were centrifuged for 5 min at 1500 rpm, 4^{o}C, cooled on ice and suspended in FBS supplemented with 10% DMSO. After transfer into 2 ml cryovials the cell suspensions were stored overnight at -20^{o}C, transferred to -80^{o}C for 2-3 days, and finally placed into liquid nitrogen (-196^{o}C) for further storage. A slow gradient of lowering freezing temperatures should limit the extent of possible damage.

2.2.1.2.2. Thawing cells

The thawing procedure is characterized by a rapid increase in temperature and fast exchange of culture medium in order to avoid toxic effects of the high DMSO content. Directly after thawing, cells were transferred into 25 ml of pre-warmed culture medium and centrifuged for 5 min at 1500 rpm. Cells were then suspended in 25 ml of fresh medium for further culture.

2.2.1.3. Isolation and culture of human peripheral T cells

Human peripheral T cells were prepared by Ficoll-Plaque density centrifugation, followed by rosetting with 2-amino-ethylisothyo-uronium-bromide-treated sheep red blood cells. 1 ml of heparin (Braun) was added to 500 ml of whole blood to inhibit clotting. 30 ml of blood was carefully layered onto 15 ml of pre-warmed (37^{o}C) Ficoll solution (Biochrom) and centrifuged (2420 rpm, 20 min, RT, without breaks). The

leukocytes (a ring between the phases) were collected and washed 2 times with pre-warmed, sterile PBS or RPMI medium (500 g, 10 min, RT, slow breaking - ”6”) and suspended in 200 ml of RPMI medium. The cell suspension was depleted of macrophages and monocytes (*i. e.* monodepletion) by their adhesion to plastic culture dishes (two 500 ml cell culture flasks) after 1 hour of incubation in a cell culture incubator. Non-adherent cells were collected, spun down (500 g, 10 min, RT) and suspended in RPMI medium (cell density: 1 x 10^7 cells/ml). Next, cells were mixed in a 2:1 ratio with 4% AET-erythrocytes for a “rosetting” reaction. The mixture was centrifuged (500 g, 10 min, RT, slow breaking – “2”). The pellet (containing “rosettes”) was resuspended, carefully layered on top of prewarmed Ficoll solution and centrifuged for 20 min at 2420 rpm and RT (without breaks). The pellet, consisting of T cells and erythrocytes, was washed with prewarmed PBS or medium (500 g, 10 min, RT, slow breaking - ”6”). The erythrocytes were lysed by addition of 4x volume (acc. to the pellet) of ACK buffer. The lysis is indicated by a color change of the mixture from turbid light red to clear dark red. Subsequently, cells were washed (2 times) with prewarmed PBS or medium, resuspended in 50 ml of RPMI, counted and diluted to a concentration of 2 x 10^6 cells/ml. For activation, resting T cells were cultured at a concentration of 2 x 10^6 cells/ml in the presence of 1 µg/ml PHA for 16 h. T cells were then cultured in RPMI medium supplemented with 10% FCS and 25 U/ml IL-2 for six days (day 6 T cells). All experiments were performed with T cells isolated from at least three different healthy donors.

2.2.2. Cell biological methods

2.2.2.1. Transfection of eukaryotic cells

2.2.2.1.1. Transfection with Fugene for generation of stable HeLa cell lines

HeLa cells were grown to 50% confluence in 10 cm cell culture dishes. 5 µg of plasmid DNA were mixed with 100 µl of OPTIMEM. The volume of Fugene was calculated with the ratio 1 µg: 3 µl (DNA:Fugene). 15 µl of Fugene were added to 300 µl of OPTIMEM and incubated for 5 minutes. Next, DNA and Fugene in OPTIMEM were mixed and incubated for another 15 minutes. Afterwards the mix was added to the cells after the medium has been changed. The cells were harvested after 36-48 hours.

2.2.2.1.2. $Ca_3(PO_4)_2$ method

HeLa cells were grown to 70-80% confluence in 10 cm cell culture dishes. 20 µg plasmids DNA were mixed with 1 ml HBS and 50 µl 2.5 M $CaCl_2$ were added. After 15 min of incubation the mix was added to the cells together with fresh media. Cells were harvested after 36 hours.

2.2.2.2. Analysis of neuraminidase-treated cells

Cells were harvested and washed in digestion buffer (20 mM Hepes, pH 7.0, 140 mM NaCl). The cells were then resuspended in digestion buffer at a volume of 1ml and at a density of 1 x 10^7 cells/ml. 100 mU/ml of Neuraminidase from *Vibrio cholerae* were added to the cells. Cells were incubated for 1 hour at 37^{o}C, 5% CO_2, and then washed with complete medium. Control cells were treated with digestion buffer only. Cells were analyzed for sensitivity to CD95-mediated apoptosis as described later. Protein lysates were also prepared from 1 x 10^7 cells and analyzed by Western blot.

2.2.1.3. Inhibition of glycosylation

The the mannosidase I inhibitor, 1-deoxymannojirimycin (DMM) was dissolved in water. The inhibitor tunicamycin, which completely inhibits N-glycosylation was dissolved in DMSO. Inhibitors were added at final concentrations of 2 mM for DMM and 2 µg/ml for tunicamycin. After a 24 h incubation, fresh glycosidase inhibitor was added to the cells at the same final concentrations. To control cells, only an equivalent amount of water or DMSO was added. The cells were harvested after 48 h, and surface expression of CD95 was measured by FACS. Protein lysates were prepared for Western blot analysis and the cells were tested for sensitivity to CD95-mediated death as described later.

2.2.2.4. Cell death analysis

The samples were analyzed using flow cytometric methods. Dying cells shrink and become more granular, resulting in a lower forward scatter index (FSC) and an increased side scatter index (SSC), respectively. Loss of membrane impermeability can be monitored by the use of propidium iodide (PI) staining (SSC/strength of PI emission signal). PI is not penetrating living cells but stains nuclei of dead cells

fluorescent red. Briefly, cells were centrifuged at 2000 rpm for 5 min (Biofuge, Heraeus (Hanau, Germany)), washed with PBS, suspended in PBS and stained by mixing with the equal volume of PI solution (5 µg/ml in PBS). Next, cells were immediately subjected to FACS analysis (PI excitation wavelength is 535 nm, emission wavelength 617 nm). Experimental results are presented as percentage of "specific cell death", calculated according to the following formula:

$$"Specific\ cell\ death"[\%] = \left(\frac{dead\ cells\,[\%] - dead\ cells\,[\%]_{(untreated\ control)}}{100 - dead\ cells\,[\%]_{(untreated\ control)}} \right) * 100$$

2.2.2.5. Cell surface staining

To analyze the surface expression of CD95, 5 x 10^5 cells were resuspended in 100 µl of FACS buffer and incubated with 10 µg/ml of anti-APO-1 antibodies or with FII23 antibodies as isotype control for 15 min on ice. The cells were washed with FACS buffer, centrifuged and resuspended in 100 µl of FACS buffer containing PE-conjugated anti-mouse IgG antibody and incubated on ice for 15 min. The cells were washed with FACS buffer and resuspended in 300 µl of FACS buffer containing 1 µg/ml PI. The staining was analysed by flow cytometry. The population was gated on living cells and the staining of isotype control was compared to the surface staining with anti-APO-1 antibody.

2.2.2.6. Immunostaining of cultured cells

5 x 10^5 HeLa cells were plated on autoclaved 12-mm coverslips into 12 -well plates and were grown overnight. Next morning they were washed with PBS and fixed with 3% PFA in PBS. Afterwards they were washed with PBS for 3 times. Membranes were permeabilized for 5 min with 0.1% Triton X-100 and washed 3 times with PBS. Blockage of uspecific signals was done with different 10% serums dependent of secondary antibodies. Staining with primary antibodies diluted in PBS was performed in 50 µl for 1 hour at RT. Cells were washed 3 times with PBS for 5 min. Next, cells were stained with diluted in PBS secondary antibodies for 1 hour and washed 3 times with PBS. Nuclei were stained with DAPI for 5 minutes and cells were washed with PBS. Last, cells were put to the objective glasses with Fluoromount G mounting media. Stainings were analyzed by fluorescence and confocal microscopy.

2.2.3. Biochemical methods

2.2.3.1. Western Blot and SDS-PAGE

Cells were lysed in TritonX-100 lysis buffer and protein concentration was measured by BCA Assay (Pierce (Bonn, Germany), USA). Aliquots of cell lysates were resolved by SDS-PAGE (180 V, 25 mA, 1 hour), transferred onto nitrocellulose membranes (Pharmacia, USA) using a semi-dry system (transfer conditions: 0.5 mA/cm^2; 2 h) and blocked by 1 hour washing in blocking solution (5 % powdered milk or 5% BSA in PBS-T). Blots were then incubated with the respective primary antibodies (suspended in 1% milk or 3% BSA in PBS-T) (2 h at room temperature or overnight at 4^{o}C) and washed (3 x 15 min) with PBS-T solution. After staining with horseradish peroxidase-conjugated secondary antibodies (1 h at room temperature) and washing with PBS-T solution (3 x 15 min), the signal was detected by enhanced chemiluminescence using Western Lightning Chemiluminescence Reagent (PerkinElmer, USA) according to the manufacturer's instructions. Signal intensities were quantified by standard scanning densitometry with the NIH Image program, version 1. 36b.

Separation Gel, 10% acrylamide (20ml)

Reagent stock	Volume (ml)
30% Acrylamide mix	6.7
1.5 M TrisHCl (pH 8.8)	5
10% SDS	0.2
10% APS	0.2
TEMED	0.008
H_2O	7.9

Stacking Gel (5ml)

Reagent stock	Volume (ml)
30% Acrylamide mix	0.83
1.5 M TrisHCl (pH 6.8)	0.68
10% SDS	0.2
10% APS	0.2
TEMED	0.008
H_2O	3.4

2.2.3.2. Preparation of total cellular lysates

1 x 10^8 cells were washed twice in 1 x PBS and subsequently lysed in buffer A (20 mM Tris/HCl, pH 7.5, 150 mM NaCl, 2 mM EDTA, 1 mM phenylmethylsulfonyl fluoride (Sigma-Aldrich (Steinheim, Germany)) protease inhibitor cocktail (Roche

(Mannheim, Germany), Switzerland), 1% Triton X-100 (Serva, Germany) and 10% glycerol) (stimulation condition) or lysed without treatment (unstimulated).

2.2.3.3. N-glycosidase F treatment of protein lysates

For N-glycosidase F treatment 1 x 10^7 cells were lysed in buffer A and, subsequently the total cellular lysates were treated with N-glycosidase F following the protocol by the manufacturer.

2.2.3.4. DISC analysis by immunoprecipitation and Western Blot

1 x 10^8 cells were treated with 1 µg/ml of anti-APO-1 antibodies at 37℃ for indicated periods of time, washed twice in 1 x PBS and subsequently lysed in buffer A (stimulation condition) or lysed without treatment (unstimulated). The CD95 DISC was immunoprecipitated overnight with 2 µg of anti-APO-1 and 30 µl protein A sepharose beads. Protein A sepharose beads were washed five times with 20 volumes of lysis buffer. The immunoprecipitates were analyzed on 8, 10 and 12 % PAAG. Subsequently, the gels were transferred to Hybond nitrocellulose membrane (Amersham Pharmacia Biotech., Germany), blocked with 5% nonfat dry milk in PBS/Tween (PBS plus 0.05% Tween 20) for 1 h, washed with PBS/Tween, and incubated with the primary antibodies in PBS/Tween at 4℃ overnight. Blots were developed with a chemoluminescence method following the manufacturer's protocol (Perkin Elmer (Jügesheim, Germany) Life Sciences, Germany).

2.2.3.5. Enzyme-linked immunosorbent assay (ELISA)

Flexible 96-well plates from BD Transduction Laboratories (Heidelberg, Germany) (USA) were coated with 100 µl of anti-CD95 (Abcam (Cambridge, Germany)) antibody in 0.05 M carbonate-bicarbonate buffer pH 9.6 (CBB) at 4℃ overnight. Then the plates were washed 3 times with distilled water, blocked with 200 µl of PBS containing 3% bovine serum albumin (BSA) at RT for 2 hours, which was followed by washing 3 times with PBS containing 0.5% Tween 20 (PBS-T). 100 µl of total cell lysates were added to each well, which was followed by incubation at RT for 1 h. After incubation, the plates were washed 3 times with PBS-T. This was followed by addition of 100 µl of peroxidase-conjugated goat anti-mouse IgG antibody (Jackson ImmunoResearch Laboratories) diluted at 1:5000 in PBS-1% BSA. The plates were incubated for 1 h at 4℃. After incubation, the plates were washed 3 times with

PBS-T and then the reaction was revealed with 100 µl of OPD 0.4 mg/ml (Sigma-Aldrich (Steinheim, Germany)) in 0.05 M phosphate-citrate buffer, pH 5.0 solution for 10-20 min at room temperature. After stopping the reaction with 100 µl of 3N H_2SO_4, the plates were read with an ELISA reader (Wallac, Gaithersburg, USA) at 490 nm.

2.2.4. Methods of molecular biology

2.2.4.1. Preparative scale isolation of plasmid DNA

The purification of plasmid DNA was performed with the Plasmid Maxi or Mini Kit (Qiagen (Hilden, Germany)). Bacteria containing the transformed plasmid were cultured in 300 ml LB medium containing 50 µg/ml ampicillin, overnight at 37ºC in an incubator (300 rpm). The next day, the bacteria were harvested by centrifugation at 6000g for 15 min at 4ºC. After discarding the supernatant, the bacterial pellet was resuspended in 10 ml of the supplied buffer P1. To lyse the cells, 10 ml of buffer P2 were added to the samples, mixed by inverting the tube 4-6 times, and incubated at RT for 5 min. To stop the lysis, 10 ml of chilled buffer P3 was added, mixed well, incubated on ice for 20 min, and then centrifuged at 13000g. The QIAGEN (HILDEN, GERMANY)-tip 500 columns were equilibrated by applying 10 ml of buffer QBT, and the column was allowed to drain by gravity. The supernatant containing the plasmid was filtered through a filter paper into the column and allowed to enter the column by gravity. The column was washed 2 times with 30 ml of buffer QC. To elute the plasmid DNA, 15 ml of buffer QF was applied to the column and the eluate was collected into a fresh tube. The DNA was precipitated by adding 0.7 volumes (10.5 ml) of isopropanol, followed by centrifugation at 4ºC at 13000 g for 30 min. The DNA pellet was washed with 5 ml of 70% ethanol and centrifuged again at 4ºC for 15 min. After pouring off the ethanol, the pellet was dried at RT and then resuspended in the required amount of sterile water.

2.2.4.2. Preparation of competent bacteria

For preparation of competent bacteria, 10 ml of an overnight culture of DH-5α *E. coli* were inoculated into 300 ml LB-media and further cultured at 37℃ in a shaker until the OD_{600} = 0.6. The bacterial culture was cooled down for 10 min and then pelleted by centrifugation at 4000 rpm at 4℃ for 5 min. The supernatant was discarded and the pellet was resuspended in 40 ml ice-cold 100 mM $CaCl_2$ buffer and incubated on ice for 10 min. This step was repeated two times. The pellet was

resuspended in 8 ml ice-cold 100 mM $CaCl_2$ buffer, incubated on ice for 10 min and aliquoted. Aliquots of 100 µl cell suspension were stored at -80℃ until usage.

2.2.4.3. Transformation of plasmid DNA in competent bacteria

Competent bacteria (100 µl) were thawn on ice and plasmid solution was gently mixed with the bacterial solution and incubated on ice for 30 min. After 30 min a heat shock was performed at 42℃ for 1 min. The reaction mix was transferred to a LB-agarose plate containing ampicillin (50 µg/ml). The plate was incubated overnight at 37℃.

2.2.4.4. Restriction enzyme digestion and ligation of DNA fragments

The plasmid DNA and DNA fragments were prepared by cutting it with suitable restriction enzymes for 1 h at 37 ºC in a following typical reaction:

Cutting of DNA fragments obtained by PCR	
5 µl	DNA fragment
1 µl	restriction enzyme
5 µl	buffer 10x
Add to 50 µl with H_2O	
Restriction digestion of plasmid DNA	
1 µg	plasmid
1 µl	restriction enzyme
5 µl	buffer 10x
Add to 50 µl with H_2O	

The fragments were separated on an agarose gel and purified out of the gel. For ligation, 1:3 molar ratio of vector:insert DNA fragments together with 1 µl of T4 DNA ligase were incubated in 1 x ligation buffer in a total volume of 20 µl at 16ºC overnight.

2.2.4.5. Measurement of DNA concentration

The concentration of DNA was determined by measuring the absorbance at 260 nm using a spectrophotometer. For measuring the absorbance, the spectrophotometer was first calibrated with 100 µl of H_2O. Then 5 µl of DNA sample was diluted with 95 µl H_2O, transferred to a quartz cuvette, and the absorbance was recorded at 260 and 280 nm. The concentration of DNA was calculated by using the following formula:

$$\text{Absorbance at 260 nm } (A_{260}) \text{ x dilution factor x 50 µg/ml = x µg/ml}$$

2.2.4.6. Site-directed mutagenesis

To generate CD95-glycomutants site-directed mutagenesis was performed. Asparagine and Threonine at 118, 136, 214 and 223 amino acid positions were changed to Glutamine by point mutations in CD95 cDNA using PCR. Primers were chosen by Stratagene Primer Designer program. All procedure was done according to manufacturer instructions and following typical reaction:

PCR mix	
19.2 µl	H_2O
3.0 µl	10x buffer
0.6 µl	dNTP mix
3.0 µl	Forward primer
3.0 µl	Reverse primer
0.6 µl	pKEX-APO-1 plasmid (5 ng/mkl)
0.6 µl	PfuUltra
Final volume 30 µl	

PCR program and DpnI treatment		
95℃	1 min	
95℃	50 sec	x18
60℃	50 sec	
68℃	9 min	
68℃	10 min	
37℃	pause	
+ 0.6 µl	DpnI	
37℃	60 min	

XL10-Gold cells were transformed according to manufacturer procedures with the ready glycomutants, plated to ampicillin agar-plates overnight. Five colonies for each mutant were picked up and cultured overnight in SOC media. Next morning plasmid was purified and presence of the mutations was analyzed by GATC sequencing service (GATC (Konstanz, Germany)).

2.2.4.7. Isolation of total cellular RNA

Total cellular RNA was isolated with the use of a RNeasy Protect Mini Kit l (Qiagen (Hilden, Germany)) reagent based method according to the manufacturer's protocol. Essentially, approximately 2 x 10^6 cells were pelleted (1500 rpm, 10 min) and suspended in 1 ml TRIzol reagent. After 10 min incubation at room temperature, 200 µl chloroform were added, the sample was mixed and further incubated for 3 min at room temperature. The mixture was centrifuged at 12000 rpm, at 4^{o}C for 15 min.

The aqueous phase was collected and transferred to a new tube avoiding contamination with the protein precipitates. The RNA was precipitated by addition of 500 µl isopropanol, incubation for 10 min at room temperature and subsequent centrifugation at 12000 rpm, 4^{o}C for 15 min. After the removal of isopropanol, the RNA was washed with 75% EtOH, centrifuged for 10 min at 12000 rpm, 4^{o}C, and dried at room temperature. RNA content was measured spectrophotometrically at a wavelength of 260 nm and purity was assayed by measurement of the 260/280 nm ratio.

2.2.4.8. Semi-quantitative RT-PCR and PCR

Total RNA was subjected to mRNA-specific RT-PCR reaction to synthesize cDNA (GeneAmp RNA PCR kit, Applied Biosystems, USA). The composition of the reaction mixture applied is listed below (volumes are given for one reaction vial). Synthesized cDNA was stored at -20^{o}C.

RT-PCR program and DpnI treatment	
95℃	5 min
4℃	2 min
42℃	60 min
70℃	15 min

cDNA synthesized in the RT-PCR step was used as a template for classical PCR reaction. The content of the reaction mixture is listed below (volumes are given for one reaction vial):

PCR program		
95℃	5 min	
95℃	60 sec	X30
52℃	60 sec	
68℃	60 sec	
68℃	10 min	
4℃	pause	

The PCR programs used are listed below. The PCR products were resolved using 1% agarose gel containing 0.001 % EtBr.

2.2.4.9. Purification of PCR products

Purification of PCR products prior to restriction enzyme digestion was done with the PCR purification kit (Qiagen (Hilden, Germany)). All centrifugation steps were performed at 10000 g in a conventional table top micro centrifuge. 5 volumes of

buffer PB, which is provided by the kit, were mixed with 1 volume of the PCR sample. A QIAquick spin column was placed in a 2 ml collection tube. The mixture was applied to the QIAquick column and centrifuged for 1 min. The flow through was discarded. 0.75 ml wash buffer PE from the kit was added to the QIAquick column and centrifuged for an additional 1 min to completely remove the residual buffer. The QIAquick column was transferred in a clean 1.5 ml microcentrifuge tube and the DNA was eluted. 50 µl H_2O was placed directly on the filter and left on the column for 2 min. Then the column was centrifuged for 1 min. DNA concentration was analyzed, using spectrophotometry.

2.2.4.10. Purification of DNA fragments from agarose gels

To obtain the desired DNA fragments, DNA was run in agarose gel and the gel was cut by using a scalpel and transferred to an eppendorf (Wesseling-Berzdorf, Germany) tube. DNA was purified according to the QIAquick Gel Extraction kit (Qiagen (Hilden, Germany)). Briefly, the DNA fragment was excised from the agarose gel. The gel slice was transferred in a tube and 3 volumes of buffer QG were added to 1 volume of gel. The mixture was incubated at 50ºC with shaking for 10 min to dissolve the gel. When the gel was dissolved completely, one gel volume of isopropanol was added to the mixture. The mixture was applied to a QIAquick column and centrifuged for 1 min. The flow-through was discarded and the QIAquick column was placed back in the same collection tube. The DNA was washed with 0.75 ml of buffer PE and centrifuged again for 1 min. The flow-through was discarded and the QIAquick column was centrifuged for an additional min and the QIAquick column was placed into a 1.5 ml eppendorf tube. DNA was eluted by adding 50 µl buffer EB to the center of the membrane and centrifuged for 1 min. DNA was stored at -20ºC before further use.

2.2.6. Bioinformatical methods

To find possible posttranslational modifications human CD95 protein sequence of the full-length receptor was submitted to several prediction programs on CBS Server of Center for Biological Sequence Analysis www.cbs.dtu.dk/services/). For prediction of palmitoylation sites CSS-Palm 2 web server has been used. Generic phosphorylation sites in CD95 have been predicted by NetPhos 2.0 server (www.cbs.dtu.dk/services/NetPhos/) (Blom et al. 1999) with a threshold of 0.5 (level

under which prediction considered as insignificant). Kinase specific phosphorylation sites have been predicted by NetPhosK 1.0 server (www.cbs.dtu.dk/services/NetPhosK/) (Blom et al. 2004) with a threshold of 0.5. C-mannosylation sites have been predicted by NetCGlyc 1.0 Server (www.cbs.dtu.dk/services/NetCGlyc/) (Julenius 2007) with a threshold of 0.5. Palmitoylation sites have been predicted by CSS-Palm 2.0 server (csspalm.biocuckoo.org/online.php) (Ren et al. 2008) with a threshold of 0.5. N-linked glycosylation sites have been predicted by NetNGlyc 1.0 server (www.cbs.dtu.dk/services/NetNGlyc/) with a threshold of 0.5. O-linked (GalNA) glycosylation sites have been predicted by NetOGlyc 3.1 server (www.cbs.dtu.dk/services/NetOGlyc/) (Julenius et al. 2005) with a threshold of 0.5.

3. RESULTS

3.1. CD95 from Type I and Type II cells shows a different protein modification pattern upon Western blot analysis

Type I cells are characterized by an increased amount of DISC formation in comparison to Type II cells despite similar CD95 expression levels on the cell surface (Fig. 6, see section 1.2.1.1.3 for details) (Scaffidi et al. 1998). A possible explanation for the difference in CD95 signaling in Type I and Type II cells could be that different posttranslational modifications or a splicing pattern of CD95 exist. To check this hypothesis CD95 expression levels and protein modification patterns in Type I and Type II cells were tested by Western blot analysis of total cellular lysates.

B lymphoblastoid SKW6.4, T leukemia Hut78 and B lymphoma BJAB cells were used as a model for Type I cells whereas Jurkat cells (subclone J16) and CEM cells served as a model for Type II cells, respectively (Scaffidi et al. 1998). Detection of CD95 was performed by anti-CD95 polyclonal antibodies C20 after Western blot (Schmitz et al. 2002). This analysis revealed significant differences in CD95 protein patterns between selected Type I and Type II cells (Fig. 13). Two different CD95 forms with corresponding molecular mass of 48 and 55 kDa were seen in Type I cells. However, only one form of the receptor with a molecular mass of approximately 50 kDa was detected in Type II cells.

Instead of 12% SDS-PAGE gels used in Fig. 13A 10% SDS-PAGE gels were also used to improve protein separation (Fig. 13B). As seen before two major bands in case of Type I cells (SKW6.4 and Hut78) as well as one major band in the case of Type II cells (JA3, J16, J27 and CEM) were observed. Thus, it has been found that there are different forms of CD95 receptor in Type I and Type II cells. An investigation of the origin for Type I/Type II CD95 signaling on the level of CD95 could, therefore, potentially explain the underlying cause for different sensitivity of cells towards CD95-induced apoptosis in these two types of cells.

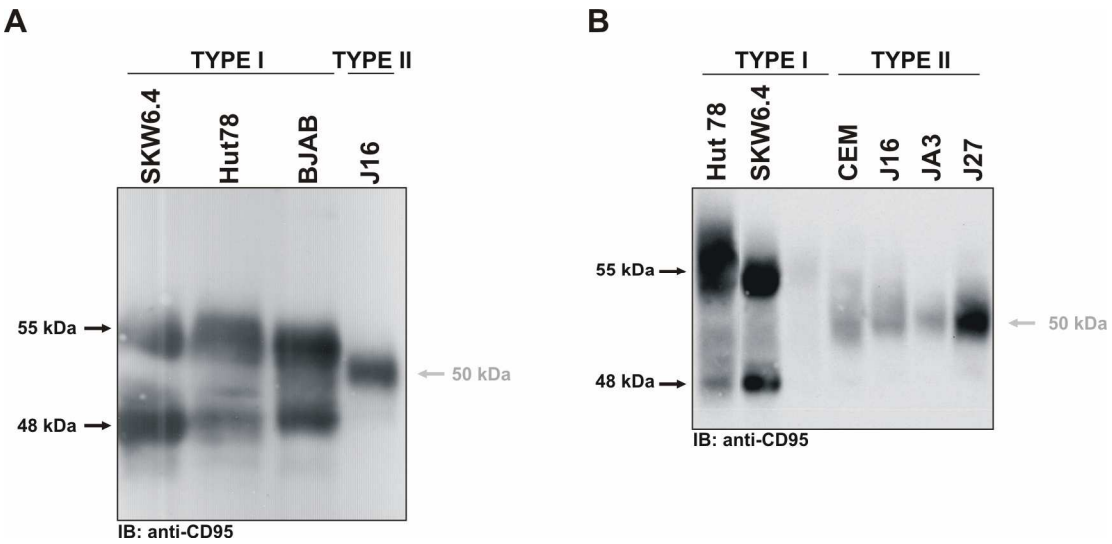

Figure 13. Different protein modification pattern of CD95 in Type I and Type II cells. A. CD95 protein patterns were analyzed in the total cellular lysates of SKW6.4, Hut78, BJAB and J16 cells on 12 % SDS-PAGE followed by Western blot with anti-CD95 polyclonal antibodies C20. **B**. CD95 protein modification patterns were analyzed in the total cellular lysates of SKW6.4, Hut78, J27, JA3, CEM and J16 cells on 10% SDS-PAGE followed by Western blot with anti-CD95 polyclonal antibodies C20. CD95 bands in Type I cells are indicated by black arrows, the CD95 band in Type II cells by a grey one.

3.2. Analysis of alternative splicing of CD95 in Type I and Type II cells

The presence of different splice variants of CD95 in Type I and Type II cells was investigated. Total mRNA was purified from Type I cells: BJAB, Hut78, SKW6.4 cells, primary T cells (day 6) and from Type II cells: J16 cells, primary T cells (day 1). RT-PCR analyses using three pairs of primers (Cascino et al. 1995) that amplify three different regions of the CD95 gene were performed (Fig. 14). The combination of these sets of primers is sufficient to identify different splice products.

RT-PCR analysis using primer pairs I and III revealed no differences in CD95 mRNA patterns between Type I and Type II cells. In all cells analyzed only one PCR product of 330 bp for primer pair I and III, respectively, was observed. RT-PCR analysis performed with primer pair II revealed one major band of 350 bp for all cell lines and an additional product in the region of 280 bp in Hut78 cells and day 1 primary T cells. This product was also observed in the other cell lines, but was barely detectable. Taken together no differences were detected between Type I and Type II

cells with different pairs of primers. Therefore, alternative splicing is not a reason for the different CD95 protein pattern in Type I and Type II cells.

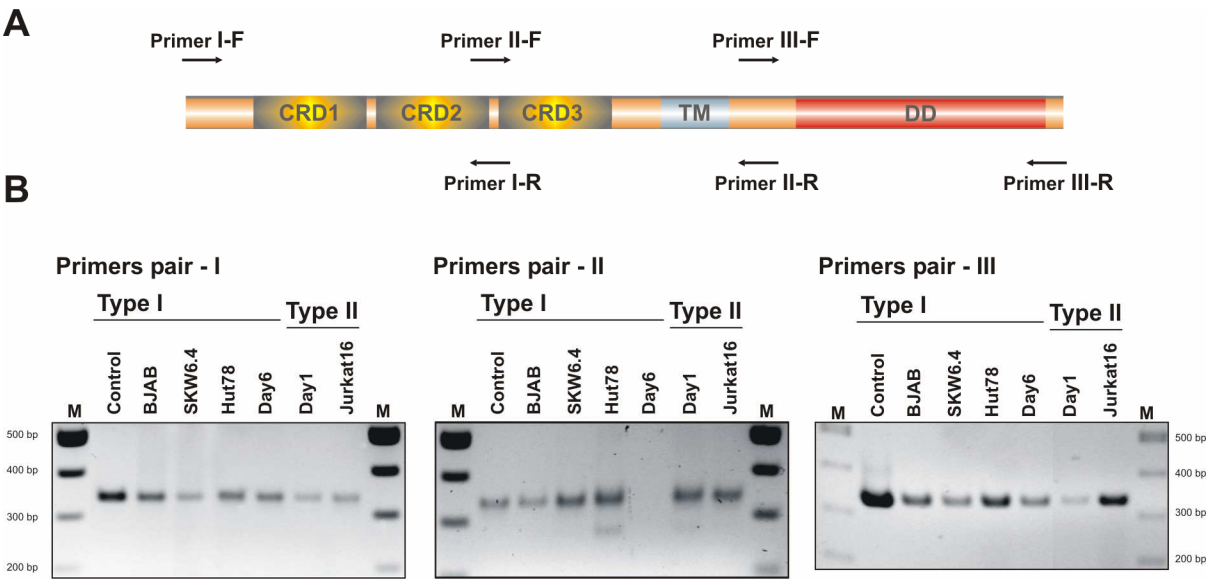

Figure 14. Analysis of alternative splicing of CD95 in Type I and Type II cell lines. **A**. Scheme of primer pairs for the analysis of possible splice variants of CD95 (adopted from (Cascino et al. 1995)). **B**. RNA was isolated from SKW6.4, Hut78, BJAB, primary T cells (day 1), primary T cells (day 6), J16 and CEM cells, reverse transcribed and amplified using primers depicted in A.

Another reason why different splicing could be ruled out was the transient overexpression of CD95 in HeLa and Cos1 cells transiently transfected with plasmid pKEX encoding the CD95 cDNA. In this case CD95 was expressed from a plasmid containing a complete CD95 gene without introns. Therefore, splicing could not take place. Nevertheless, two different forms of CD95 were observed upon Western blot analysis (Fig. 15). This indicates that the different bands of CD95 proteins in Type I and Type II cells do not result from alternative splicing. GFP was used as a control for transfection efficiency and as a negative control.

It was next analyzed whether posttranslational modifications of CD95 could be the reason for the presence of different forms of CD95 in Type I and Type II cells.

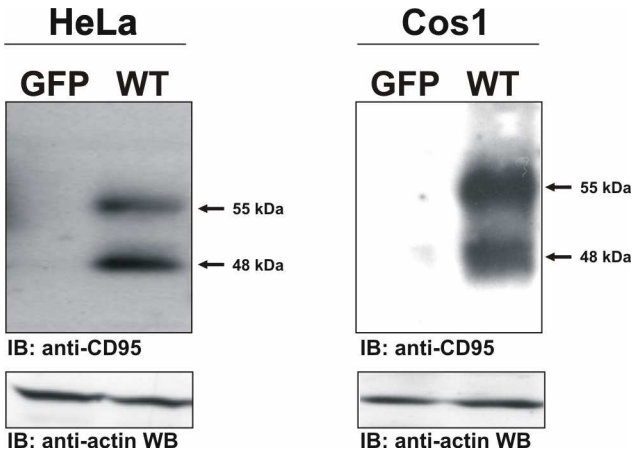

Figure 15. Transiently transfected HeLa and Cos1 cells overexpressing CD95 revealed the presence of two different forms of CD95. Plasmid pKEX encoding CD95 (Oehm et al., 1992) was transfected into HeLa cells as well as into Cos1 cells. Anti-CD95 Western blot analysis was performed to control protein expression. Anti-actin Western blot was used as a loading control.

3.3. *In silico* predictions of possible posttranslational modifications of CD95

Possible modifications of CD95 were investigated with prediction programs. As CD95 is a type I transmembrane protein the possibility for proteolytic cleavage, phosphorylation, palmytoilation, mannosylation and glycosylation was tested.

To find possible posttranslational modifications, the human CD95 protein sequence of the full-length receptor was submitted to several prediction programs on the CBS Server of the Center for Biological Sequence Analysis (www.cbs.dtu.dk/services/). For prediction of palmitoylation sites the CSS-Palm 2 webserver was used.

A possible explanation for the different observed CD95 protein modification patterns in Type I and Type II cells different posttranslational modifications or the presence of different splice variants of CD95 were considered.

CD95 was reported to be cleaved by MMP7 (Martilysin) as the first physiologically relevant protease that can specifically cleave CD95 (Strand et al. 2004). Cleavage of CD95 by matrix metalloproteinase-7 induces apoptosis resistance in tumor cells.

Microsequencing of the positions in CD95 cleaved by MMP7 revealed two sites in the N-terminal extracellular domain of CD95, important for preligand assembly of CD95. The resulting cleavage product of CD95 is several kDa smaller than

noncleaved CD95. MMP7 cleavage of CD95 results in reduced CD95 surface expression and decreased CD95-mediated apoptosis sensitivity of tumor cells. Treatment of MMP7-positive HT-29 tumor cells with MMP7-antisense oligonucleotides led to an increase in CD95-mediated apoptosis sensitivity (Strand et al. 2004).

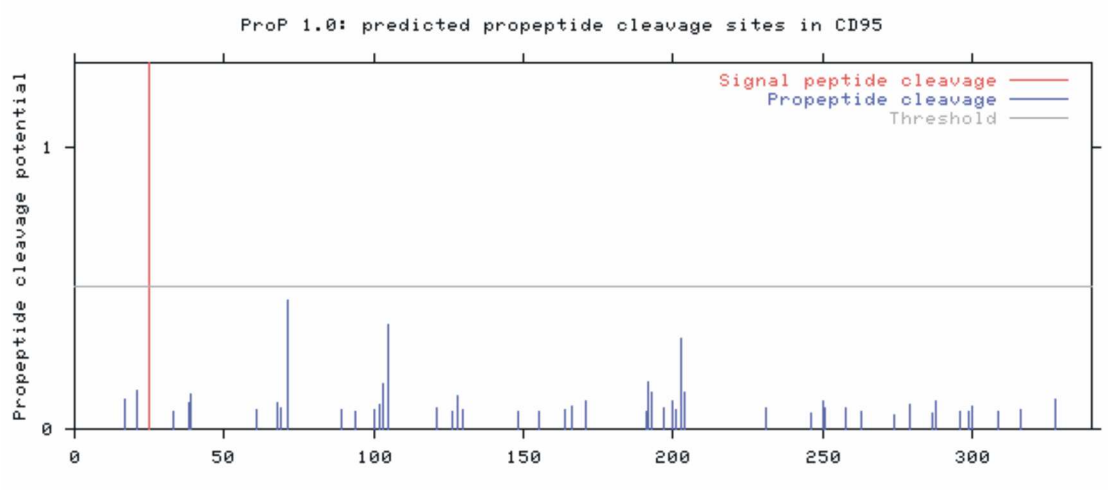

Figure 16. Prediction potential arginine and lysine propeptide cleavage sites in CD95. The output from PropP 1.0 is graphically represented.

The possibility of proteolitic cleavage of CD95 was predicted by ProP 1.0 Server (www.cbs.dtu.dk/services/ProP/) (Duckert et al. 2004) with a threshold of 0.5. Many potential arginine and lysine propeptide cleavage sites were found (Fig. 16). No proteases cleavage sites were found with the threshold equal or higher than 0.5. Therefore other reasons for the presence of two CD95 bands were checked.

3.3.1. Generic and kinase specific phosphorylation sites

Generic phosphorylation sites in CD95 were predicted by NetPhos 2.0 server (www.cbs.dtu.dk/services/NetPhos/) (Blom et al. 1999) with a threshold of 0.5. Results are summarized in Fig. 17. Bioinformatic analyses have shown that CD95 has many generic phosphorylation sites, which involve phosphorylation of Thr, Tyr and Ser residues.

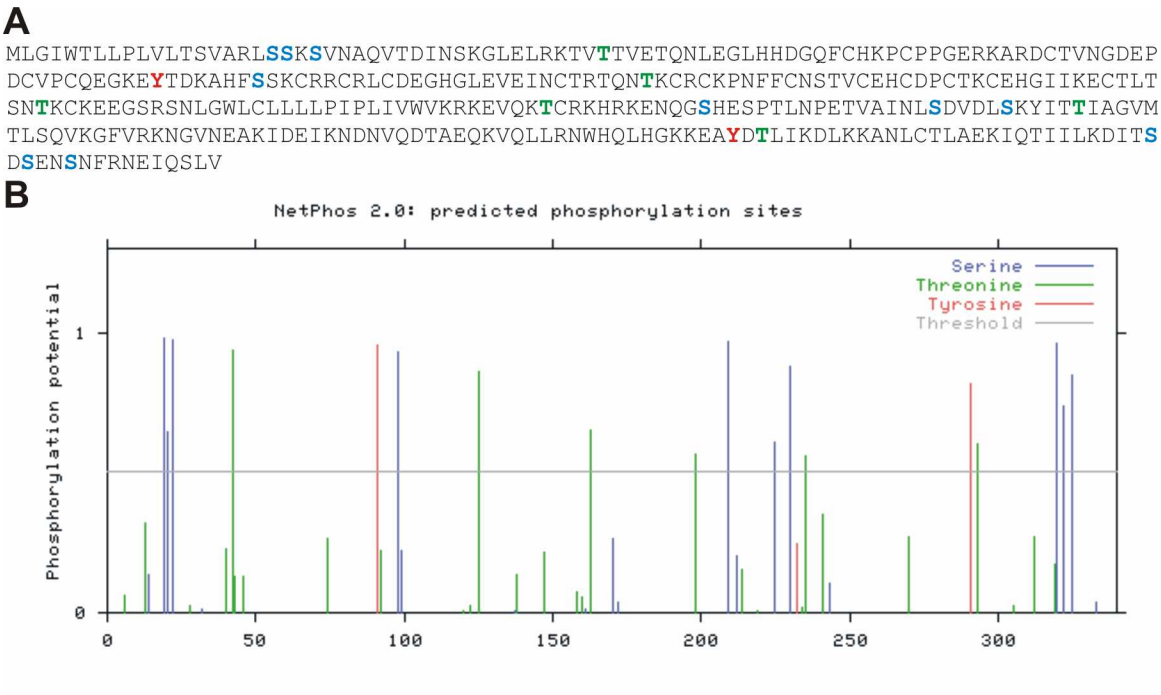

Figure 17. Prediction of generic phosphorylation sites in CD95. A. Sequence of human CD95 followed by an assignment field describing the predicted category for each residue. Residues having a prediction score above the threshold are indicated by 'S', 'T' or 'Y', respectively. **B**. Graphical representation of predictions with indicated scores generated by the server.

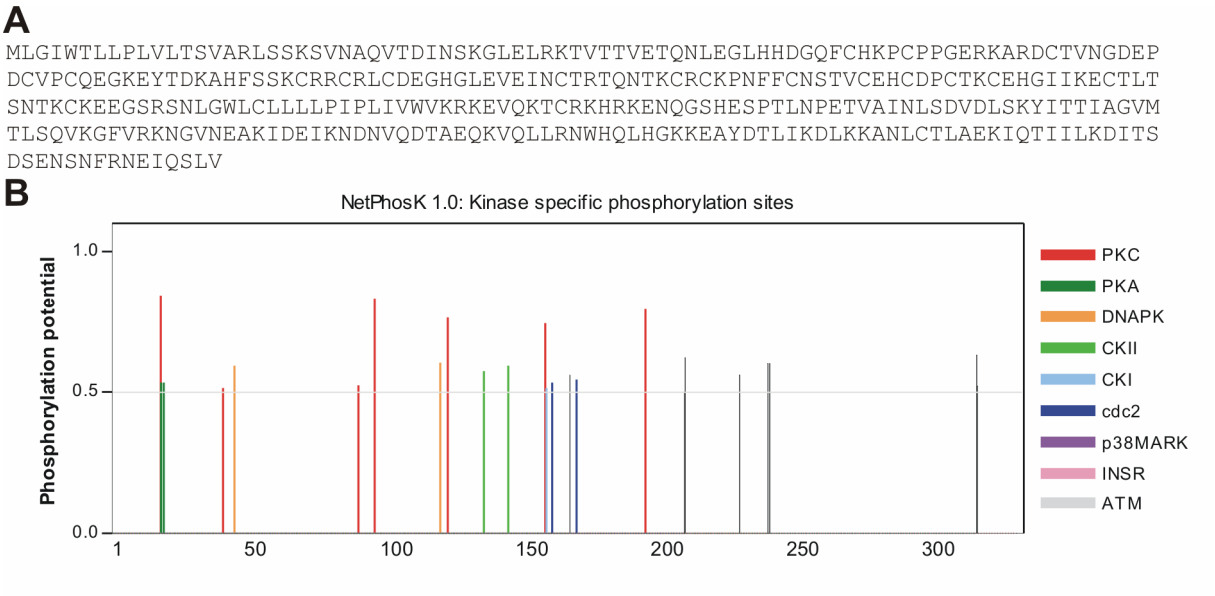

Figure 18. Prediction of kinase specific phosphorylation sites in CD95. A. Sequence of CD95. **B.** Potential kinase specific phosphorylaion sites with thresholds more than 0.5 were labeled with colors depicted on the right.

Kinase specific phosphorylation sites were predicted by NetPhosK 1.0 server (www.cbs.dtu.dk/services/NetPhosK/) (Blom et al. 2004) with a threshold of 0.5. Results are summarized in Fig. 18. Consistent with previous reports PKC, p38, CKI and CKII were revealed by this prediction. Nevertheless, there are a number of kinases, which have not been reported to be associated with CD95 signaling.

3.3.2. C-mannosylation, palmitoylation, N-linked and O-linked glycosylation sites

C-mannosylation sites were predicted by NetCGlyc 1.0 Server (www.cbs.dtu.dk/services/NetCGlyc/) (Julenius 2007) with a threshold 0.5. Results are summarized in Fig. 19. There are only four mannosylation sites predicted in CD95. Nevertheless, the probabilities for CD95 being mannosylated at these sites are low as their score were below the threshold.

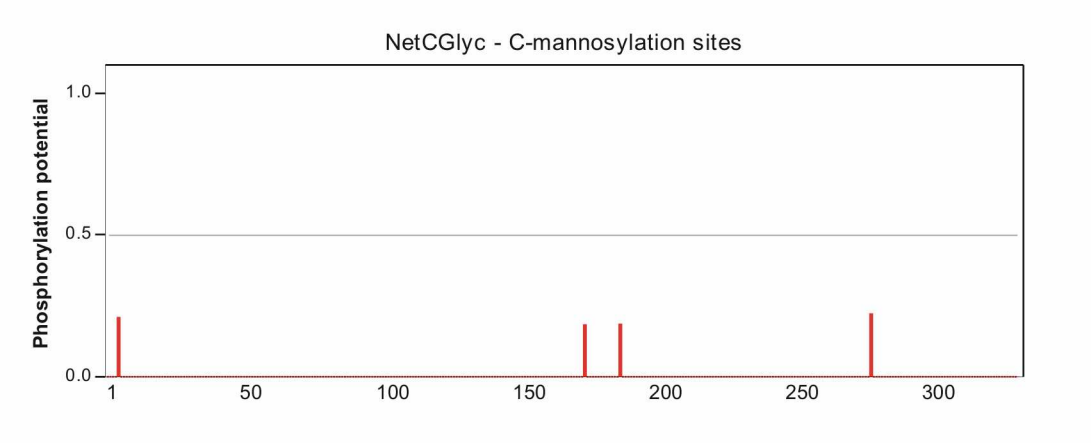

Figure 19. Prediction of C-mannosylation sites in CD95. The output from NetCGlyc is graphically represented.

Palmitoylation sites were predicted by CSS-Palm 2.0 server (csspalm.biocuckoo.org/online.php) (Ren et al. 2008) with a threshold of 0.5. Results are summarized in Fig. 20. There are many palmitoylation sites in CD95 predicted. Nevertheless only two of them have a high prediction score level and have a high probability to be palmitoylated (pos. 104 and 199).

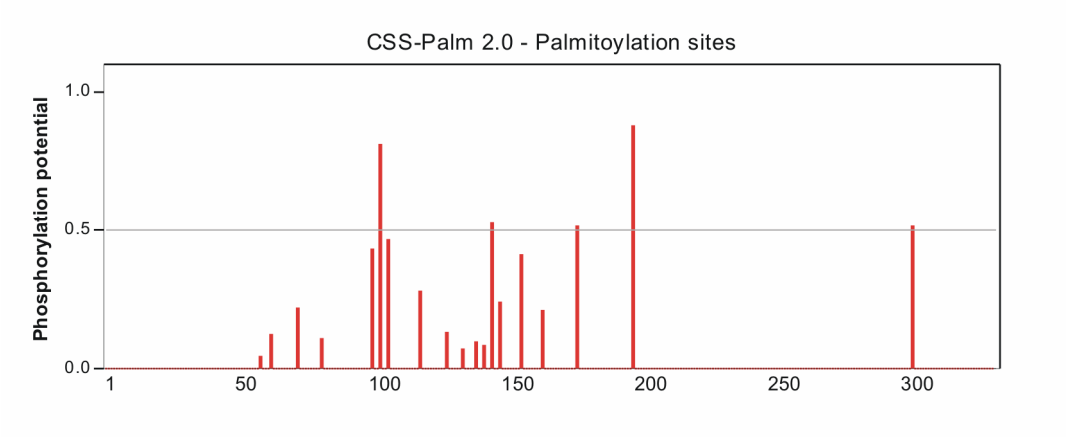

Figure 20. Prediction of palmitoylation sites in CD95. Potential phosphorylation sites are represented with indicated scores generated by server.

A

MLGIWTLLPLVLTSVARLSSKSVNAQVTDINSKGLELRKTVTTVETQNLEGLHHDGQFCHKPCPPGERKARDCTVNGDEP
DCVPCQEGKEYTDKAHFSSKCRRCRLCDEGHGLEVEI**NCT**RTQNTKCRCKPNFFC**NST**VCEHCDPCTKCEHGIIKECTLT
SNTKCKEEGSRSNLGWLCLLLLPIPLIVWVKRKEVQKTCRKHRKENQGSHESPTLNPETVAI**NLS**DVDLSKYITTIAGVM
TLSQVKGFVRKNGVNEAKIDEIKNDNVQDTAEQKVQLLRNWHQLHGKKEAYDTLIKDLKKANLCTLAEKIQTIILKDITS
DSENSNFRNEIQSLV

B

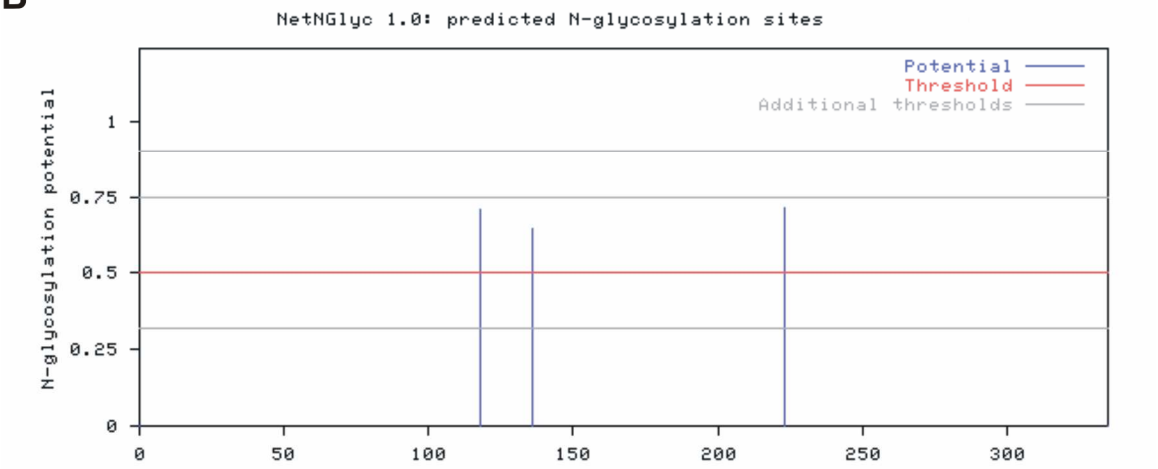

Figure 21. Prediction of N-linked glycosylation sites in CD95. A. Sequence of human CD95 followed by an assignment field describing the predicted category for each residue. Asn-Xaa-Ser/Thr sequons in the sequence are highlighted in blue. Asparagines predicted to be N-glycosylated are highlighted in red. If the residue was predicted not to be glycosylated, either because the score was below the threshold or because the residue was not Asn, then the position is not marked. Residues having a prediction score above the threshold are indicated by 'N'. **B**. Graphical representation of prediction with indicated scores generated by the server.

N-linked glycosylation sites were predicted by NetNGlyc 1.0 server (www.cbs.dtu.dk/services/NetNGlyc/) with a threshold of 0.5. Results are

summarized in Fig. 21. Bioinformatic analyses have demonstrated that there are only three putative N-linked glycosylation sites in CD95. Two in the extracellular domain (Asn118 and Asn136) and one in the intracellular domain (Asn223).

O-linked (GalNA) glycosylation sites were predicted by NetOGlyc 3.1 server (www.cbs.dtu.dk/services/NetOGlyc/) (Julenius et al. 2005) with a threshold of 0.5. Results are summarized in Fig. 22. Bioinformatic analysis demonstrated that there was only one O-linked glycosylation site with a high probability in CD95 (Thr214).

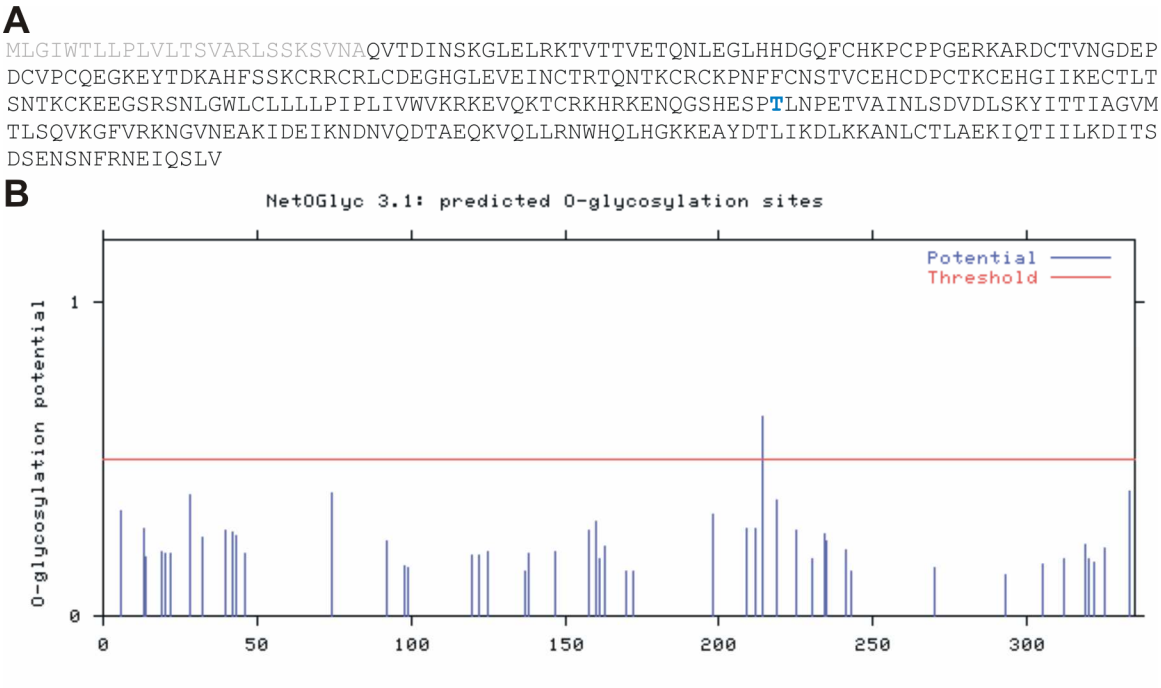

Figure 22. Prediction of O-linked glycosylation sites in CD95. A. Sequence of human CD95 followed by an assignment field describing the predicted category for each residue. Residues having a prediction score above the threshold are indicated by blue 'S' or 'T', respectively. **B**. Graphical representation of prediction with indicated scores generated by the server.

From all modifications, provided by bioinformatics analysis, our experimental efforts were concentrated mostly on glycosylation of CD95, because glycosylation might account for the significant shifts in molecular mass observed. Phosphorylation was also analyzed to a minor extent. Other modifications of CD95 and their role in CD95 signaling will have to be analyzed in future studies.

3.3. Phosphorylation is not a reason for several CD95 forms

According to the predictions CD95 has many potential phosphorylation sites. To analyze if the differences in the molecular mass of the two CD95 forms are due to phosphorylation HeLa cells stably overexpressing CD95 (HeLa-CD95 cells) were used. Under these conditions two bands of CD95 are detected. CD95 was immunoprecipitated from cellular lysates of HeLa in the presence of the phosphate inhibitor (sodium vanadate) using anti-APO-1 antibody. The presence of phosphorylated groups was analyzed by Pro-Q Diamond staining which can detect phosphate groups attached to tyrosine, Ser or Thr residue. It allows detection of as little as 50 nanograms of phosphoprotein (Fig. 23A). The efficiency of the immunoprecipitation was controlled by anti-CD95 Western blot (Fig. 23B).

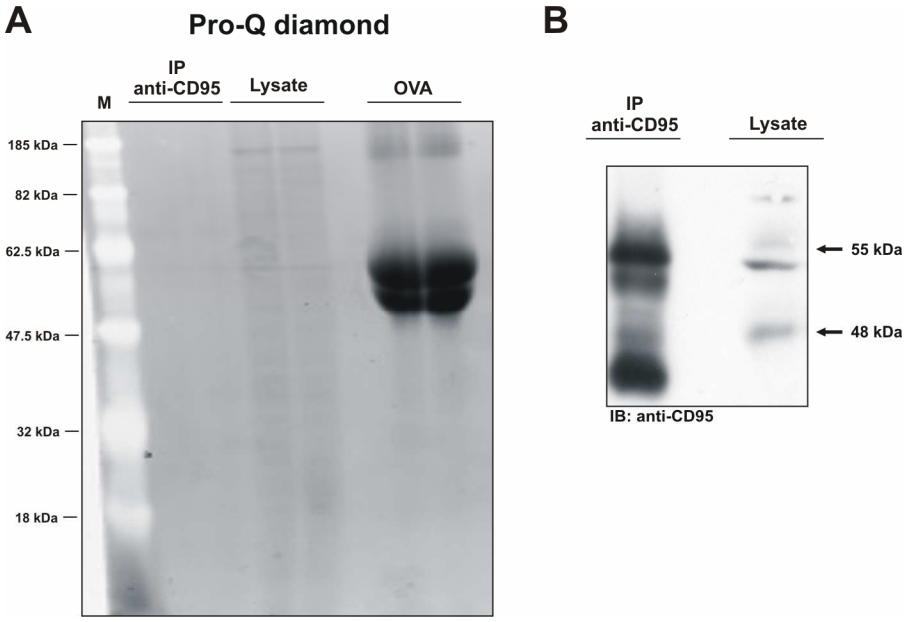

Figure 23. Analysis of CD95 phosphorylation. A. CD95 immunoprecipitated from HeLa-CD95 cells, HeLa-CD95 total cellular lysates and control phosphoprotein Ovalbumin were analyzed with Pro-Q Diamond phosphoprotein gel stain. **B**. The presence of CD95 in the samples was controlled by Western blot.

No phosphorylation of CD95 was detected. This does not exclude that CD95 could be phosphorylated at low levels. It is likely that the sensitivity of this approach was not sufficient to detect low levels of phosphorylation. Therefore, the main modification of CD95 seems to be glycosylation and the study focused on this modification.

3.4 Treatment with N-glycosidase F resulted in different CD95 protein modification patterns in Type I and Type II cells

According to the prediction, the second very prominent modification of CD95 was glycosylation. As mentioned before, CD95 is a sialylated N-glycosylated protein (Peter et al., 1995) (see section 1.2.2.2.4. for details). Therefore, it was assumed that the different CD95 protein modification patterns in Type I and Type II cells result from the different degree of N-glycosylation of CD95 in these cells. Protein modification patterns of CD95 were analyzed upon complete N-deglycosylation with N-glycosidase F, which cleaves all N-glycans from a protein (Fig. 24A). Cellular lysates from Type I and Type II cells treated with N-glycosidase F were analyzed for CD95 protein modification patterns in a 10 % SDS-PAGE with subsequent Western blot analysis. Untreated Type I and Type II cells were used as a control. The treatment with N-glycosidase F resulted in a clear shift of the two major bands in Type I cells (SKW6.4) to a decreased molecular mass (Fig. 24C). One major band in Type II cells (J27 and JA3) also shifted to a decreased molecular mass (Fig. 24C). Interestingly, the molecular mass of deglycosylated CD95 in Type I and Type II cells was different. Type II cells contain only one form of CD95 which seems to be less glycosylated than the “higher molecular mass form” from Type I cells and higher glycosylated than the ”lower molecular mass form” from Type I cells. CD95 in Type I cells seems to have an enhanced level of N-glycosylation and subsequently sialylation in comparison to CD95 in Type II cells. Treatment with N-glycosidase F did not result in a similar CD95 pattern in Type I and Type II cells. The data show clearly that there is another modification in addition to glycosylation. Nevertheless, there are various glycosylated forms of the receptor in both cell types. These differences might lead to the differences in signaling. Therefore, N-glycosylation was addressed in more detail. Treatment with N-glycosidase F could not be used since this enzyme showed a high level of unspecific deglycosylation. To further analyze the role of glycosylation other enzymes and inhibitors of N-glycosylation were applied such as a *Vibrio Cholerae* Neuraminidase (VCN), tunicamycin and deoxymannojirimycin (DMM).

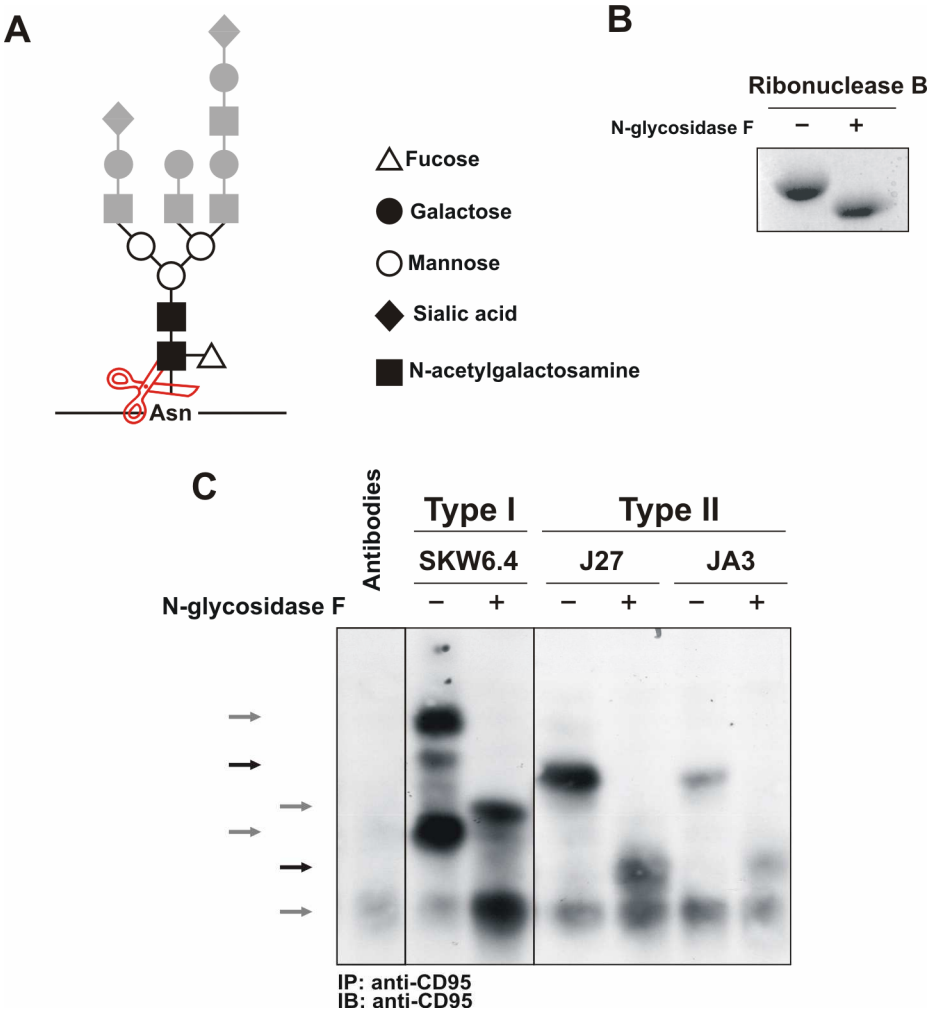

Figure 24. The analysis of deglycosylation of CD95 with N-glycosidase F. A. The mechanism of action of N-glycosidase F. Variable structures of glycan side chains are presented in grey. **B.** The action of N-glycosidase F on the Ribonuclease B. **C.** CD95 pattern in indicated cell lines after N-glycosidase F treatment was analyzed by Western blot analysis using anti-CD95 polyclonal antibodies C20.

3.5. Inhibition of CD95 N-glycosylation by tunicamycin

3.5.1. Tunicamycin treatment leads to a change in CD95 glycosylation pattern

Type I cells seems to have an enhanced level of glycosylation of CD95 compared to Type II cells. SKW6.4 and Hut78 were used to test if a decrease of various glycosylation forms of CD95 might convert Type I to Type II cells. The influence of N-glycosylation on CD95 signaling in cells was analyzed using tunicamycin. Tunicamycin acts at the ER level blocking the first step of protein N-glycosylation - the addition of the NacGlc from Dol-P-P to the Asn of a protein.

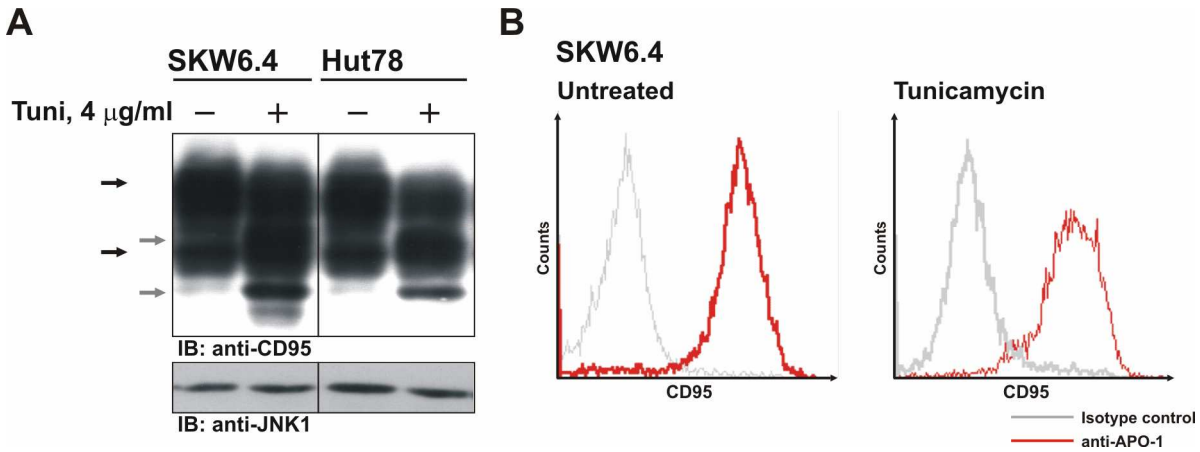

Figure 25. The analysis of deglycosylation of CD95 in Type I cells with the inhibitor of N-glycosylation tunicamycin. SKW6.4 and Hut78 were cultured with tunicamycin for 20 hours, followed by analysis of tunicamycin-treated *vs.* untreated cells. **A.** CD95 pattern was analyzed by Western blot. Anti-JNK1 Western blot was used as a loading control. CD95 bands in non-treated cells are indicated with black arrows, while shifts of CD95 bands in tunicamycin-treated cells are indicated with grey arrows. **B.** CD95 surface expression was analyzed in SKW6.4 cells.

Tunicamycin treatment for 20 hours resulted in a shift of the relative molecular mass of CD95 as detected by Western blot (Fig. 25A). Three bands of CD95 were observed in tunicamycin-treated cells. Two lower bands resulted from the deglycosylation shift. The upper one apparently corresponds to the fully glycosylated CD95, which was already expressed before tunicamycin treatment. CD95 has been reported to have an estimated turnover time of about 24 hours (Peter et al. 1995). Thus, after incubation with tunicamycin significant amounts of fully glycosylated CD95 were still present. Typically, using this approach more than 50% deglycosylation of CD95 was observed. This conclusion can be drawn based on comparison of the intensity of deglycosylated and glycosylated bands in the Western blot (Fig. 25A).

3.5.2. Tunicamycin treatment does not prevent partially deglycosylated CD95 from being transported to the cell surface

It has been shown before that the partially deglycosylated extracellular domain of CD95 is still expressed on the cell surface upon tunicamycin treatment, while the nonglycosylated form is retained intracellularly (Li et al. 2007). Whether the treatment with tunicamycin inhibits the translocation of the deglycosylated CD95 to the cell

surface was analyzed by cell surface staining. (Fig. 25B). There were no significant differences between CD95 surface expression of tunicamycin-treated and untreated cells. The identification of the amount of nonglycosylated CD95 was performed by Western blot and revealed about 10% of the total cellular content of CD95.

3.5.3. CD95 DISC formation upon tunicamycin treatment

The central event in CD95 signaling is the formation of the DISC. CD95 DISC formation was analyzed in untreated and tunicamycin-treated cells. SKW6.4 and Hut78 were treated with 4 µg/ml of tunicamycin for 20 hours. Untreated and inhibitor-treated cells were stimulated with 500 ng/ml anti-APO-1 antibody (Trauth et al. 1989) for 10 minutes at 37^{o}C to allow DISC formation (Fig. 26). The level of procaspase-8 as well as its cleavage product p43/p41 at the DISC was similar in tunicamycin treated *vs.* untreated cells. At the same time a decrease in c-FLIP levels at the DISC was observed.

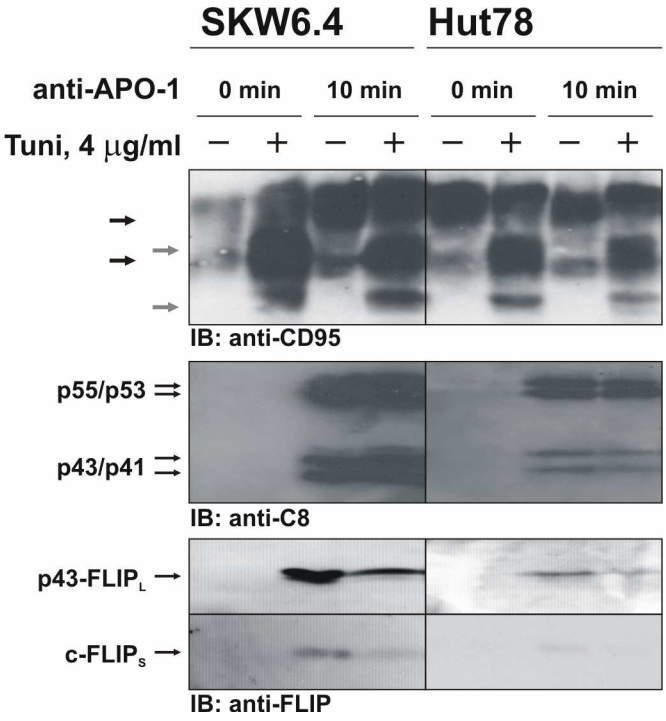

Figure 26. The analysis of DISC formation in Type I cells upon inhibition of N-glycosylation with tunicamycin. The SKW6.4 and Hut78 cells were treated for 24 h with 4 µg/ml of tunicamycin or left untreated. CD95 DISCs were analyzed after stimulation with 500 ng/ml of anti-APO-1 antibody for indicated time points. Western blot analysis of the DISCs was performed with antibodies against CD95, procaspase-8 and c-FLIP. CD95 bands in non-treated cells are indicated with black arrows, while shifts of CD95 bands in tunicamycin-treated cells are indicated with grey arrows.

3.5.4. Tunicamycin treatment resulted in CD95-independent cell death

Next, signaling downstream from the CD95 DISC was analyzed. The main events which occur downstream of the CD95 DISC are caspase-8 activation and induction of cell death.

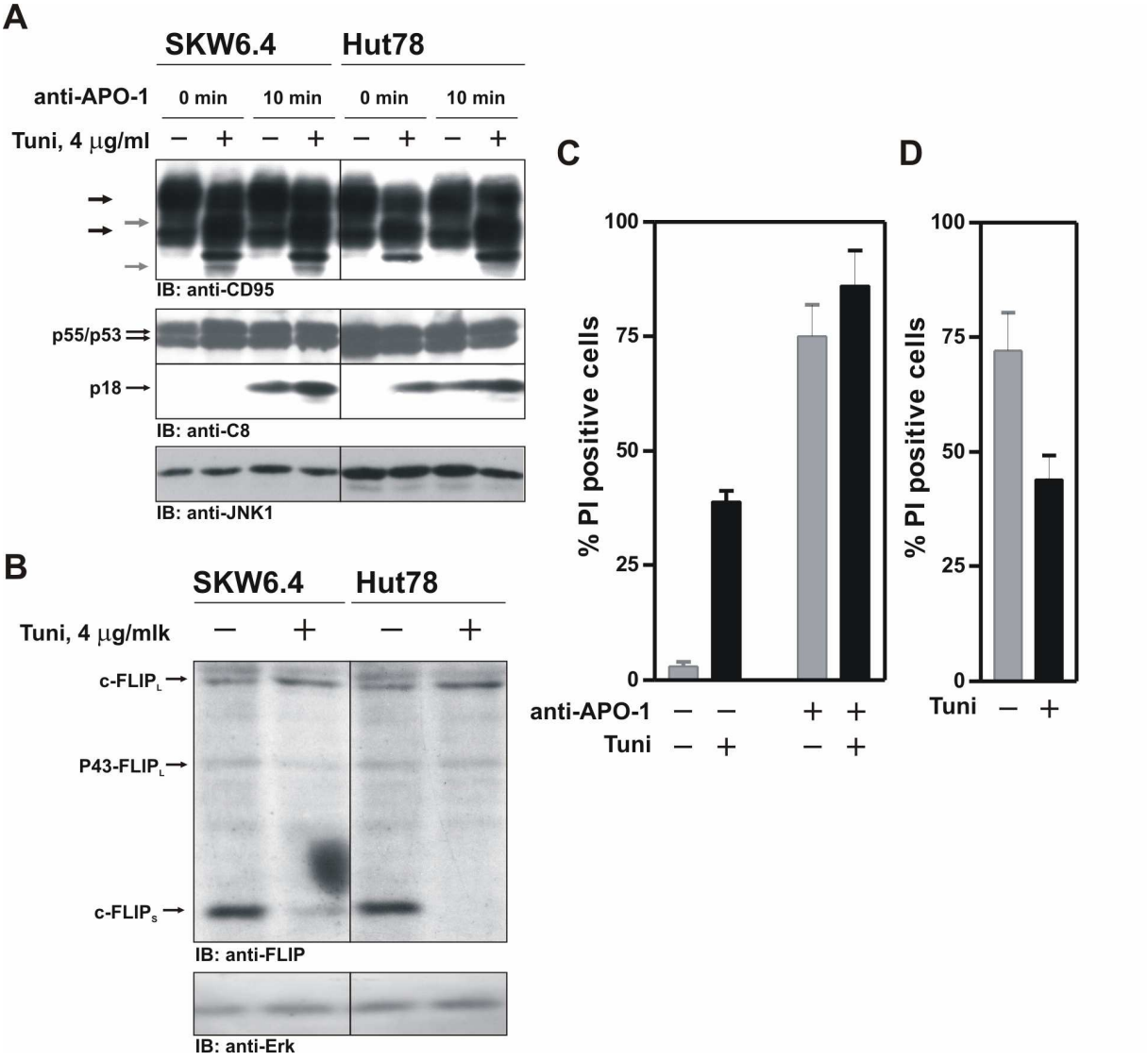

Figure 27. Tunicamycin treatment causes a strong cell death. A. Total cellular lysates were analyzed after treatment with 1 µg/ml of anti-APO-1 antibody using Western blot with polyclonal antibodies C20 and monoclonal antibodies C15 against procaspase-8. Anti-JNK1 Western blot was used as a loading control. **B.** c-FLIP expression was analyzed by Western blot using monoclonal NF6 antibodies. **C.** Apoptotic cell death was measured with PI staining in SKW6.4 cells. **D**. Specific cell death calculated from data in C.

The level of caspase-8 activation was analyzed by Western blot analysis and showed an enhanced level of caspase-8 activation upon tunicamycin treatment (Fig. 27A). The analysis of cell death by propidium iodide (PI) staining in SKW6.4 has

revealed that tunicamycin causes a strong CD95-independent cell death up to 35% (Fig. 27B). Upon overnight stimulation with anti-APO-1 cell death in tunicamycin-treated cells was 20% higher than in the untreated cells and reached 95%. But the level of CD95 specific cell death was decreased to 20% due to high background cell death (Fig. 27C).

Tunicamycin was reported to block translation. To further investigate the mechanism of tunicamycin-induced sensitization towards CD95-induced apoptosis the tunicamycin effects on protein synthesis in the system of DR-induced apoptosis were analyzed. C-FLIP proteins have a short turnover and are the central inhibitors of CD95-induced apoptosis. Their expression upon addition of tunicamycin was checked by Western blot. A significant decrease in the c-FLIP$_S$ levels were detected (Fig. 27D). This downregulation of c-FLIP$_S$ should certainly lead to enhanced sensitivity towards CD95-induced apoptosis as c-FLIP$_S$ protein was reported to block caspase-8 activation at the DISC (Scaffidi et al. 1999).

Thus, the action of tunicamycin in addition to N-deglycosylation results in a number of side effects such as the inhibition of translation leading to the downregulation of c-FLIP proteins and unspecific cell death. Therefore, tunicamycin was not ideal for the functional studies of N-deglycosylation of CD95. For further experimental analysis the influence of partial deglycosylation on CD95 signaling were tested by using enzymatic approaches.

3.6. Analysis of the role of CD95 sialylation in CD95 signaling using *Vibrio Cholerae* Neuraminidase (VCN)

3.6.1. DISC formation upon VCN treatment

CD95 is highly sialylated protein (Keppler et al. 1999). Analysis of the influence of sialic acid on CD95 signaling was carried out. A set of different sialidases (for more details see materials and methods) was tested and it was found that *Vibrio Cholerae* Neuraminidase (VCN) from Sigma-Aldrich (Steinheim, Germany) which preferentially hydrolyzes a (α2-3)-linkages of sialic acid (Fig. 28A) was the best for the following experiments. The conditions under which effective removal of sialic acid occurred within the shortest period of time were found (see materials and methods for details).

Treatment of SKW6.4 and Hut78 cells with VCN for one hour substantially reduced the relative molecular mass of CD95. The shift to the lower molecular mass was observed for CD95 indicating removal of sialic acid.

To test whether sialylation of CD95 plays a role in signal transduction the differences in CD95 signaling upon desialylation of CD95 starting with DISC formation were investigated. CD95 DISC formation was compared in SKW6.4 and Hut78 cells treated *vs.* untreated with VCN (Fig. 28B). The cells were first treated with VCN for one hour. After complete desialylation of CD95, the cells were stimulated with agonistic anti-APO-1 antibody and the CD95 DISC was immunoprecipitated and analyzed as described before. CD95 DISCs were detected both upon and without VCN treatment. However, lower amounts of procaspase-8a/b, its cleavage product p43/p41 and the cleavage product of c-$FLIP_L$, p43-$FLIP_L$ were observed in comparison to the DISCs from VCN-untreated cells (Fig. 28C). The full-length c-$FLIP_L$ was not detected at the DISC as it was immediately processed in accordance with previous publications (Chang et al. 2002; Lavrik et al. 2007). Notably, the amount of DED-containing proteins and processed caspase-8 at the DISC were reduced.

To control that the reduced DISC formation upon VCN treatment is not due to the decreased affinity of anti-APO-1 antibody to desialylated CD95, ELISA analysis was carried out using two types of anti-CD95 antibodies. The primary antibodies were rabbit polyclonal antibodies and interact with the C-terminus of CD95, which should not be glycosylated. As secondary antibodies anti-APO-1 antibodies were used (Fig. 28C). The binding of desialyated and sialylated CD95 to anti-APO-1 antibodies was shown to be similar. Thus, the reduced DISC formation is the consequence of VCN treatment.

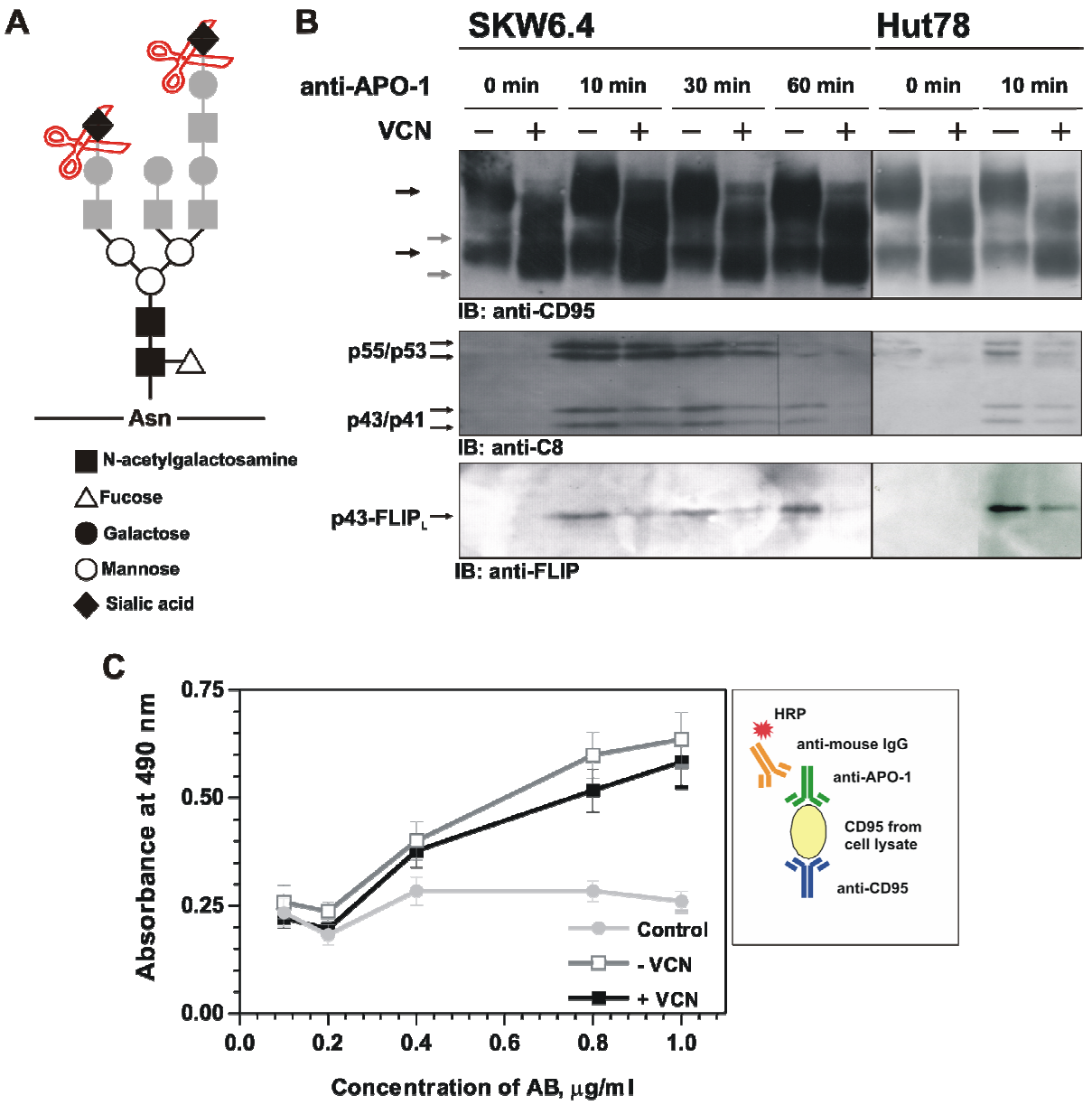

Figure 28. DISC formation upon VCN treatment. A. The mechanism of action of VCN. Variable structures of glycan side chains are presented in grey. **B.** CD95 DISCs were analyzed after treatment with 1 µg/ml of anti-APO-1 antibody for indicated time points. Western blot analysis of the DISCs was performed with antibodies against CD95, procaspase-8 and c-FLIP. CD95 bands in untreated cells are indicated with black arrows, while shifts of CD95 bands in VCN-treated cells are indicated with grey arrows. **C.** ELISA analysis for the binding of anti-APO-1 antibody to CD95 from the lysates of untreated and VCN-treated SKW6.4 cells.

3.6.2. Decreased formation of CD95$_n$ oligomers upon VCN treatment

CD95 is published to form SDS-stable CD95 oligomers (CD95$_n$) upon stimulation with the ligand or agonistic antibodies (Feig et al. 2007). The first interesting

observation was the reduction molecular mass of the $CD95_n$ oligomers from 220 kDa to 116 kDa upon treatment with VCN in Type I SKW6.4 cells (Fig. 29). These differences in mobility might be a result of the decreased amount of CD95 oligomers or because of the different mobility on the gel due to different charge or conformational changes of the protein upon deglycosylation.

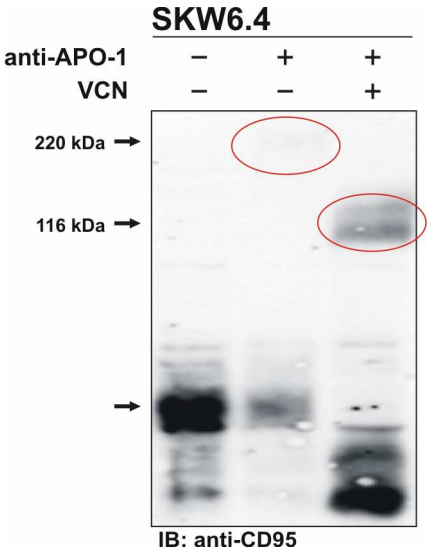

Figure 29. The analysis of desialylation of CD95 in Type I cells with *Vibrio Cholerae* Neuraminidase (VCN). SKW6.4 cells were treated with VCN for 1 hour at 37^0C, followed by the analysis of VCN-treated *vs.* untreated cells. $CD95_n$ oligomers were analyzed by Western blot for CD95. Oligomeric structures are marked with red circles.

Interestingly, the desialylated upper band of CD95 in Type I cells had a molecular mass similar to the one of CD95 in Type II cells. This suggests that one of the differences in CD95 modification in Type I and Type II cells could be the higher level of sialylation of CD95 in Type I cells.

3.6.3. VCN treatment resulted in CD95-independent cell death

Apoptotic signaling in SKW6.4 and Hut78 downstream of the DISC was analyzed. Untreated and VCN-treated cells were stimulated with anti-APO-1 for 10 min at 37^oC. Total cellular lysates were analyzed by Western blot using anti-caspase-8, anti-Bid and anti-caspase-3 antibodies. In contrast to the DISC, in total cellular lysates more active caspase-8 was detected upon VCN treatment than without VCN treatment (Fig. 30A). Moreover, caspase-3 and Bid cleavage were significantly enhanced upon VCN treatment (Fig. 30B).

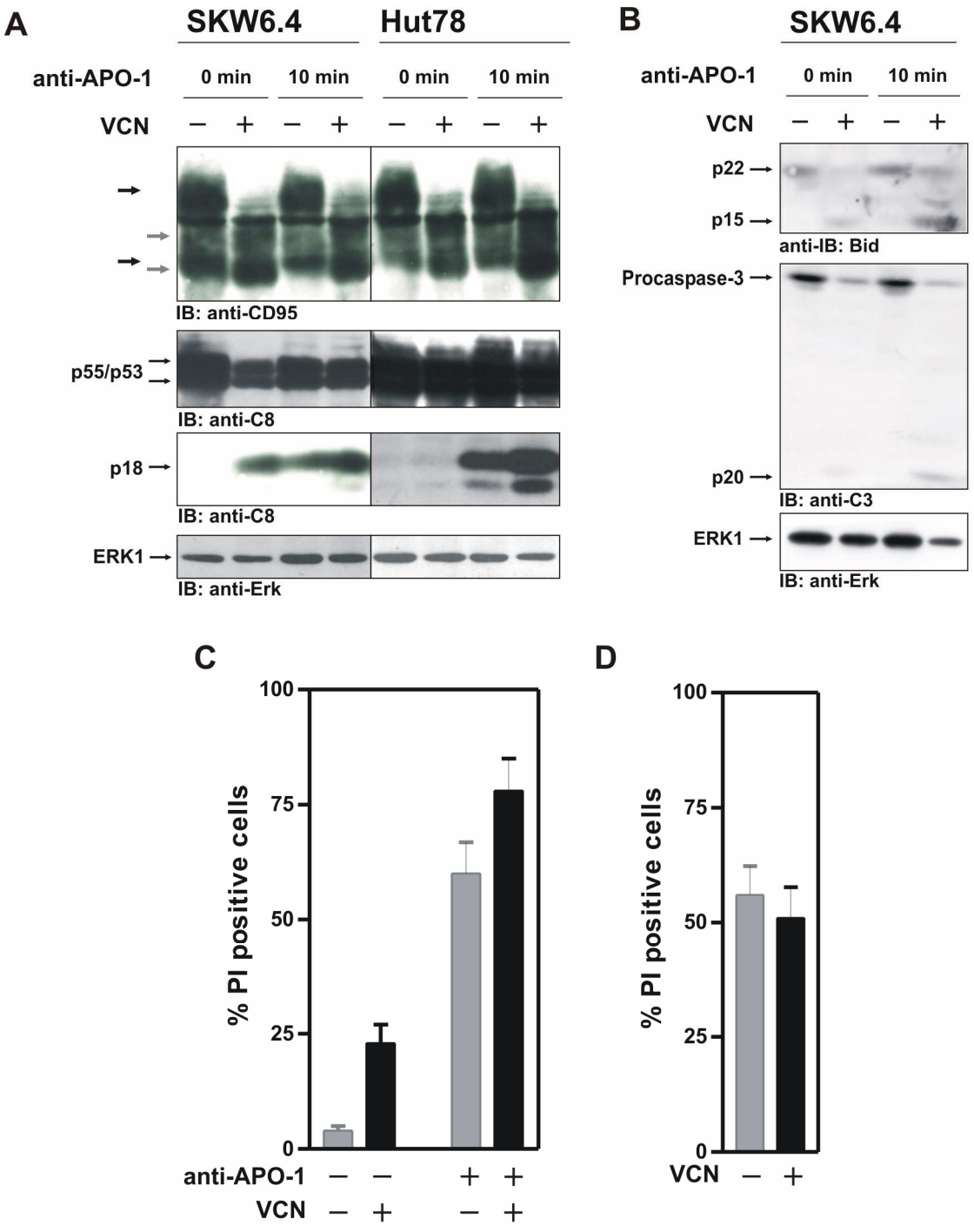

Figure 30. Treatment with VCN resulted in unspecific cell death. A. Total cellular lysates were analyzed after treatment with 1 µg/ml of anti-APO-1 antibody by Western blot for CD95 and caspase-8. Anti-Erk1 Western blot was used as a loading control. **B.** Caspase-3 processing and Bid cleavage were analyzed in untreated and VCN-treated SKW6.4 cells using Western blot. **C.** Apoptotic cell death in SKW6.4 was measured with PI staining. **D**. Specific cell death calculated from data in C.

To address the observed contradiction between the reduced level of procaspase-8 processing at the DISC upon VCN treatment and the enhanced level of caspase-8 activation in the total cellular lysates upon VCN treatment cell death was measured by PI staining. It was found that the VCN treatment alone resulted in significant increase of cell death (Fig. 30C). The mechanism of this cell death is not described and possibly involves desialylation of other surface receptors leading to the blockage of many important cellular pathways, which results in apoptosis induction. Therefore, the cells pretreated with VCN showed an increased level of apoptosis in a CD95-independent way, but CD95 specific cell death was diminished (Fig. 30D). This provides an explanation for the increased caspase-8 activity in total cellular lysates (Fig. 30A) upon VCN treatment. Therefore, VCN could not be applied for functional studies in CD95 signaling as it causes significant CD95-independent cell death.

3.7. Analysis of the role of complex and hybrid N-glycans in CD95 signaling using Deoxymannojirimycin (DMM)

To evaluate the effect of complex and hybrid glycans 1-deoxymannojirimycin (DMM) was applied. DMM inhibits the ER mannosidases and Golgi mannosidase I, resulting in the accumulation of high-mannose oligosaccharide structures that can not be further modified by the terminal addition of different carbohydrate moieties (Varki et al. 2009). Different concentrations of inhibitor were tested and a nontoxic concentration which did not influence the quality of inhibition. The optimal concentration for DMM was 2 mM and treatment was performed for 48 hours (data not shown).

3.7.1. DMM treatment resulted in a different CD95 protein modification pattern than after tunicamycin and VCN treatments. DMM does not change surface expression of CD95 and had no toxic effect.

DMM treatment in SKW6.4 cells was performed for 48 hours with a daily medium change. Total cell lysates were analyzed by Western blot in order to check whether DMM altered the glycosylation patterns of CD95. The reduction in relative mass of CD95 corresponded to approximately 5-6 kDa for DMM-treated cells compared to untreated cells (Fig. 31A). Different CD95 protein modification patterns were observed upon DMM treatment in comparison to tunicamycin and VCN treated cells.

Three bands of CD95 were observed in DMM-treated cells. Two lower bands apparently result from a shift of deglycosylation. The third upper one probably corresponds to glycosylated CD95.

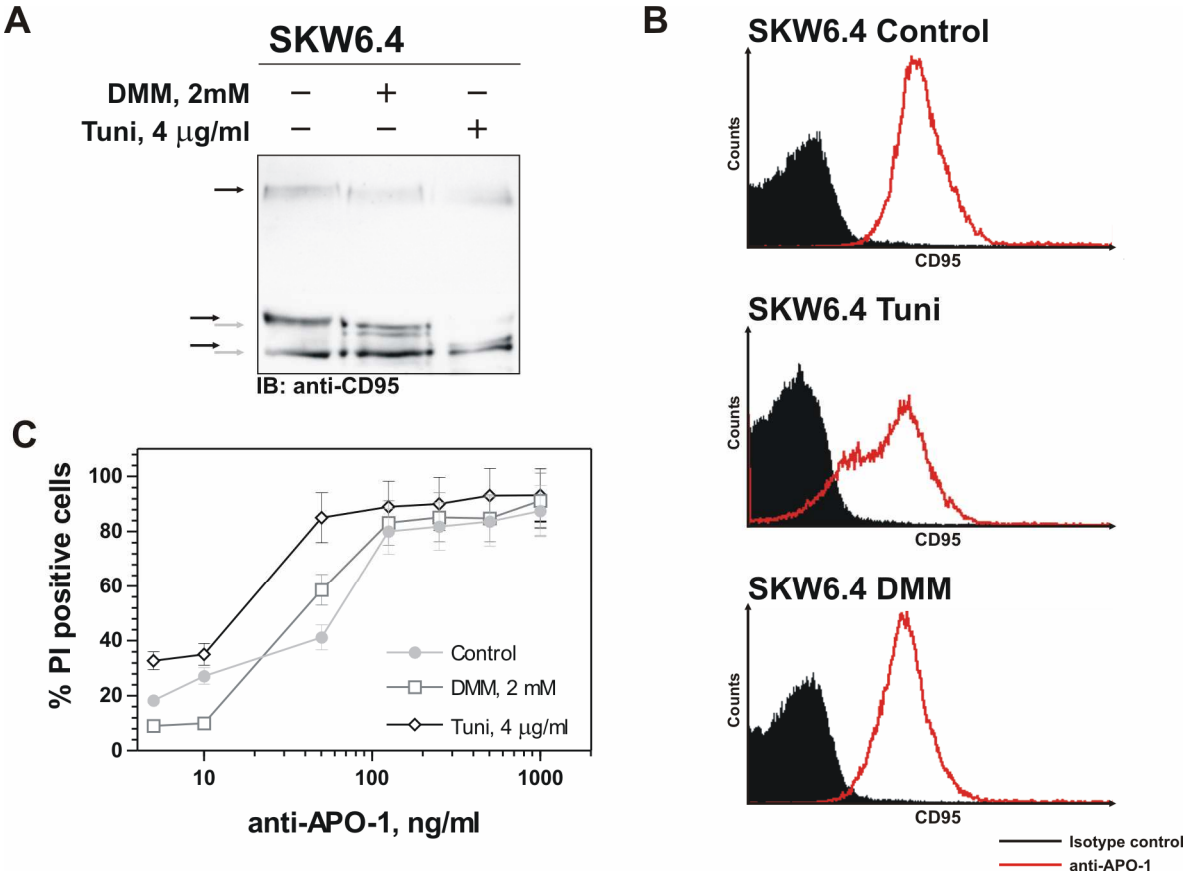

Figure 31. **Analysis of deglycosylation of CD95 in SKW6.4 cells with the inhibitor of N-glycosylation, DMM.** SKW6.4 cells were cultured with DMM for 48 h, followed by the analysis of DMM-treated *vs.* untreated cells. **A.** The CD95 pattern was analyzed by Western blot analysis using anti-CD95 polyclonal antibodies C20. CD95 bands in untreated cells are indicated with black arrows, while shifts of CD95 bands in DMM-treated cells are indicated with grey arrows. **B.** CD95 surface expression was analyzed in SKW6.4 cells. **C**. Apoptotic cell death in SKW6.4 cells was measured with propidium iodide staining.

Cell surface expression of the N-glycosylated proteins treated with DMM should not be influenced because they undergo proper folding in the ER. Therefore the amount of CD95 on the cell surface in untreated and DMM-treated SKW6.4 cells was analyzed. No differences were found between treated and untreated cells (Fig. 31B). Thus, DMM treatment does not regulate CD95 apoptotic signaling *via* cell surface expression.

To analyze sensitivity to CD95 induced apoptosis in DMM-treated cells cell death was determined by PI-staining upon incubation with different amounts of antagonistic anti-APO-1 antibody (Fig. 31C). DMM treatment modulated the sensitivity to CD95 induced apoptosis at low anti-APO-1 concentrations. The level of cell death was the same upon stimulation with high anti-APO-1 concentrations.

3.7.2. CD95 DISC formation upon DMM treatment

To analyze the influence of DMM on CD95 DISC formation DISC levels were compared in untreated and DMM-treated SKW6.4 cells (Fig. 32).

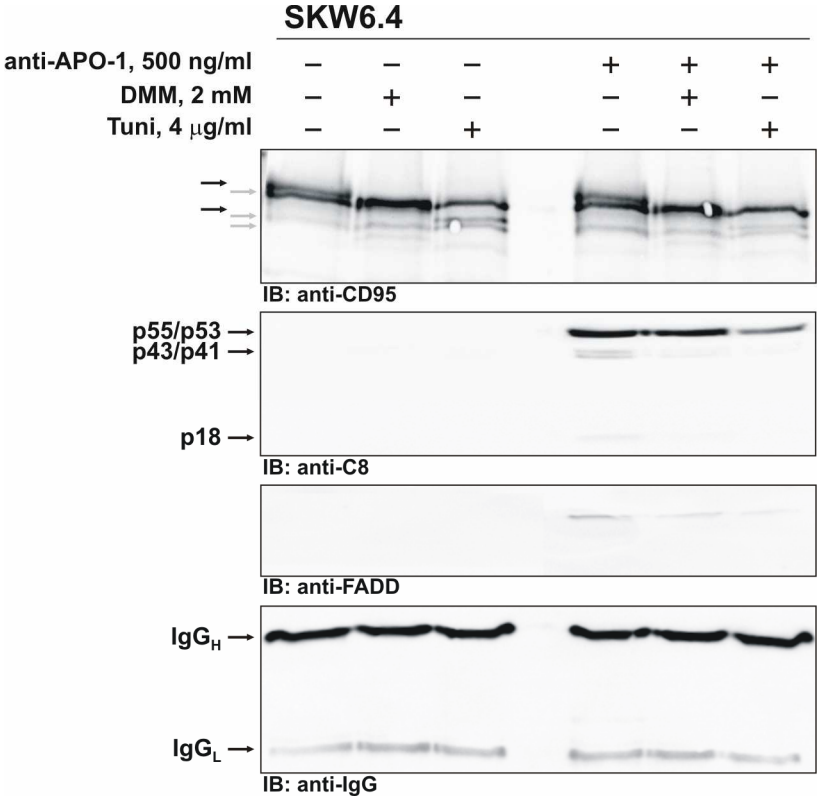

Figure 32. **DISC formation upon DMM treatment is reduced.** CD95 DISCs were analyzed after treatment with 500 ng/ml of anti-APO-1 antibody for 15 min. Western blot analysis of the DISCs was performed with antibodies against CD95, procaspase-8 and FADD. Anti-IgG Western blot was used as a loading control for the immunoprecipitation. CD95 bands in non-treated cells are indicated with black arrows, while CD95 bands in DMM-treated cells are indicated with grey arrows.

As a control for the diminished CD95 DISC formation SKW6.4 cells treated with tunicamycin as described above were used. The cells were treated with DMM for 48 hours which resulted in a complete inhibition of formation of the CD95 complex and hybrid glycans. After 48 hours cells were stimulated with agonistic anti-APO-1

antibodies and the CD95 DISC was immunoprecipitated and analyzed. The levels of active caspase-8 and FADD at the DISC were marginally decreased upon DMM treatment compared to untreated cells and higher than in tunicamycin-treated cells (Fig. 32). This observation suggests that complex and hybrid glycans are important for the proper CD95 DISC formation and apoptotic signaling of CD95.

3.8. Investigation of the role of CD95 glycosylation by site-directed mutagenesis

3.8.1. Single aminoacid substitutions as a specific approach to generate CD95 glycosylation mutants

Analysis of glycosylation patterns of the receptor using enzymatic and inhibitory approaches was informative, but it was not applicable for functional analysis due to the unspecific deglycosylation of many cellular proteins that resulted in a high degree of CD95-independent cell death. To specifically study CD95 glycosylation sites-deficient glycosylation mutants were generated by site-directed mutagenesis. Asparagine and threonine residues were changed for glutamine in order to not significantly change the local structure and charge of CD95. Single and double mutants in different combinations were used (Fig. 33A).

HeLa cells were used to study CD95 glycosylation mutants. In all cases, the impact of N-glycosylation on CD95 function was assessed by surface staining, DISC formation and cell death analysis after transient transfection or in cell lines stably expressing CD95 WT or corresponding glycosylation mutants.

3.8.2. Construction of single and double glycosylation mutants of CD95

As discussed above, CD95 has three potential N-glycosylation sites (Asn118, Asn136 and Asn223) and one O-glycosylation site (Thr214) (Fig. 33A).

Accordingly, the CD95 single mutations were named CD95 (N118Q,) CD95 (N136Q), CD95 (T214Q) and CD95 (N223Q) and CD95 (N118Q/N136Q), CD95 (N118Q/T214Q), CD95 (N118Q/N223Q), CD95 (N136Q/T214Q) and CD95 (N136Q/N223Q) for the double mutants, respectively.

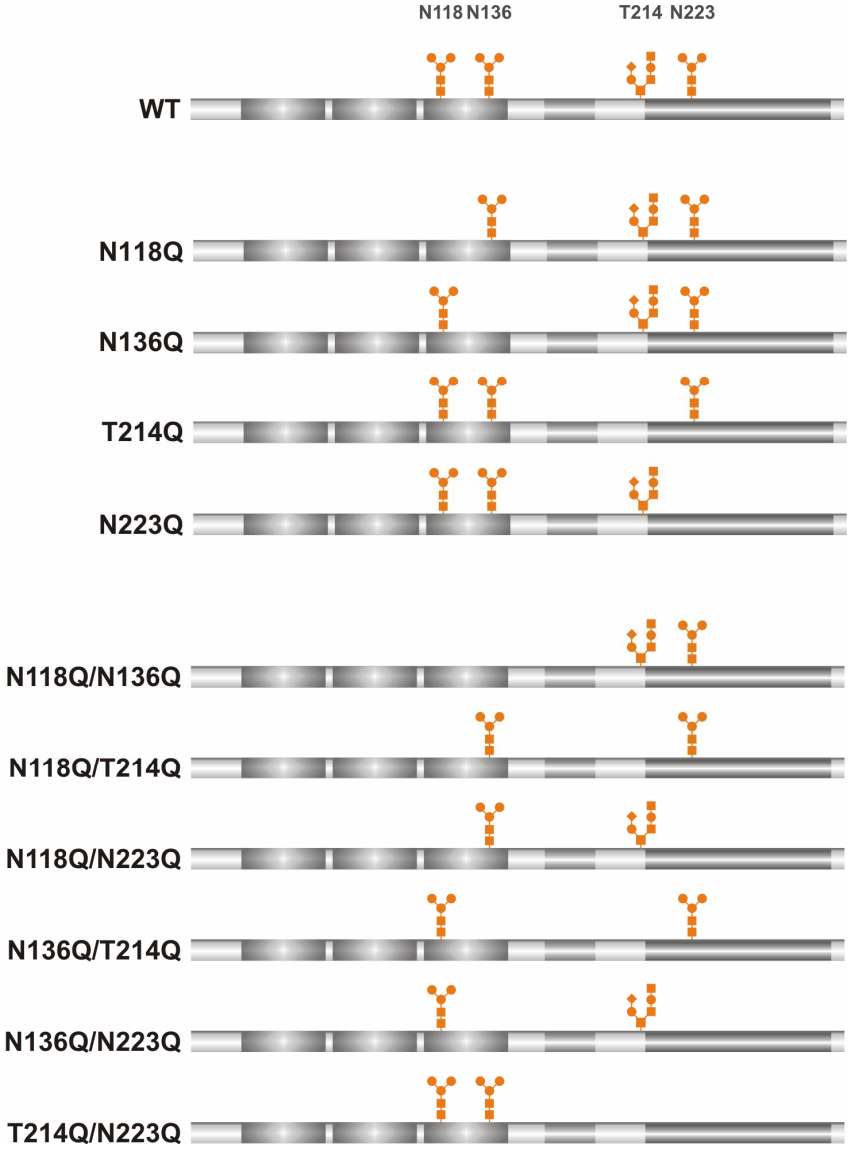

Figure 33. **Generation of CD95 glycosylation mutants**. Scheme of all created glycosylation mutants for CD95.

3.8.3. Analysis of CD95 glycosylation mutants in HeLa cells

3.8.3.1. Expression of WT and mutant CD95 in HeLa cells

CD95 glycosylation mutants were expressed in HeLa cells upon transient transfection (Fig. 34A) and detected by Western blot. Upon expression of wild-type CD95 (WT) two bands were detected.

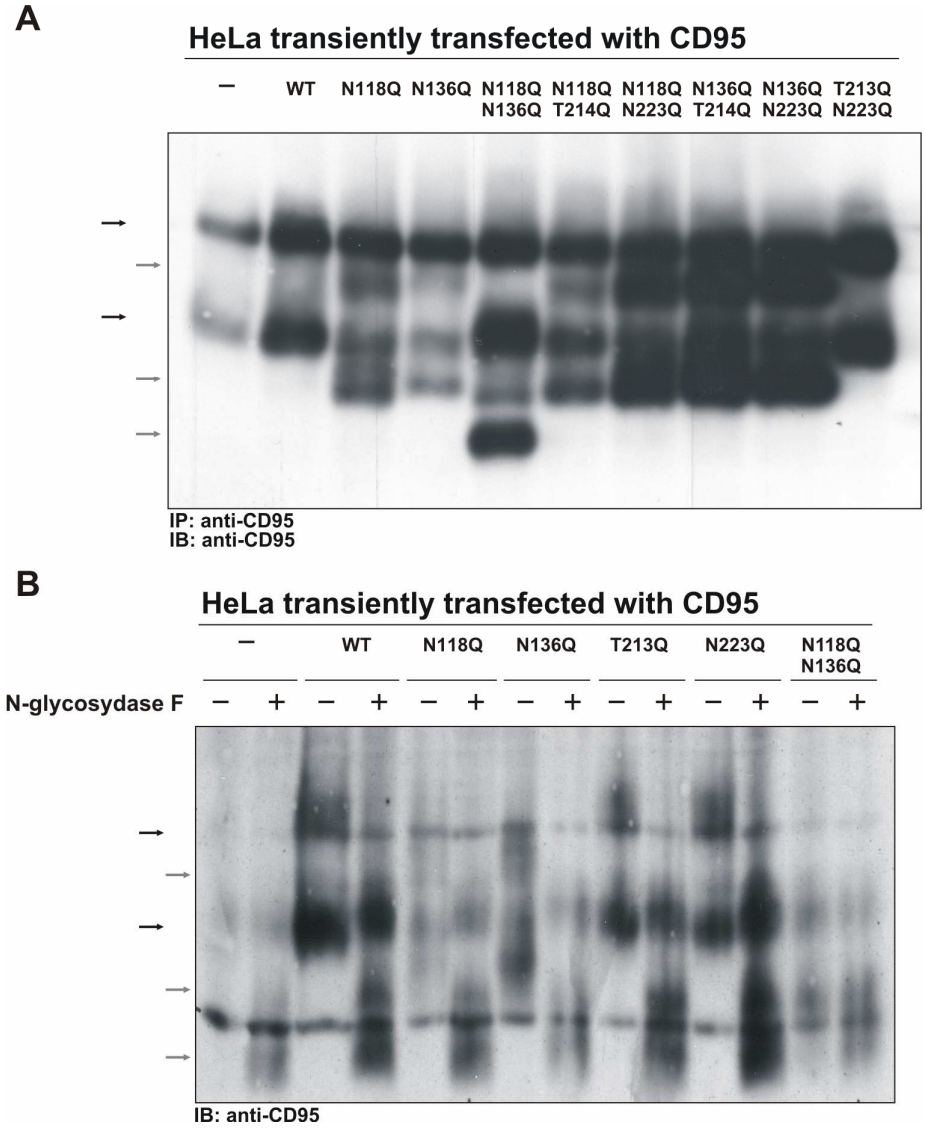

Figure 34. **Expression of CD95 glycosylation mutants upon transient transfection**. **A.** Expession of CD95 glycosylation mutants in HeLa cells. The pattern of CD95 was analyzed by Western blot analysis using anti-CD95 polyclonal antibodies C20. CD95 (WT) bands are indicated with black arrows, while CD95 bands from glycosylation mutants are indicated with grey arrows. **B.** CD95 pattern in HeLa cells transfected with CD95 (WT) and CD95 glycosylation mutants after N-Glycosidase F treatment was analyzed by Western blot analysis using anti-CD95 polyclonal antibodies C20.

In case of expression of glycosylation mutants deficient on one of the extracellular glycosylation sites three CD95 bands were observed. All of them correspond to the differentially glycosylated CD95.

No differences in CD95 protein modification pattern for the CD95 (T214Q/N223Q) mutant were found in comparison with WT CD95. This shows the absence of intracellular glycosylation of CD95. The most remarkable difference in CD95 protein

modification pattern was observed in the case of CD95 (N118Q/N136Q) mutant, where an additional lower band was observed. This band likely corresponds to the nonglycosylated CD95.

3.8.3.2. Analysis of CD95 glycosylation mutants using N-glycosidase F

To check that the CD95 protein modification pattern in case of the CD95 (N118Q/N136Q) double mutant corresponds to those of completely deglycosylated CD95, lysates from cells transiently expressing glycosylation mutants were treated with N-glycosidase F. As expected, all mutants except the CD95 (N118Q/N136Q) double mutant which lacks both extracellular glycosylation sites demonstrated a shift of CD95 protein modification pattern upon treatment with this enzyme (Fig. 34B). Only in case of CD95 (N118Q/N136Q) the protein modification pattern was not changed. This result suggests that this mutant does not contain any N-glycans. Nevertheless, even in the case of CD95 (N118Q/N136Q) a double band in CD95 protein modification pattern was still observed.

3.8.3.3. Comparison of cell surface expression and DISC formation in HeLa cells transiently transfected with glycosylation mutants

First, cell surface expression and DISC formation of CD95 glycosylation mutants were checked. Transiently transfected with the same amounts of the CD95 constructs HeLa cells were analyzed 36 hours after transfection. Cell surface expression was analyzed by surface staining with anti-APO-1 antibody by FACS. The ability to form a DISC after triggering of the receptor was tested under conditions described above (Fig. 35A).

CD95 surface staining has demonstrated that all the mutant proteins are translocated to the cell surface (Fig. 35A). These results suggest that the protein folding of the mutants occur normally and glycosylation mutants are not retained in the ER. Moreover, no significant differences in DISC formation were observed (Fig. 35B).

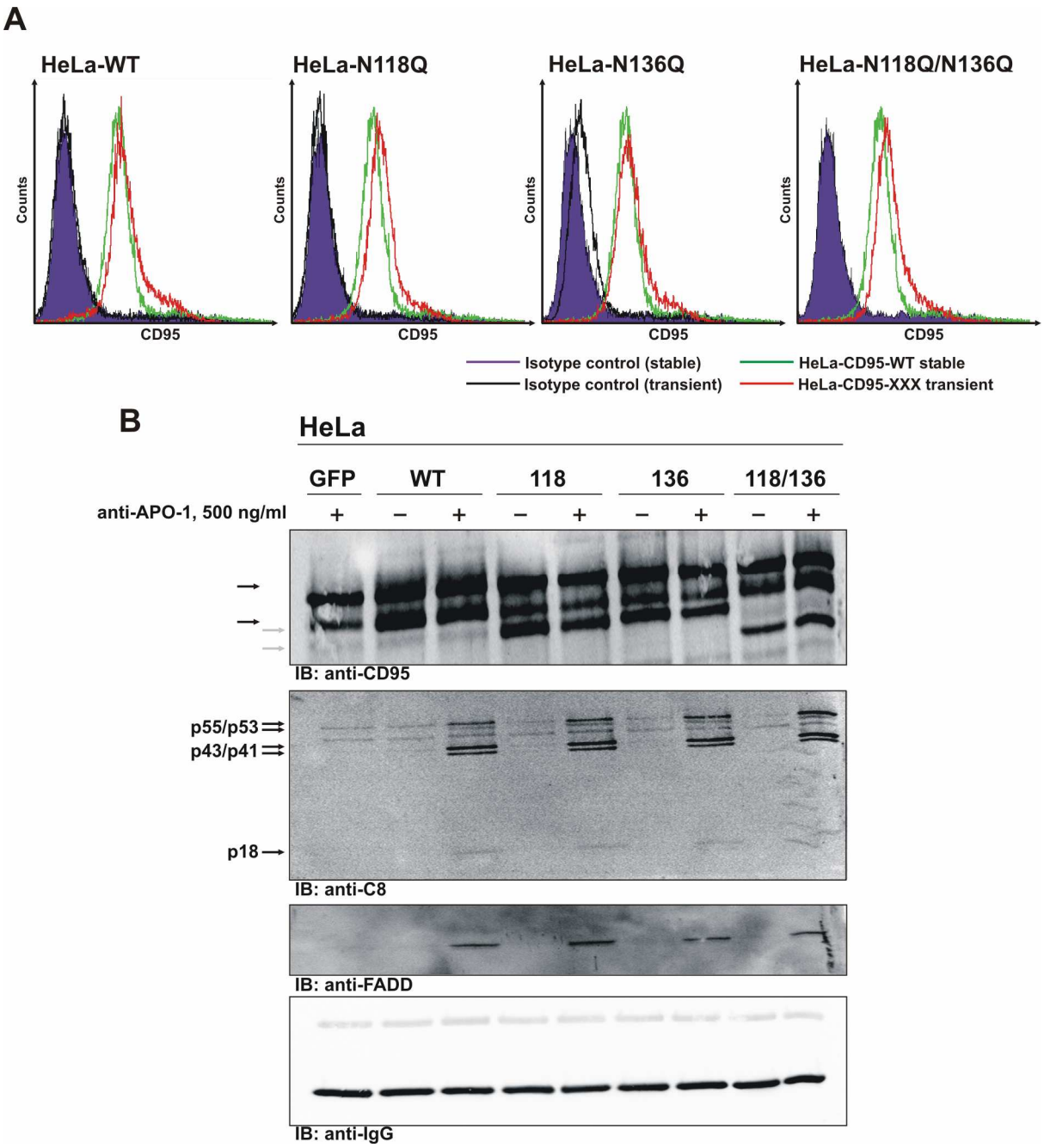

Figure 35. Cell surface expression and DISC formation in HeLa cells transiently transfected with CD95 glycosylation mutants. A. Cell surface staining of WT CD95 and CD95 glycosylation mutants for transiently transfected HeLa cells was performed with anti-APO-1 IgG3 antibodies (red line). As isotype control FII23 IgG3 antibodies were used (Black and violet lines). To control efficiency of CD95 surface expression the HeLa-CD95 stable cell line was used (green line) (Neumann et al., in press). **B.** The CD95 DISC was analyzed after treatment with 500 ng/ml of anti-APO-1 antibody for 15 min. Western blot analysis of the DISCs was performed with antibodies against CD95, procaspase-8, FADD. CD95 bands of CD95 (WT) are indicated with black arrows, while bands of CD95 glycosylation mutants are indicated with grey arrows.

To overcome variations of CD95 expression upon transient transfection and study CD95 glycosylation mutants under more physiological conditions HeLa cell lines stably expressing different CD95 glycosylation mutants were created and cell lines with similar expression levels of CD95 mutants were selected.

3.8.4. Analysis of CD95 glycosylation in cell lines stably expressing CD95 glycosylation mutants

3.8.4.1. Generation and characterization of cell lines stably expressing CD95 glycosylation mutants

To generate HeLa-CD95 cell lines stably expressing different glycosylation mutants, HeLa cells were transfected with 200 ng of a pIRES-CD95 construct (Neumann et al., in press), a coding for a WT or mutants of the CD95 gene. Cells with a stable integration of a CD95 cassette were selected upon puromycin treatment.

Cell lines expressing CD95 (N118Q), CD95 (N223Q) and CD95 (T214Q) single glycosylation mutants were generated. CD95 (N136Q) single and CD95 (N118Q/N136Q) double glycosylation mutants did not survive puromycin selection.

3.8.4.2. CD95 (WT) and glycosylation mutants protein modification patterns are the same in transiently transfected and stably expressing cells

To check the CD95 expression levels in the produced cell lines stably expressing CD95 (WT) and glycosylation mutants the CD95 protein modification patterns from these cells were analyzed as described above. The same CD95 (WT) and glycosylation mutant protein modification patterns were found for transiently transfected HeLa cells expressing the same CD95 constructs. Moreover, for the single mutants deficient in intracellular glycosylation sites (N223Q and T214Q) no differences were found in comparison to WT receptor, where only two forms of CD95 were detected. For the extracellular glycosylation site mutant CD95 (N118Q) three forms of CD95- two of those with relatively lower molecular mass- were detected (Fig. 36A). These findings are in good agreement with the results obtained from transiently transfected HeLa cells.

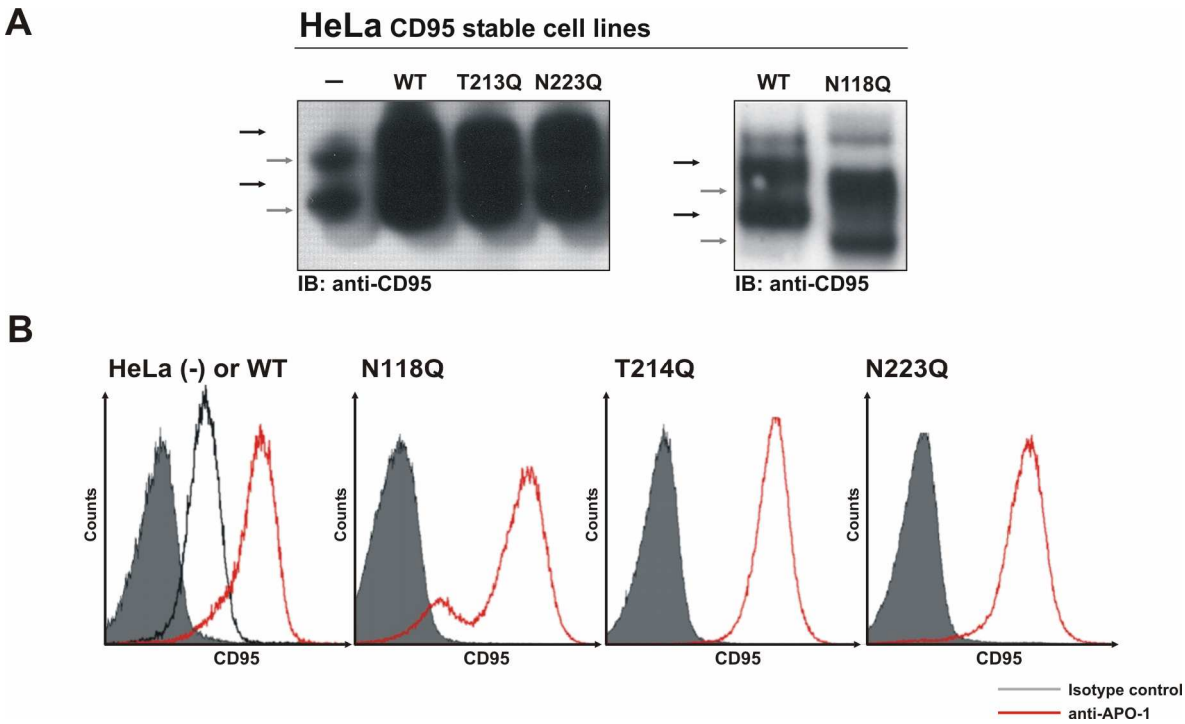

Figure 36. Production of cell lines stably expressing CD95 WT and glycosylation mutants. A. CD95 protein modification pattern in cell lines stably expressing CD95 glycomutants was analyzed by Western blot analysis using anti-CD95 polyclonal antibodies C20. WT CD95 bands are indicated with black arrows, while CD95 bands from glycosylation mutants are indicated with grey arrows. **B.** Cell surface staining of CD95 (WT) and CD95 glycosylation mutants in stable cell lines was performed with anti-APO-1 IgG3 antibodies. As isotype control FII23 IgG3 antibodies were used.

3.8.4.3. Cell surface localization of CD95 (WT) and glycosylation mutants in HeLa stably expressing cell lines

For the functional studies of the CD95 signaling the cell surface expression of the receptor plays a critical role. To select cell lines with a similar expression efficiency of CD95 (WT) and glycosylation mutants more than 120 cell lines, which include pools and single clones, were analyzed for the levels of CD95 total protein and cell surface expression by Western blot and flow cytometry, respectively (data not shown). On the basis of these analysis HeLa stably transfected cell lines which express the same amount of CD95 at the cell surface and contain equal amount of CD95 in total cell lysates were selected (Fig. 36B).

3.8.4.4. CD95 WT and glycosylation mutants have a similar localization within the cell

To compare the localization of CD95 WT and glycosylation mutants in stably transfected HeLa cells immunoflourecence staining and confocal microscopy analysis of these cells were performed. All membrane proteins undergo a glycosylation procedure in order to be transported to the membrane (Parodi 2000). To check the possibility that abrogation of CD95 glycosylation leads to accumulation of the protein in the ER co-stainings for the ER marker calreticulin and the Golgi marker GM130 were performed. No differences in the distribution of CD95 WT and glycosylation mutants within HeLa stably transfected cell were found (Fig. R37).

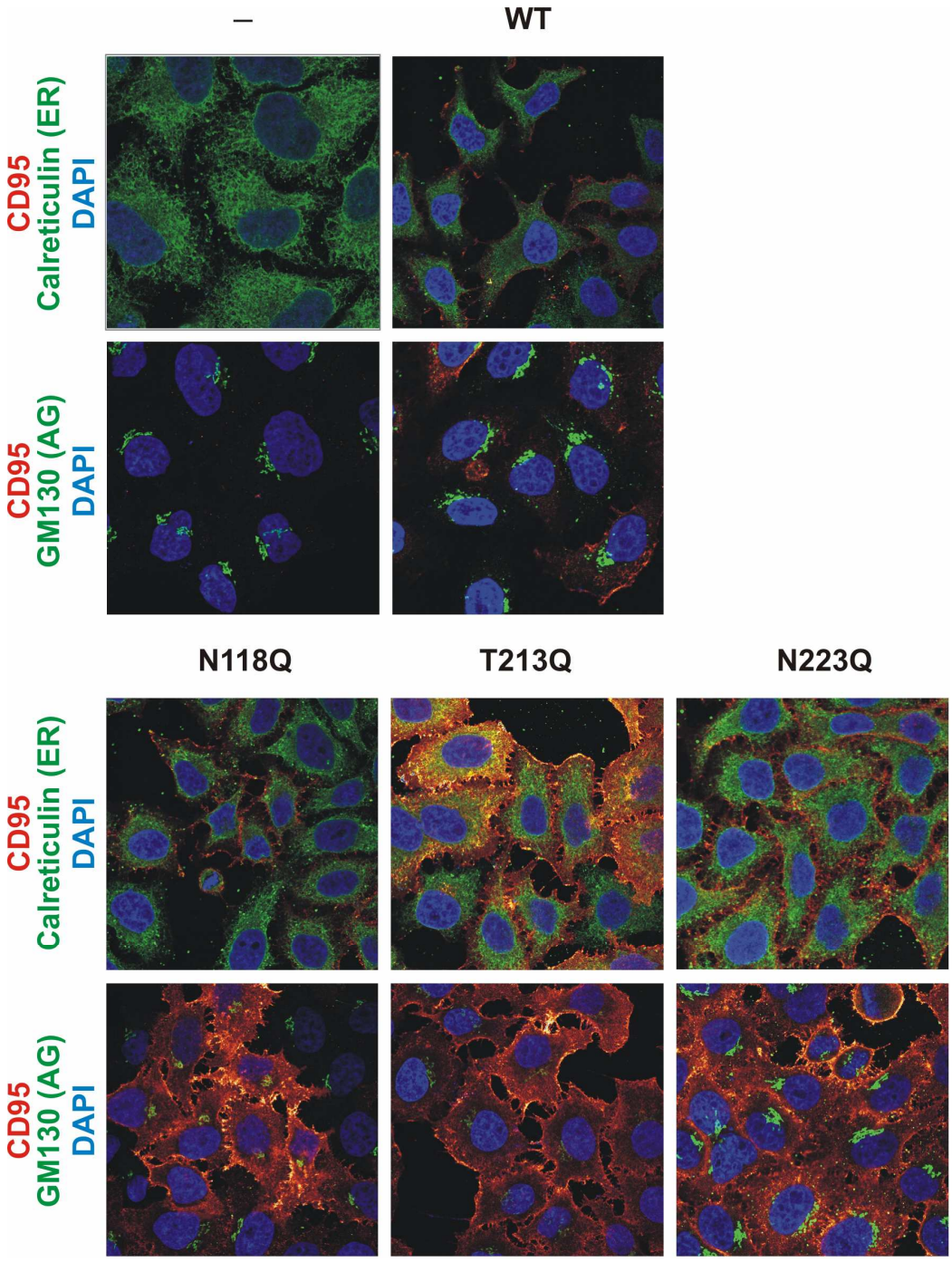

Figure 37. CD95 WT and glycosylation mutants distribution within the cell by confocal microscopy. HeLa, HeLa stably transfected with WT CD95 and CD95 glycosylation mutants were plated on glass slides, fixed, stained with anti-APO-1 antibody for CD95, with anti-calreticulin as a specific marker for ER and with anti-GM130 as a specific marker for Golgi antibodies. Localization of CD95 was visualized by Alexa594-coupled secondary antibodies and localization of GM130 and calreticulin was visualized by Alexa488-coupled antibodies. Nuclei were stained with DAPI. Representative fluorescence micrographs are shown.

3.8.4.6. CD95 glycosylation mutants have the same affinity to anti-APO-1 antibody as CD95 WT

All previous data show that HeLa cells stably transfected with CD95 mutants express CD95 on the cell surface. Therefore, these mutants are an excellent tool to analyze the role of glycosylation in CD95 signaling. This gave a basis to analyze the CD95 signaling events upon anti-APO-1 treatment. However, it remained unclear, whether the absence of glycans induces changes in CD95 conformation, which, in turn, causes differences in the binding affinity of the agonistic anti-APO-1 antibody. To analyze this possibility binding of the anti-APO-1 antibody to CD95 (WT) and glycosylation mutants was measured by ELISA analysis as was described above (Fig. 38).

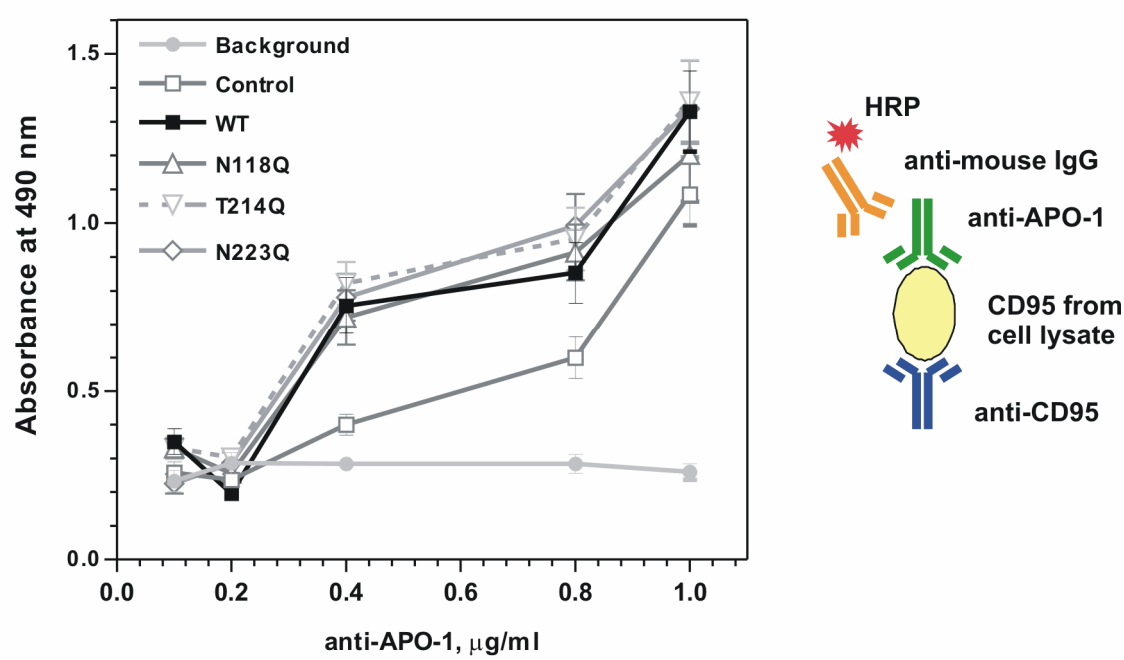

Figure 38. Binding of CD95 WT and glycosylation mutants to anti-APO-1 antibody. Cellular lysates from HeLa cells stably transfected with CD95 WT and glycosylation mutants were used for anti-APO-1 specific ELISA analysis. Anti-APO-1 was used at concentrations of 0.1, 0.2, 0.4, 0.8 and 1 μg/ml.

We determined that CD95 (WT) and glycosylation mutants were bound to the anti-APO-1 antibody with a similar efficiency at different concentrations of anti-APO-1. Thus, HeLa cells stably transfected with glycosylation mutants could be used to analyze DISC formation and cell death sensitivity.

3.8.4.7. Analysis of CD95-induced death in stable cell lines overexpressing CD95 glycosylation mutants

To analyze the influence of glycosylation on CD95-induced of cell death HeLa cells stably transfected with CD95 (WT) or glycosylation mutants were treated with 500 ng/ml of anti-APO-1 for 24 and 48 hours. To control specificity of the induced cell death another cell death inducer staurosporine was used as a positive control. Cell death was analyzed by PI-staining. All cell lines showed a similar level of cell death upon treatment with staurosporine (Fig. 39A). However, upon anti-APO-1 treatment a slightly higher level of CD95-induced cell death was detected in HeLa cells expressing CD95 (WT) in comparison with HeLa cells expressing CD95 glycosylation mutants (Fig. 39B).

3.8.4.8. DISC formation

To check if the observed differences in CD95-induced cell death are due to diminished CD95 signaling, DISC formation at the different time points was investigated for HeLa cell lines stably transfected with CD95 WT and glycosylation mutants. Three time points 10, 30 and 60 minutes were checked. Untransfected HeLa cells which contain endogenous CD95 were used as a control for DISC formation. The amount of the endogenous CD95 is at least ten times smaller than in HeLa cell line stably transfected with CD95 (WT) (Neumann et al., in press).

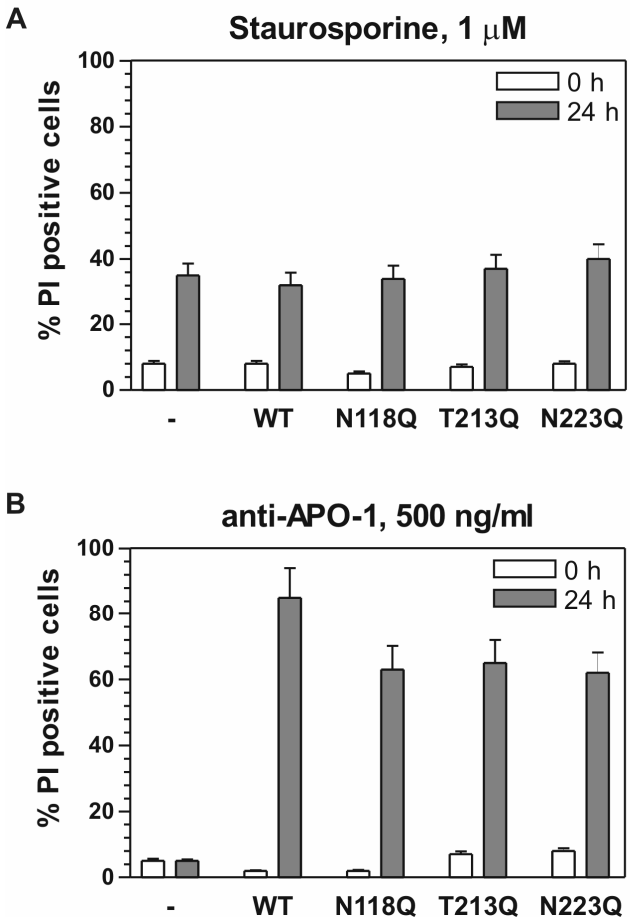

Figure 39. CD95-induced cell death in HeLa cells stably transfected with CD95 (WT) and glycosylation mutants. Apoptotic cell death was measured with propidium iodide staining in control untransfected HeLa cells and HeLa cells stably transfected with CD95 (WT) and glycosylation mutants. **A**. Cells were treated with staurosporin to induce intrinsic apoptosis as a control for CD95-induced cell death. **B.** Cells were treated with 500 ng/ml of anti-APO-1 antibody to induce CD95-specific apoptosis.

It was found that in HeLa cells stably transfected with CD95 (N118Q) glycomutant the amount of the CD95 DISCs formed at the latest time points are similar to those of CD95 (WT) and other glycosylation mutants (Fig, 40). However, the kinetic of procaspase-8 activation appeared slower in case of the CD95 (N118Q) glycomutant (Fig, 40, Lysates panel). Thus, slower kinetics of caspase-8 activation were observed at the DISC formed with glycosylation mutants.

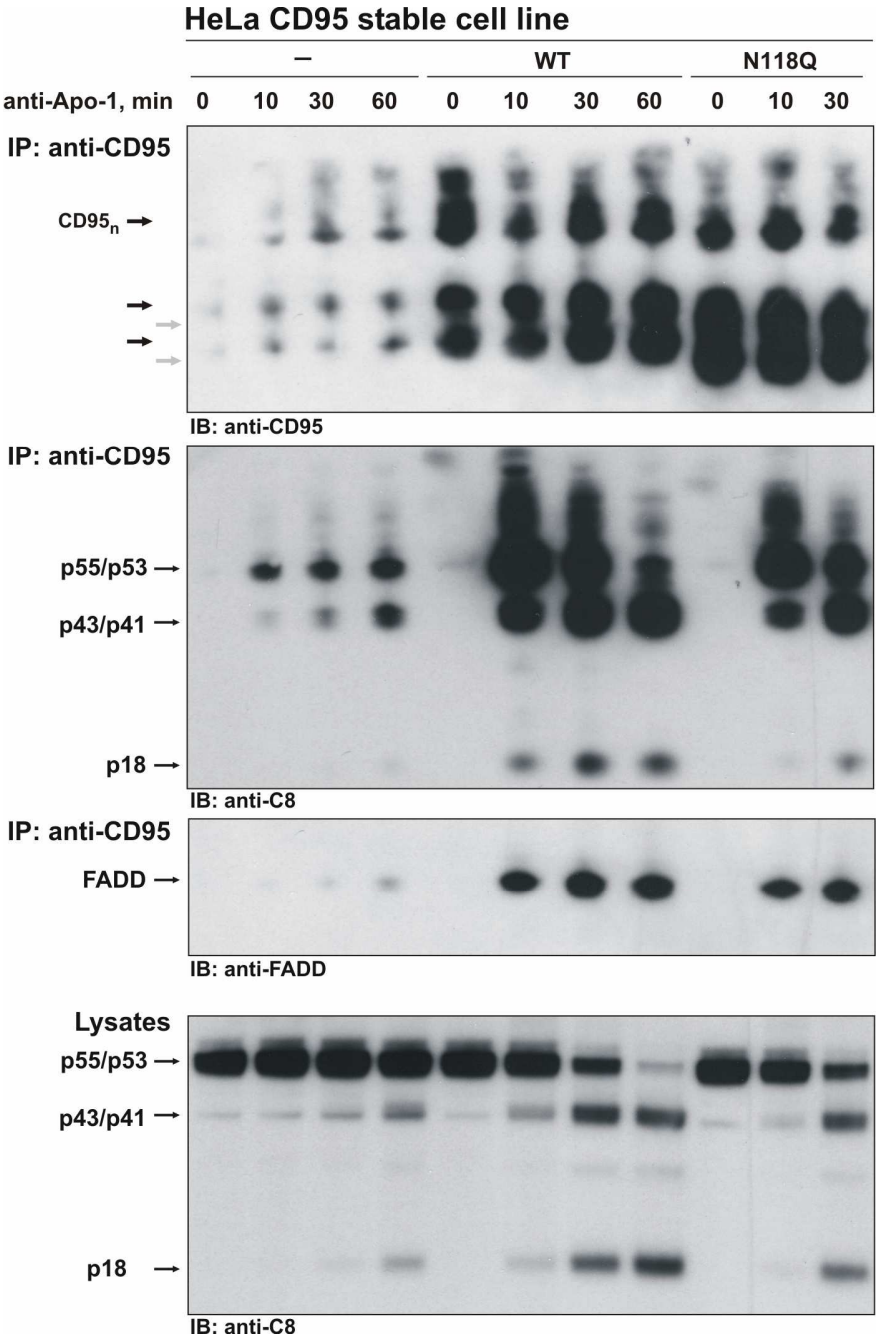

Figure 40. DISC formation. CD95 DISCs were analyzed after treatment with 500 ng/ml of anti-APO-1 antibody for the indicated time points. Western blot analyses were performed with antibodies against CD95, procaspase-8 and FADD. CD95 bands in HeLa cells stably transfected with WT and glycomutated CD95 are indicated with black arrows, while glycomutated CD95 bands are indicated with grey arrows.

Taken together, the experimental results demonstrate that CD95 glycosylation plays a role in CD95 signaling by influencing DISC formation and CD95-induced cell death.

4. DISCUSSION

4.1. Possible reasons for the presence of different forms of CD95

Signaling of CD95 is one of the best-studied apoptotic signaling pathways. A lot of studies were performed to understand main CD95 mediated events such as DISC formation, procaspase-8 activation and signaling in Type I and Type II cells (Schmitz et al. 1999). CD95 exists as 45 and 55 kDa forms recognized by C20 antibodies in Type I cells and as one form in Type II cells (Fig. 13). The nature of these forms is poorly understood but all of them are capable of forming the DISC. There are two possible reasons for the presence of different receptor forms – alternative splicing and posttranslational modifications.

4.2. Alternative splicing of CD95 is not the reason for the presence of two CD95 forms

It was shown that alternative splicing does not contribute to the presence of several CD95 protein forms in the investigated cell lines. RT-PCR analysis of mRNA purified from these cell lines revealed the same PCR products in the case of all primer combinations used (Fig. 15). Additional evidence against alternative splicing was that transient overexpression of CD95 in HeLa and Cos1 cells resulted in the presence of two CD95 bands. Since CD95 was expressed from a plasmid containing a complete gene without introns, alternative splicing can be ruled out. Therefore, only posttranlational modifications of CD95 could explain the presence of two different CD95 bands.

4.3. Analysis of possible modifications of CD95: proteolytic cleavage, phosphorylation, mannosylation, palmitoylation and glycosylation

The possibility of CD95 proteolysis which might result in the second lower band in Type I cells also was not excluded. The presence of a Type I specfic protease might explain the second 45 kDa band. CD95 was published to be cleaved by MMP7 (Strand et al. 2004). MMP7 is produced by the tumour cells themselves at early stages of tumour development. Treatment of MMP7-positive tumour cells with MMP7-antisense oligonucleotides led to an increase in CD95-mediated apoptosis sensitivity

(Strand et al. 2004). Processing of CD95 by MMP7 results in a smaller differences in molecular mass of the CD95 than the two forms observed in Type I cells. Therefore, the proteolytic cleavage by MMP7 was excluded as a reason for the two forms of CD95 in Type I cells.

The possibility of CD95 proteolitic cleavage was analyzed and many potential sites for different proteases were found. Nevertheless, no proteases were found to cleave CD95 with the threshold of equal or higher 0.5 (Fig. 14). Hence, proteolytic cleavage of CD95 was not addressed in more detail. Therefore other reasons for two CD95 bands were checked.

Detailed understanding of phosphorylation of CD95 is missing. CD95 is reported to be phosphorylated intracellulary and extracellulary (Lautrette et al. 2006; Eberle et al. 2007) (Fig. 17 and 18). The potential intracellular phosphorylation sites located predominantly in the DD of CD95 and might influence apoptotic signaling *via* modulation of the binding of adaptor proteins. One of the potential extracellular phosphorylation sites is located in PLAD. Therefore, phosphorylation of this site may directly modulate CD95L-independent oligomerisation of CD95 and apoptosis signaling by blocking pre-association of the receptors. Two others are located in the ligand-binding region. Phosphorylation at this area might modulate CD95L binding to the receptor. CD95 phosphorylation was analyzed before in our laboratory by means of phospho-specific antibodies. CD95 phosphorylation was not detected by this approach (T. Mock, Diploma thesis). The method of analysis used is very sensitive to a number of conditions including the quality of phospho-specific antibodies. However, it leads not always to a proper detection of phosphorylated residues in proteins. To exclude phosphorylation as the reason for different CD95 forms Pro-Q Diamond staining was applied to analyze CD95 phosphorylation in HeLa cells in which overexpression of two forms of the receptor had been detected. Pro-Q Diamond staining is highly specific and can detect phosphate groups at the scale of several nanogramms of phosphorylated protein (Schabacker et al. 2006). Analysis with the Pro-Q Diamond staining proved that phosphorylation was not the reason for the presence of several forms of CD95. This allowed us to concentrate further on other types of posttranslational modifications – mannosylation, palmitoylation and glycosylation.

Bioinformatics analysis revealed no potential C-mannosylation sites with a probability score higher then 0.5 (Fig. 19). Several potential palmitoylation (Fig. 20)

and N- and O-glycosylation sites were predicted (Fig. 21 and 22). Recent studies revealed that CD95 is a palmitoylated protein and that CD95 palmitoylation facilitates induction of apoptosis. Formation of CD95 SDS-stable aggregates has been shown to be regulated by palmitoylation of CD95 at cysteine 199 and was suggested to be important for caspase-8 activation (Feig et al. 2007). However, palmitoylation of CD95 does not result in large differences in relative molecular mass, as mutants of the palmitoylated site did not have an altered mobility in SDS-PAGE (Feig et al. 2007). These results rules out palmitoylation as the reason for two forms of CD95. Taken together, mannosylation and palmytoilation could be excluded. Therefore our main focus was on glycosylation, since this modification might potentially lead to the largest difference in molecular mass of the modified proteins.

4.4. Glycosylation of CD95 is important for DISC formation and procaspase-8 activation

Several methods to obtain the deglycosylated receptor including enzymatic deglycosylation and inhibition of CD95 glycosylation and the generation of CD95 mutants on glycosylation sites were used in the present work to study the contribution of glycans to the presence of different forms of CD95 as well as to CD95 signaling in Type I and Type II cells.

Therefore, we analyzed CD95 patterns in Type I and Type II cells with N-glycosidase F. This enzyme cleaves all N-glycans from the protein. All cell lines contain highly glycosylated CD95. Upon treatment with the N-glycosidase F two forms of CD95 were detected in Type I cells. Our results suggest, that another modification is responsible for the presence of different forms of the receptor in Type I cells. Due to the high level of deglycosylation of many cellular receptors and unspecific cell death N-glycosidase F could not be applied for the cell culture experiments. Thus, to study the role of N-glycosylation in cell culture another approach based on inhibition of N-glycosylation was used. Tunicamycin inhibits N-glycosylation completely. Upon treatment with tunicamycin, an increased CD95-independent cell death was observed. Moreover, DISC formation could not be compared in untreated and tunicamycin-treated cells since tunicamycin treatment led to inhibition of translation. This resulted in downregulation of c-FLIP expression. c-FLIP is the central inhibitor of procaspase-8 activation at the DISC. Low expression

of c-FLIP resulted in an increased level of procaspase-8 activation and, therefore, in an increased level of CD95-induced apoptosis (Krueger et al. 2001; Krueger et al. 2001; Krammer et al. 2007). Thus, tunicamycin could not be applied for our functional studies *in vitro*.

Until recently, only few studies addressed the role of N-glycosylation of CD95 in the context of sensitivity and resistance to induction of apoptosis. The high sialylation level of CD95 in different cell lines was suggested to be a factor defining resistance (Peter et al. 1995; Keppler et al. 1999). To address this question in detail partial deglycosylation was performed using *Vibrio Cholerae* neuraminidase (VCN) in SKW6.4 and Hut78 cells. Recombinant VCN enzyme preferentially hydrolyzes α(2-3)-linkages of sialic acid from the glycans. VCN treatment was shown to lead to reduced procaspase-8 activation at the DISC. Thus, sialic acids in the CD95 glycans might play an important role in proper DISC formation and procaspase-8 activation. However, signaling downstream from the DISC using VCN could not be analyzed because treatment of cells with this enzyme resulted in a high level of CD95-independent unspecific cell death, which could result from desialylation of many of the surface receptors.

Application of an inhibitor of glycosylation, DMM, was an alternative to analyze the influence of N-glycosylation and in particular, the role of complex and hybrid N-glycans on CD95 function. This inhibitor does not block high mannose N-glycans formation. The presence of high mannose N-glycans is sufficient for proper folding of proteins and therefore does not induce ER stress. No toxic effects of DMM were observed on the cells. This observation suggests that complex and hybrid glycans on CD95 are needed for proper DISC formation and fine CD95 apoptotic signaling.

Analysis of glycosylation patterns of the receptor using enzymatic and inhibitory approaches was not applicable due to the unspecific deglycosylation of many cellular proteins that resulted in a high degree of CD95-independent cell death. To specifically study CD95 glycosylation site-deficient glycosylation mutants were generated by site-directed mutagenesis.

All methods together showed that deglycosylation of CD95 did not significantly impair CD95 DISC formation but diminished procaspase-8 activation. These effects were detectable only upon stimulation with low concentrations of CD95 antagonists. Under these so-called threshold conditions the amount of CD95 DISCs is low and the amount of caspase-8 just high enough to trigger apoptosis (Bentele et al. 2004;

Lavrik et al. 2007). Therefore, the decrease of caspase-8 caused by deglycosylation of CD95 might result in a blockage of apoptosis.

Inhibitors of glycosylation with an exception of tunicamycin as well as glycosylation mutants demonstrated a decrease of procaspase-8 activation at the DISC. A reduction of CD95-induced apoptosis was observed upon treatment with DMM, tunicamycin and VCN. In contrast to tunicamycin and VCN, DMM did not possess any toxicity towards the cells tested. Upon DMM treatment combined with CD95 stimulation cell death was mediated by deglycosylated CD95. In contrast, treatment with VCN and tunicamycin was toxic to the cells and the effects on cell death mediated by deglycosylated CD95 were difficult to consider independently from toxicity.

Recently, it was reported that O-glycosylation of TRAILR1 (DR4) and TRAILR2 (DR5) plays a central role in sensitivity and resistance regulation towards TRAIL-induced apoptosis (Wagner et al. 2007). Only one predicted O-glycosylation T214 site was found for CD95. T214 was not glycosylated and did not play any role in CD95 function (Fig. 41). CD95 glycomutant T214Q as well as N223Q showed the same CD95 protein pattern upon SDS-PAGE analysis and no influence on DISC formation and CD95-mediated cell death. Furthermore, N-glycosylation of CD95 does not have a strong effect in the regulation of CD95-induced apoptosis. These results show that CD95 is not modified at the potential intracellular glycosylation sites T214 and N223. The CD95 extracellular glycosylation sites N118 and N136 were addressed in more detail.

Analysis of cell death showed a different kinetics upon anti-APO-1 stimulation. This revealed that cells with mutation CD95 (N118Q) showed slower kinetics of caspase-8 activation compared to cells with CD95 (WT). Moreover, this phenomenon was specific for cells expressing the CD95 (N118Q) mutant. A control experiments with staurosporine, which induces intrinsic apoptosis, showed an equal level of cell death in all cell lines. Formation of the DISC upon anti-APO-1 stimulation was diminished in the case of cells expressing the CD95 (N118Q) mutant compared to cells expressing CD95 (WT) receptors and intracellular glycosylation sites mutants.

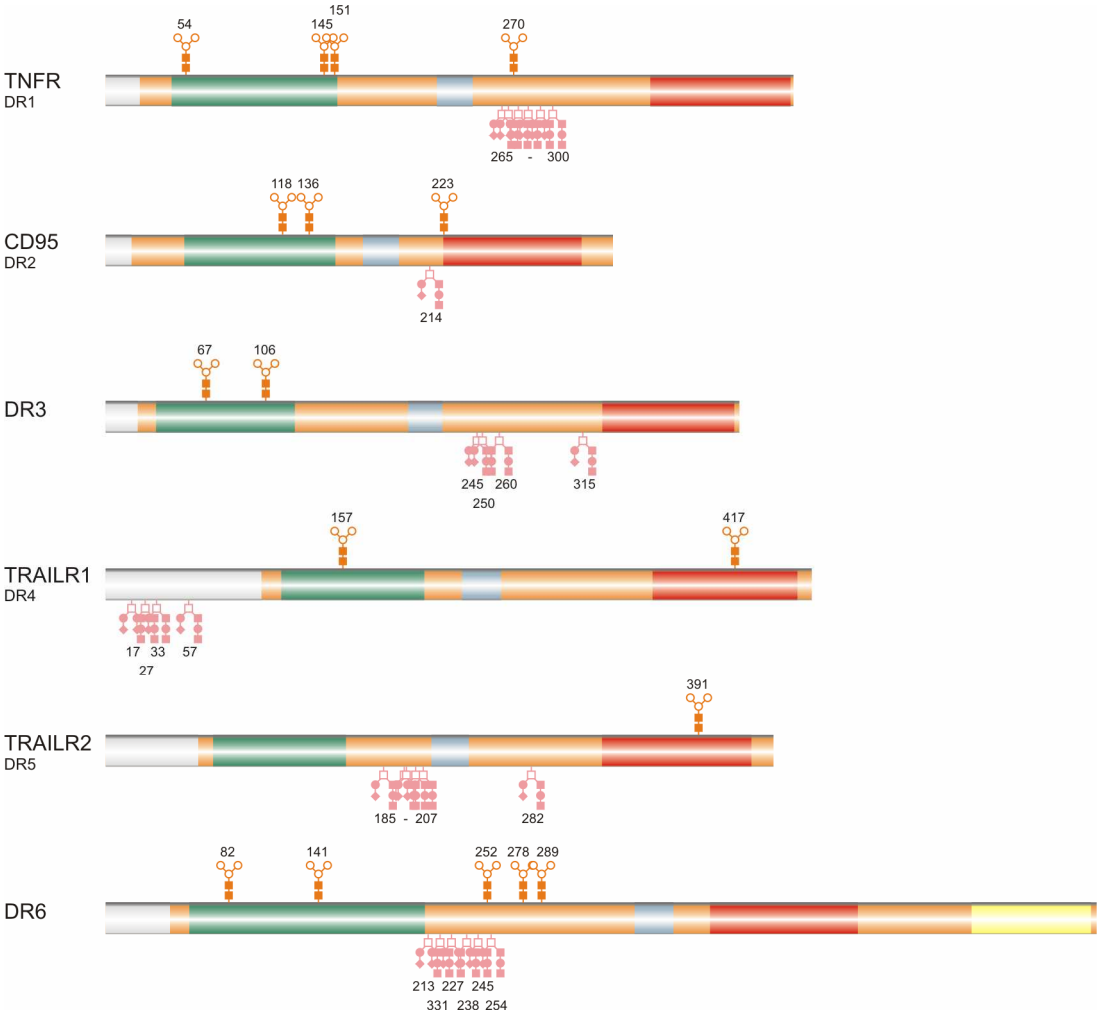

Figure 41. Predicted N- and O-glycosylation sites in all members of the death receptors family. Results of N-glycosylation and O-glycosylation sites in death receptors were predicted by NetNGlyc 1.0 and NetOGlyc 3.1 servers, respectively. Cysteine-rich domains are in green, transmembrane domains are in light blue, death domains are in red. The CARD-like domain at the C-terminus of DR6 was found by bioinformatic analysis and is depicted in yellow. Potential N-glycosylation and O-glycosylation sites are shown as schematic orange and pink oligosaccharides above and below the protein, respectively.

4.5. Only one glycosylation site of CD95 is conservative between species

Analysis of the alignment of 16 sequences of CD95 from different species indicates that the N residue of the first N-glycosylation site, which corresponds to N118 in human CD95, is the most conserved one, while the second and third N-glycosylation sites, which correspond to N136 and N223 in human CD95, are less conserved (Fig. 42).

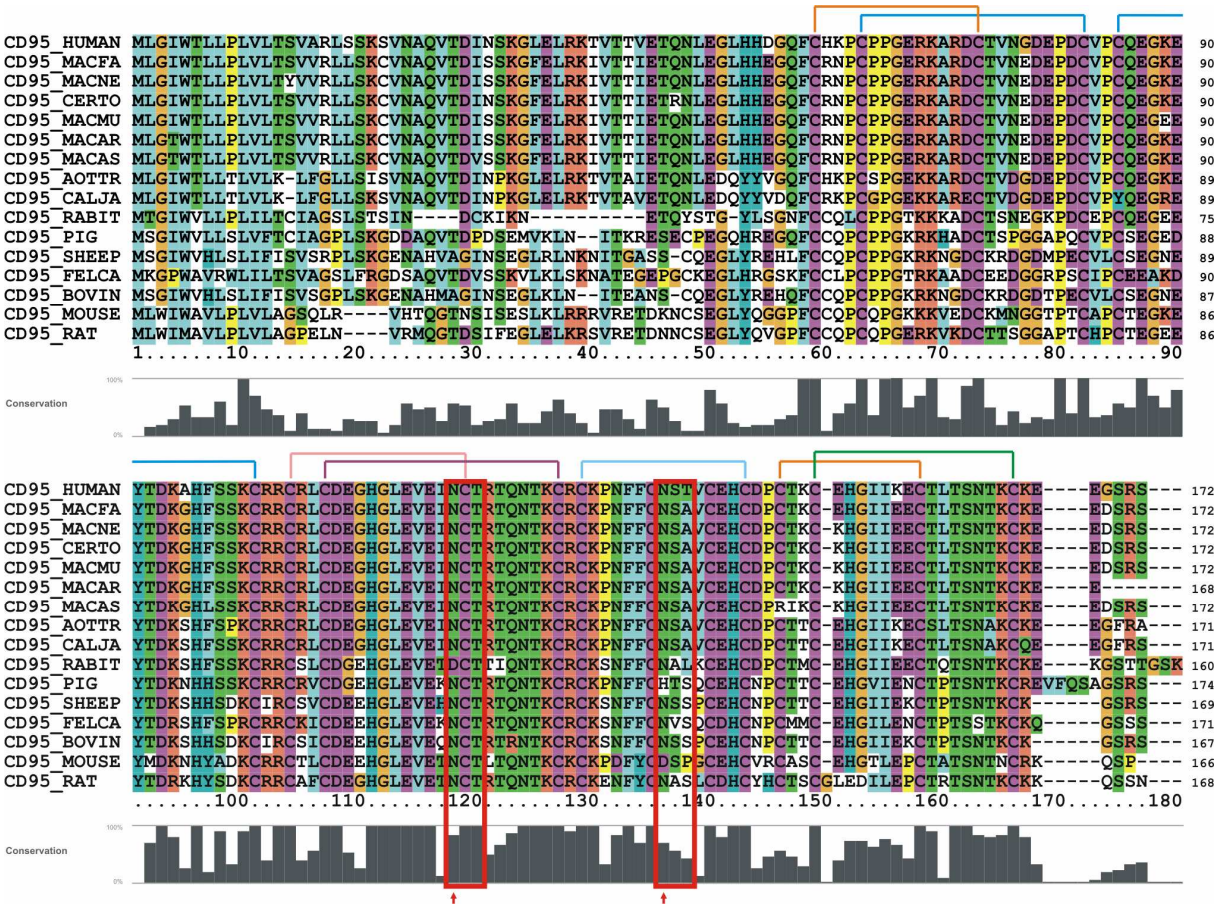

Figure 42. Alignment of CD95 sequences from different organisms. ClustalX2 sequence alignment of CD95 ECD across different species. Sequence abbreviations: *Homo sapiens* (HUMAN); *Macaca fascicularis* (MACFA); *Macaca nemestrina* (MACNE); *Cercocebus torquatus* (CERTO); *Macaca mulatta* (MACMU); *Macaca arctoides* (MACAR); *Macaca assamensis* (MACAS); *Aotus trivirgatus* (AOTTR); *Callithrix jacchus* (CALJA); *Oryctolagus cuniculus* (RABIT); *Sus scrofa* (PIG); *Ovis aries* (SHEEP); *Felis catus* (FELCA); *Bos taurus* (BOVIN); *Mus musculus* (MOUSE) and *Rattus norvegicus* (RAT). Sequences from NCBI Protein databank. Color lines on the top of the alignment indicate Cysteine residues forming disulphide bonds in human CD95. Asn-Xaa-Ser/Thr sequons are indicated by red boxes.

Moreover, Asn-Xaa-Ser/Thr sequon in case of the second N-glycosylation site N136 is less conserved. Only in three organisms from all that were analyzed the probability of N136 residue to be potentially glycosylated is given (Fig. 43).

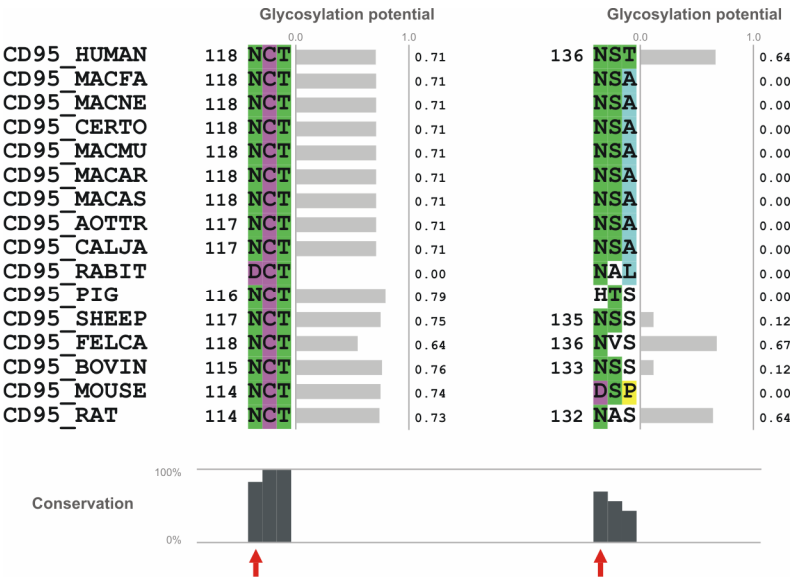

Figure 43. Prediction of glycosylation potentials for two extracellular CD95 glycosylation sites. Probability of glycosylation (glycosylation potential) of sequons at positions 118 and 136 in human CD95 and their analogues in CD95 from other species was calculated by NetNGlyc 1.0 server.

4.6. *In silico* modelling of CD95 DISC core structure and network showed that both glycosylation sites might play and important role in CD95 signaling

The possible explanation for the role of CD95 glycans in initial CD95 DISC formation and later on in the formation of a complex CD95 DISC network on the membranes could be obtained from 3D modeling of the CD95 system (Shatnyeva et al. Manuscript in preparation and Kubarenko et al. Unpublished data and personal communication).

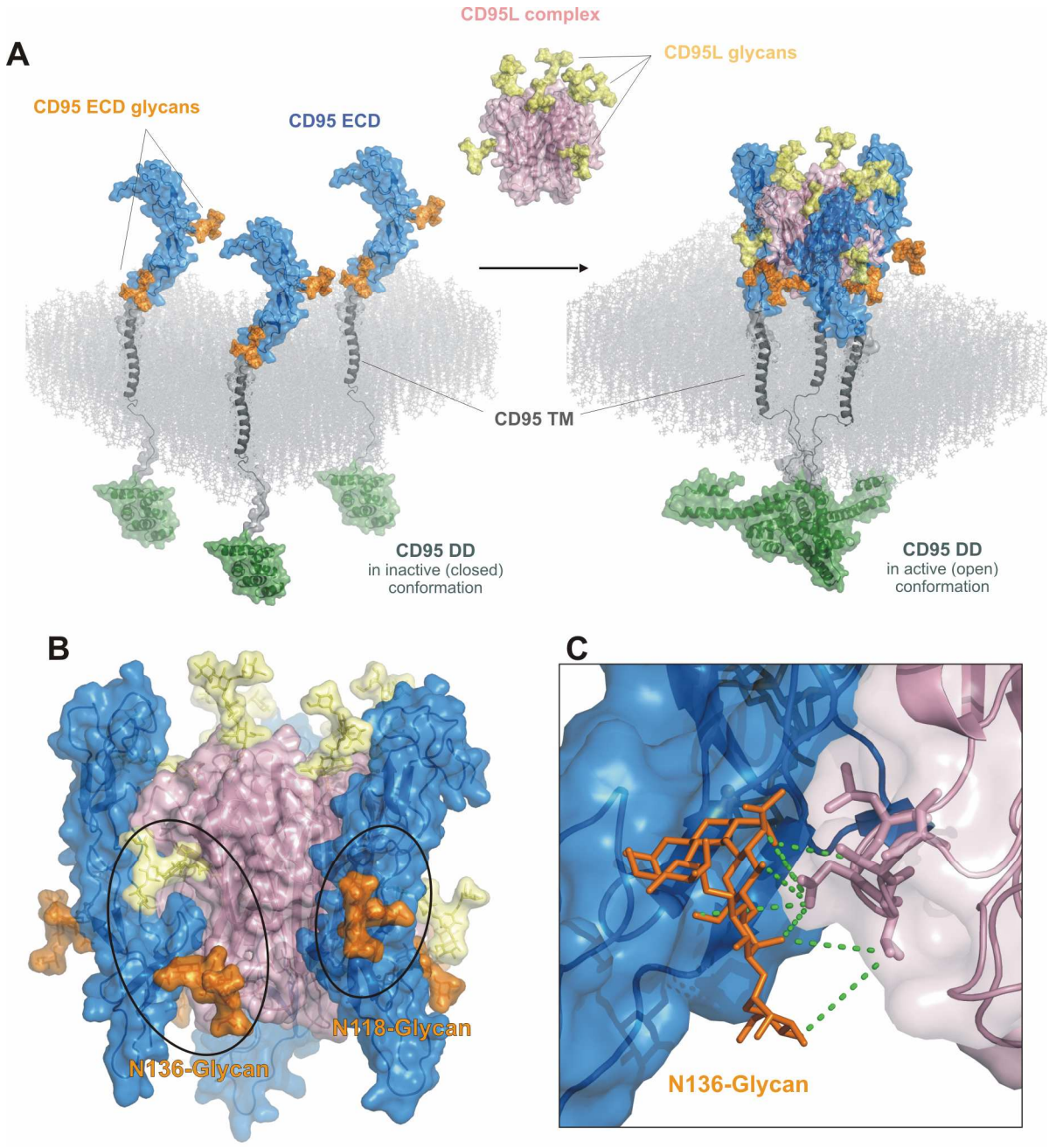

Figure 44. Formation of the human CD95 DISC core structure. A. Formation of a CD95-CD95L trimer upon binding of CD95 ECDs to the CD95L ECDs. **B**. Close look on the interface between CD95 and CD95L ECDs. Glycan attached to the N118 of CD95 is far away from CD95L ECD. **C**. Glycan attached to the N136 of CD95 is in a close proximity to CD95L ECD and could form extensive hydrogen bonds (green dotted lines) with the residues 200-204 of CD95L. In all cases: light blue - CD95 ECD (ectodomain); orange - glycan, attached to CD95 ECD; grey - CD95 TM (transmembrane domain); green - CD95 DD (death domain); light pink - CD95L ECD; light yellow - glycans, attached to CD95L ECD; membrane is depicted in light grey. Pictures were adopted with kind permission from Dr. A. Kubarenko (Shatnyeva et al. Manuscript in preparation).

The presence of a CD95L trimeric complex might lead to the formation of the CD95 DISC core structure. This structure is composed of three molecules of CD95 and three CD95L (Fig. 44A). Upon formation of this CD95 DISC core structure, a glycan moiety attached to N136 of CD95 could be important for complex formation and/or stability a it is located in close proximity to one of the CD95L molecules (Fig. 44B). It could form extensive hydrogen bonds with residues 200-204 of CD95L (Fig. 44C). At the same time, a glycan attached to the N118 residue of CD95 is most probably not important for the formation and/or stability of CD95 DISC core structure. It is located more distal from the CD95-CD95L interface (Fig. 44B).

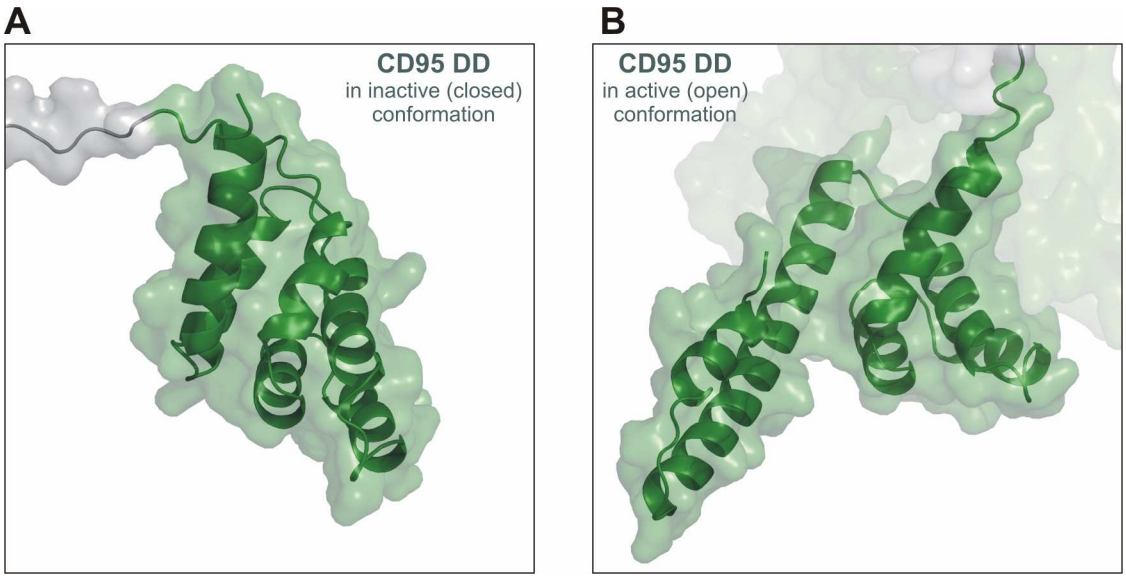

Figure 45. Structure of the closed and open forms of human CD95 DD. A. CD95 DD in closed (inactive) conformation in the free receptor. **B.** CD95 DD in an open (active) conformation in the CD95-CD95L complex. Pictures were adopted with kind permission from Dr. A. Kubarenko (unpublished data and personal communication).

CD95 DISC core structure formation leads to interaction of DD on the other side of the membrane of corresponding CD95 molecules (Fig. 44A). This interaction results in the stabilization of the “open” (active) conformation of DD (Fig. 44B and 45B) capable to interact with FADD as it was proposed by Scott et al. 2009(Scott et al. 2009). Moreover, in the intracellular core structure of CD95 DISC formed by three “open” CD95 DDs (Fig. 44A) exposed extended helices of death domains could interact with similar helices of the death domains of other CD95 DISC core structures. Assembly of CD95-CD95L trimers results in the formation of a branched 2D CD95 network on the membrane with six CD95 DISC complexes forming one network (Fig. 46).

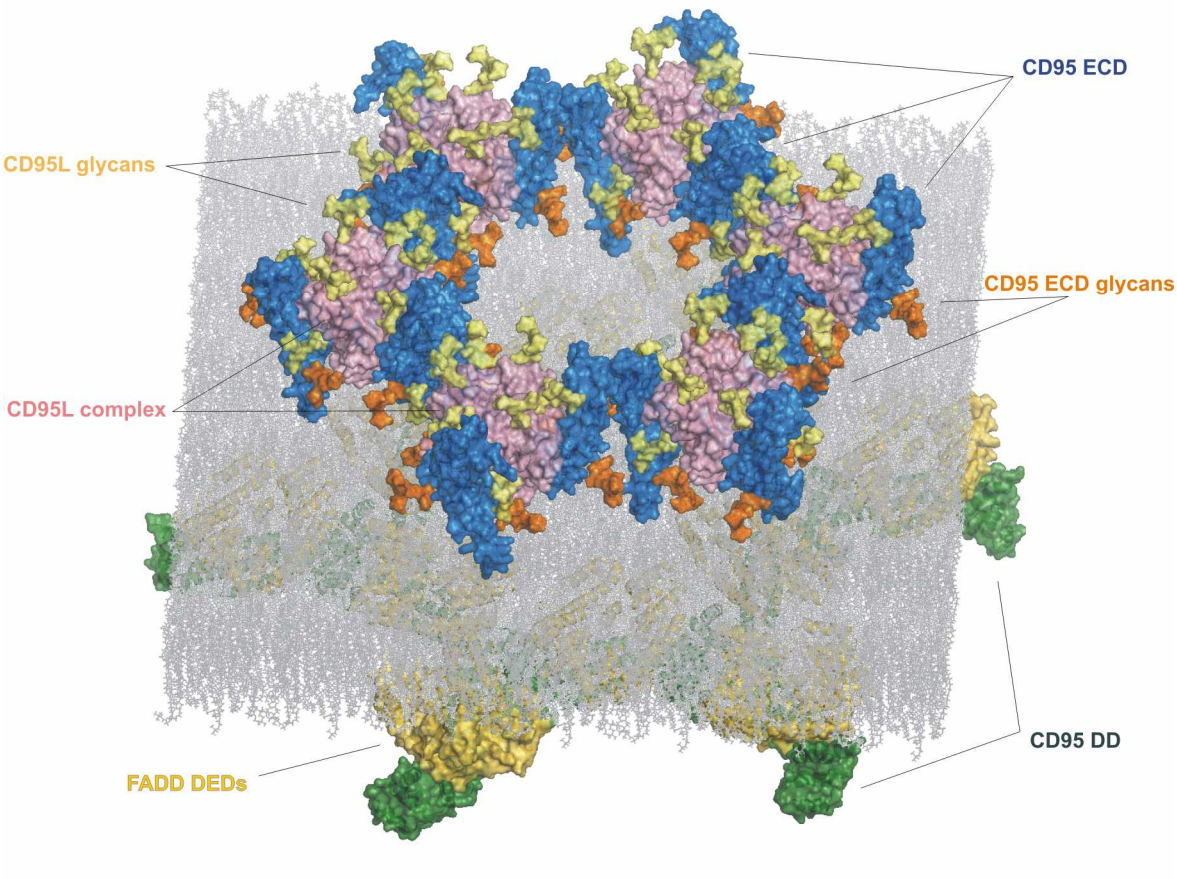

Figure 46. Formation of a potential human CD95 DISC network. Structure of six CD95-CD95L complexes on a membrane forming the basic element of a CD95 DISC network. Light blue - CD95 ECD (ectodomain); orange - glycan, attached to CD95 ECD; grey - CD95 TM (transmembrane domain); green - CD95 DD (death domain); light pink - CD95L ECD; light yellow - glycans, attached to CD95L ECD; dark yellow - FADD DED (death effector domains); membrane is in the sticks representation in light grey. Pictures were adopted with kind permission from Dr. A. Kubarenko (unpublished data and personal communication).

The model of the CD95 DISC interaction network is in an agreement with the formation of single ring-like structures upon CD95 DD - FADD DD. As it could be seen from the model of CD95 DISC interaction in the network glycans attached to N118 distant from CD95-CD95L interface in the single DISC core complex could be important for the interactions between two DISCs (Fig. 47).

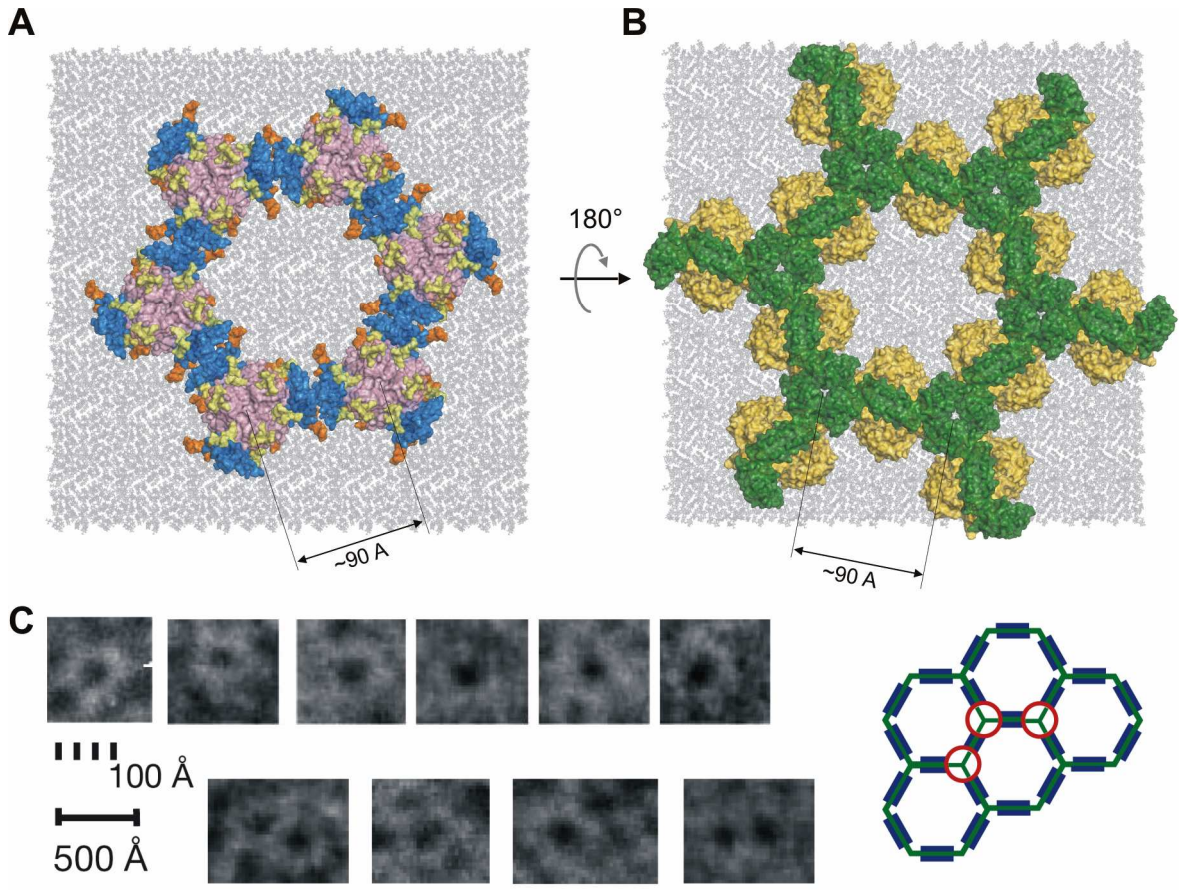

Figure 47. Extracellular and intracellular interactions upon formation of the CD95 DISC network. A. View of the basic elements of the CD95 DISCs network from the extracellular space where CD95 and CD95L ECDs are located. **B**. View of the basic elements of the CD95 DISCs network from the intracellular space where CD95 DD and FADD are located. Distance between centers of DISCs approximately 90 Å. In all cases: light blue - CD95 ECD (ectodomain); orange - glycand, attached to CD95 ECD; grey - CD95 TM (transmembrane domain); green - CD95 DD (death domain); light pink - CD95L ECD; light yellow - glycans, attached to CD95L ECD; dark yellow - FADD DED (death effector domain); membrane is in the sticks representation in light grey. Pictures were adopted with kind permission from Dr. A. Kubarenko (unpublished data and personal communication). **C**. Formation of DISC-like structures and proposed mechanism of CD95 network formation adopted from (Scott et al. 2009).

Open cavities and interacting extended helices of two CD95 DDs from neighboring CD95 DISC core complexes provide the binding region for the two FADD molecules (Fig. 48).

While formation of the CD95 DISCs network is initiated by interaction of open CD95 DD of different CD95 DISC core structures inside the cell, the glycan attached to the residue of CD95 ECD could be important for the stabilization of the DISC-DISC

interaction. Removal of this glycan upon mutation of N118 to Q could lead to decreased stability of the CD95 DISC network and as a result less stable binding of procaspase-8 to its binding site at the CD95 DD - FADD interface and to less rapid caspase-8 activation.

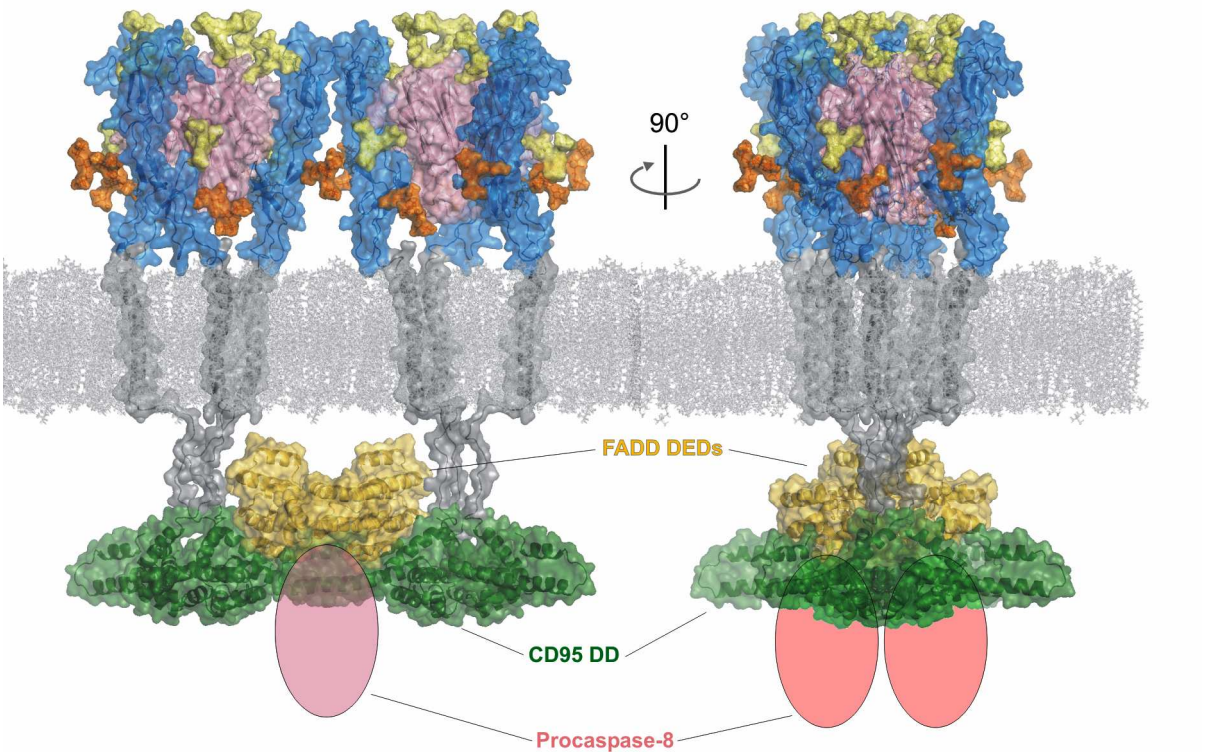

Figure 48. Composition and interactions in the CD95 DISC. Figure: light blue - CD95 ECD (ectodomain); orange - glycans, attached to CD95 ECD; grey - CD95 TM (transmembrane domain); green - CD95 DD (death domain); light pink - CD95L ECD; light yellow - glycans, attached to CD95L ECD; dark yellow - FADD DED (death effector domains); pink – schematic representation of procaspase-8. Pictures were adopted with kind permission from Dr. A. Kubarenko (Shatnyeva et al. Manuscript in preparation).

Our findings provide evidence that the CD95 glycostructure can contribute to DISC formation and a potential DISC network and, thus, to the threshold of apoptotic signaling defining cell death initiation. This regulation might be important for cancer cells when a subtle difference in the amount of activated caspase-8 regulates life or death of the cell (Lavrik et al. 2007). Further insight into the organisation of CD95 and the DISC in the future will also come from sophisticated direct microscopy observation.

5. REFERENCES

Acehan, D., X. Jiang, et al. (2002). "Three-dimensional structure of the apoptosome: implications for assembly, procaspase-9 binding, and activation." Mol. Cell **9**(2): 423-32.

Akama, T. O., H. Nakagawa, et al. (2002). "Germ cell survival through carbohydrate-mediated interaction with Sertoli cells." Science **295**(5552): 124-7.

Algeciras-Schimnich, A., L. Shen, et al. (2002). "Molecular ordering of the initial signaling events of CD95." Mol. Cell. Biol. **22**(1): 207-20.

Ameisen, J. C. (2001). "Apoptosis subversion: HIV-Nef provides both armor and sword." Nat Med **7**(11): 1181-2.

Arthos, J., C. Cicala, et al. (2002). "The role of the CD4 receptor versus HIV coreceptors in envelope-mediated apoptosis in peripheral blood mononuclear cells." Virology **292**(1): 98-106.

Badley, A. D., A. A. Pilon, et al. (2000). "Mechanisms of HIV-associated lymphocyte apoptosis." Blood **96**(9): 2951-64.

Bajorath, J. (1998). "Detailed comparison of two molecular models of the human CD40 ligand with an x-ray structure and critical assessment of model-based mutagenesis and residue mapping studies." J. Biol. Chem. **273**(38): 24603-9.

Bajorath, J. (1999). "Analysis of Fas-ligand interactions using a molecular model of the receptor-ligand interface." J. Comput. Aided Mol. Des. **13**(4): 409-18.

Bajorath, J. (1999). "Identification of the ligand binding site in Fas (CD95) and analysis of Fas-ligand interactions." Proteins **35**(4): 475-82.

Bajorath, J., N. J. Chalupny, et al. (1995). "Identification of residues on CD40 and its ligand which are critical for the receptor-ligand interaction." Biochemistry **34**(6): 1833-44.

Banner, D. W., A. D'Arcy, et al. (1993). "Crystal structure of the soluble human 55 kd TNF receptor-human TNF beta complex: implications for TNF receptor activation." Cell **73**(3): 431-45.

Barnhart, B. C., E. C. Alappat, et al. (2003). "The CD95 type I/type II model." Semin. Immunol. **15**(3): 185-93.

Behrmann, I., H. Walczak, et al. (1994). "Structure of the human APO-1 gene." Eur. J. Immunol. **24**(12): 3057-62.

Bentele, M., I. Lavrik, et al. (2004). "Mathematical modeling reveals threshold mechanism in CD95-induced apoptosis." J. Cell. Biol. **166**(6): 839-851.

Blom, N., S. Gammeltoft, et al. (1999). "Sequence and structure-based prediction of eukaryotic protein phosphorylation sites." J. Mol. Biol. **294**(5): 1351-62.

Blom, N., T. Sicheritz-Ponten, et al. (2004). "Prediction of post-translational glycosylation and phosphorylation of proteins from the amino acid sequence." Proteomics **4**(6): 1633-49.

Bodmer, J. L., K. Burns, et al. (1997). "TRAMP, a novel apoptosis-mediating receptor with sequence homology to tumor necrosis factor receptor 1 and Fas(Apo-1/CD95)." Immunity **6**(1): 79-88.

Bogin, O., M. Kvansakul, et al. (2002). "Insight into Schmid metaphyseal chondrodysplasia from the crystal structure of the collagen X NC1 domain trimer." Structure **10**(2): 165-73.

Boldin, M. P., T. M. Goncharov, et al. (1996). "Involvement of MACH, a novel MORT1/FADD-interacting protease, in Fas/APO-1- and TNF receptor-induced cell death." Cell **85**(6): 803-15.

Boldin, M. P., E. E. Varfolomeev, et al. (1995). "A novel protein that interacts with the death domain of Fas/APO1 contains a sequence motif related to the death domain." J. Biol. Chem. **270**(14): 7795-8.

Bouillet, P. and A. Strasser (2002). "BH3-only proteins - evolutionarily conserved proapoptotic Bcl-2 family members essential for initiating programmed cell death." J. Cell. Sci. **115**(Pt 8): 1567-74.

Cantarel, B. L., P. M. Coutinho, et al. (2009). "The Carbohydrate-Active EnZymes database (CAZy): an expert resource for Glycogenomics." Nucleic Acids Res **37**(Database issue): D233-8.

Cascino, I., C. Ballerini, et al. (1998). "Fas gene polymorphisms are not associated with systemic lupus erythematosus, multiple sclerosis and HIV infection." Dis. Markers **13**(4): 221-5.

Cascino, I., G. Fiucci, et al. (1995). "Three functional soluble forms of the human apoptosis-inducing Fas molecule are produced by alternative splicing." J. Immunol. **154**(6): 2706-2713.

Cha, S. S., B. J. Sung, et al. (2000). "Crystal structure of TRAIL-DR5 complex identifies a critical role of the unique frame insertion in conferring recognition specificity." J. Biol. Chem. **275**(40): 31171-7.

Chamond, R. R., A. J.C., et al. (1999). "Apoptosis and disease." Alergol. Inmunol. Clin. **14**(6): 367-374.

Chang, D. W., Z. Xing, et al. (2003). "Interdimer processing mechanism of procaspase-8 activation." EMBO J. **22**(16): 4132-42.

Chang, D. W., Z. Xing, et al. (2002). "c-FLIP(L) is a dual function regulator for caspase-8 activation and CD95-mediated apoptosis." EMBO J. **21**(14): 3704-3714.

Chang, L., H. Kamata, et al. (2006). "The E3 ubiquitin ligase itch couples JNK activation to TNFalpha-induced cell death by inducing c-FLIP(L) turnover." Cell **124**(3): 601-13.

Cheng, J., C. Liu, et al. (1995). "Characterization of human Fas gene. Exon/intron organization and promoter region." J Immunol **154**(3): 1239-45.

Chinnaiyan, A. M., K. O'Rourke, et al. (1995). "FADD, a novel death domain-containing protein, interacts with the death domain of Fas and initiates apoptosis." Cell **81**(4): 505-12.

Chinnaiyan, A. M., K. O'Rourke, et al. (1996). "Signal transduction by DR3, a death domain-containing receptor related to TNFR-1 and CD95." Science **274**(5289): 990-2.

Chu, K., X. Niu, et al. (1995). "A Fas-associated protein factor, FAF1, potentiates Fas-mediated apoptosis." Proc. Natl. Acad. Sci. USA **92**(25): 11894-8.

Chui, D., M. Oh-Eda, et al. (1997). "Alpha-mannosidase-II deficiency results in dyserythropoiesis and unveils an alternate pathway in oligosaccharide biosynthesis." Cell **90**(1): 157-67.

Colley, K. J. (1997). "Golgi localization of glycosyltransferases: more questions than answers." Glycobiology **7**(1): 1-13.

Cory, S. and J. M. Adams (2002). "The Bcl2 family: regulators of the cellular life-or-death switch." Nat. Rev. Cancer. **2**(9): 647-56.

Coutinho, P. M., E. Deleury, et al. (2003). "An evolving hierarchical family classification for glycosyltransferases." J. Mol. Biol. **328**(2): 307-17.

Cursi, S., A. Rufini, et al. (2006). "Src kinase phosphorylates Caspase-8 on Tyr380: a novel mechanism of apoptosis suppression." EMBO J. **25**(9): 1895-905.

de Bruin, E. C. and J. P. Medema (2008). "Apoptosis and non-apoptotic deaths in cancer development and treatment response." Cancer Treat Rev **34**(8): 737-49.

Dorrie, J., K. Sapala, et al. (2002). "Interferon-gamma increases the expression of glycosylated CD95 in B-leukemic cells: an inducible model to study the role of glycosylation in CD95-signalling and trafficking." Cytokine **18**(2): 98-107.

Duckert, P., S. Brunak, et al. (2004). "Prediction of proprotein convertase cleavage sites." Protein Eng. Des. Sel. **17**(1): 107-112.

Ea, C. K., L. Deng, et al. (2006). "Activation of IKK by TNFalpha requires site-specific ubiquitination of RIP1 and polyubiquitin binding by NEMO." Mol Cell **22**(2): 245-57.

Eberle, A., R. Reinehr, et al. (2007). "CD95 tyrosine phosphorylation is required for CD95 oligomerization." Apoptosis **12**(4): 719-729.

Eckhart, L., M. Henry, et al. (2001). "Alternative splicing of caspase-8 mRNA during differentiation of human leukocytes." Biochem. Biophys. Res. Commun. **289**(4): 777-81.

Edinger, A. L. and C. B. Thompson (2004). "Death by design: apoptosis, necrosis and autophagy." Curr. Opin. Cell. Biol. **16**(6): 663-9.

Eramo, A., M. Sargiacomo, et al. (2004). "CD95 death-inducing signaling complex formation and internalization occur in lipid rafts of type I and type II cells." Eur. J. Immunol. **34**(7): 1930-40.

Faccio, L., C. Fusco, et al. (2000). "Characterization of a novel human serine protease that has extensive homology to bacterial heat shock endoprotease HtrA and is regulated by kidney ischemia." J. Biol. Chem. **275**(4): 2581-8.

Falschlehner, C., C. H. Emmerich, et al. (2007). "TRAIL signalling: decisions between life and death." Int. J. Biochem. Cell. Biol. **39**(7-8): 1462-75.

Feig, C., V. Tchikov, et al. (2007). "Palmitoylation of CD95 facilitates formation of SDS-stable receptor aggregates that initiate apoptosis signaling." EMBO J. **26**(1): 221-231.

Fernandes-Alnemri, T., R. C. Armstrong, et al. (1996). "In vitro activation of CPP32 and Mch3 by Mch4, a novel human apoptotic cysteine protease containing two FADD-like domains." Proc. Natl. Acad. Sci. USA **93**(15): 7464-9.

French, L. E. and J. Tschopp (2003). "Protein-based therapeutic approaches targeting death receptors." Cell Death Differ. **10**(1): 117-23.

Fulda, S. (2009). "Caspase-8 in cancer biology and therapy." Cancer Lett. **281**(2): 128-33.

Fulda, S. and K. M. Debatin (2006). "Extrinsic versus intrinsic apoptosis pathways in anticancer chemotherapy." Oncogene **25**(34): 4798-811.

Golks, A., D. Brenner, et al. (2005). "c-FLIPR, a new regulator of death receptor-induced apoptosis." J. Biol. Chem. **280**(15): 14507-14513.

Goltsev, Y. V., A. V. Kovalenko, et al. (1997). "CASH, a novel caspase homologue with death effector domains." J. Biol. Chem. **272**(32): 19641-4.

Green, D. R. and J. C. Reed (1998). "Mitochondria and apoptosis." Science **281**(5381): 1309-12.

Gschwind, M. and G. Huber (1995). "Apoptotic cell death induced by beta-amyloid 1-42 peptide is cell type dependent." J. Neurochem. **65**(1): 292-300.

Hanahan, D. and R. A. Weinberg (2000). "The hallmarks of cancer." Cell **100**(1): 57-70.

Henkler, F., E. Behrle, et al. (2005). "The extracellular domains of FasL and Fas are sufficient for the formation of supramolecular FasL-Fas clusters of high stability." J. Cell. Biol. **168**(7): 1087-98.

Herbeuval, J. P., J. C. Grivel, et al. (2005). "CD4+ T-cell death induced by infectious and noninfectious HIV-1: role of type 1 interferon-dependent, TRAIL/DR5-mediated apoptosis." Blood **106**(10): 3524-31.

Himeji, D., T. Horiuchi, et al. (2002). "Characterization of caspase-8L: a novel isoform of caspase-8 that behaves as an inhibitor of the caspase cascade." Blood **99**(11): 4070-8.

Hong, H. Y., J. S. Choi, et al. (2008). "Detection of apoptosis in a rat model of focal cerebral ischemia using a homing peptide selected from in vivo phage display." J Control Release **131**(3): 167-72.

Hua, Z. C., S. J. Sohn, et al. (2003). "A function of Fas-associated death domain protein in cell cycle progression localized to a single amino acid at its C-terminal region." Immunity **18**(4): 513-21.

Huang, B., M. Eberstadt, et al. (1996). "NMR structure and mutagenesis of the Fas (APO-1/CD95) death domain." Nature **384**(6610): 638-41.

Hueber, A. O., A. M. Bernard, et al. (2002). "An essential role for membrane rafts in the initiation of Fas/CD95-triggered cell death in mouse thymocytes." EMBO Rep. **3**(2): 190-6.

Hughes, M. A., N. Harper, et al. (2009). "Reconstitution of the death-inducing signaling complex reveals a substrate switch that determines CD95-mediated death or survival." Mol. Cell **35**(3): 265-79.

Hymowitz, S. G., H. W. Christinger, et al. (1999). "Triggering cell death: the crystal structure of Apo2L/TRAIL in a complex with death receptor 5." Mol. Cell **4**(4): 563-71.

Imai, Y., T. Kimura, et al. (1999). "The CED-4-homologous protein FLASH is involved in Fas-mediated activation of caspase-8 during apoptosis." Nature **398**(6730): 777-85.

Inohara, N., T. Koseki, et al. (1997). "CLARP, a death effector domain-containing protein interacts with caspase-8 and regulates apoptosis." Proc. Natl. Acad. Sci. USA **94**(20): 10717-22.

Irmler, M., M. Thome, et al. (1997). "Inhibition of death receptor signals by cellular FLIP." Nature **388**(6638): 190-5.

Itoh, N. and S. Nagata (1993). "A novel protein domain required for apoptosis. Mutational analysis of human Fas antigen." J. Biol. Chem. **268**(15): 10932-7.

Jackson, C. E. and J. M. Puck (1999). "Autoimmune lymphoproliferative syndrome, a disorder of apoptosis." Curr. Opin. Pediatr. **11**(6): 521-7.

Jin, Z., Y. Li, et al. (2009). "Cullin3-based polyubiquitination and p62-dependent aggregation of caspase-8 mediate extrinsic apoptosis signaling." Cell **137**(4): 721-35.

Jones, E. Y., D. I. Stuart, et al. (1989). "Structure of tumour necrosis factor." Nature **338**(6212): 225-8.

Jost, P. J., S. Grabow, et al. (2009). "XIAP discriminates between type I and type II FAS-induced apoptosis." Nature **460**(7258): 1035-9.

Julenius, K. (2007). "NetCGlyc 1.0: prediction of mammalian C-mannosylation sites." Glycobiology **17**(8): 868-76.

Julenius, K., A. Molgaard, et al. (2005). "Prediction, conservation analysis, and structural characterization of mammalian mucin-type O-glycosylation sites." Glycobiology **15**(2): 153-164.

Kabra, N. H., C. Kang, et al. (2001). "T cell-specific FADD-deficient mice: FADD is required for early T cell development." Proc. Natl. Acad. Sci. USA **98**(11): 6307-12.

Kamitani, T., H. P. Nguyen, et al. (1997). "Activation-induced aggregation and processing of the human Fas antigen. Detection with cytoplasmic domain-specific antibodies." J. Biol. Chem. **272**(35): 22307-14.

Kang, T. B., T. Ben-Moshe, et al. (2004). "Caspase-8 serves both apoptotic and nonapoptotic roles." J. Immunol. **173**(5): 2976-84.

Kataoka, T., R. C. Budd, et al. (2000). "The caspase-8 inhibitor FLIP promotes activation of NF-kappaB and Erk signaling pathways." Curr. Biol. **10**(11): 640-8.

Keppler, O. T., M. E. Peter, et al. (1999). "Differential sialylation of cell surface glycoconjugates in a human B lymphoma cell line regulates susceptibility for CD95 (APO-1/Fas)-mediated apoptosis and for infection by a lymphotropic virus." Glycobiology **9**(6): 557-569.

Kerr, J. F., A. H. Wyllie, et al. (1972). "Apoptosis: a basic biological phenomenon with wide-ranging implications in tissue kinetics." Br J Cancer **26**(4): 239-57.

Kim, R., M. Emi, et al. (2006). "The role of apoptosis in cancer cell survival and therapeutic outcome." Cancer Biol Ther **5**(11): 1429-42.

Kischkel, F. C., S. Hellbardt, et al. (1995). "Cytotoxicity-dependent APO-1 (Fas/CD95)-associated proteins form a death-inducing signaling complex (DISC) with the receptor." EMBO J. **14**(22): 5579-5588.

Kischkel, F. C., P. Kioschis, et al. (1998). "Assignment of CASP8 to human chromosome band 2q33-->q34 and Casp8 to the murine syntenic region on chromosome 1B-proximal C by in situ hybridization." Cytogenet. Cell. Genet. **82**(1-2): 95-6.

Kitson, J., T. Raven, et al. (1996). "A death-domain-containing receptor that mediates apoptosis." Nature **384**(6607): 372-5.

Kontny, U. and H. Kovar (2005). Regulation of Death Receptors. Death Receptors in Cancer Therapy. W. S. El-Deiry. Totowa, New Jersey, Humana Press**:** 163-175.

Korsmeyer, S. J., M. C. Wei, et al. (2000). "Pro-apoptotic cascade activates BID, which oligomerizes BAK or BAX into pores that result in the release of cytochrome c." Cell Death Differ **7**(12): 1166-73.

Krammer, P. H. (2000). "CD95's deadly mission in the immune system." Nature **407**(6805): 789-95.

Krammer, P. H., R. Arnold, et al. (2007). "Life and death in peripheral T cells." Nat. Rev. Immunol. **7**(7): 532-542.

Kroemer, G., L. Galluzzi, et al. (2009). "Classification of cell death: recommendations of the Nomenclature Committee on Cell Death 2009." Cell Death Differ. **16**(1): 3-11.

Krueger, A., S. Baumann, et al. (2001). "FLICE-inhibitory proteins: regulators of death receptor-mediated apoptosis." Mol Cell Biol **21**(24): 8247-54.

Krueger, A., I. Schmitz, et al. (2001). "Cellular FLICE-inhibitory protein splice variants inhibit different steps of caspase-8 activation at the CD95 death-inducing signaling complex." J. Biol. Chem. **276**(23): 20633-40.

Kuang, A. A., G. E. Diehl, et al. (2000). "FADD is required for DR4- and DR5-mediated apoptosis: lack of trail-induced apoptosis in FADD-deficient mouse embryonic fibroblasts." J. Biol. Chem. **275**(33): 25065-8.

Kundu, M. and C. B. Thompson (2008). "Autophagy: basic principles and relevance to disease." Annu Rev Pathol **3**: 427-55.

Lacronique, V., A. Mignon, et al. (1996). "Bcl-2 protects from lethal hepatic apoptosis induced by an anti-Fas antibody in mice." Nat Med **2**(1): 80-6.

Lautrette, C., E. Loum-Ribot, et al. (2006). "Increase of Fas-induced apoptosis by inhibition of extracellular phosphorylation of Fas receptor in Jurkat cell line." Apoptosis **11**(7): 1195-204.

Lavrik, I., A. Golks, et al. (2005). "Death receptor signaling." J. Cell. Sci. **118**(Pt 2): 265-7.

Lavrik, I., A. Krueger, et al. (2003). "The active caspase-8 heterotetramer is formed at the CD95 DISC." Cell Death Differ. **10**(1): 144-145.

Lavrik, I. N., A. Golks, et al. (2005). "Caspases: pharmacological manipulation of cell death." J. Clin. Invest. **115**(10): 2665-2672.

Lavrik, I. N., A. Golks, et al. (2007). "Analysis of CD95 threshold signaling: triggering of CD95 (FAS/APO-1) at low concentrations primarily results in survival signaling." J. Biol. Chem **282**(18): 13664-13671.

Legembre, P., S. Daburon, et al. (2006). "Modulation of Fas-mediated apoptosis by lipid rafts in T lymphocytes." J. Immunol. **176**(2): 716-20.

Legler, D. F., O. Micheau, et al. (2003). "Recruitment of TNF receptor 1 to lipid rafts is essential for TNFalpha-mediated NF-kappaB activation." Immunity **18**(5): 655-64.

Leithauser, F., J. Dhein, et al. (1993). "Constitutive and induced expression of APO-1, a new member of the nerve growth factor/tumor necrosis factor receptor superfamily, in normal and neoplastic cells." Lab. Invest. **69**(4): 415-29.

Letai, A. (2005). "Pharmacological manipulation of Bcl-2 family members to control cell death." J Clin Invest **115**(10): 2648-55.

Li, H., M. Kobayashi, et al. (2006). "Ubiquitination of RIP is required for tumor necrosis factor alpha-induced NF-kappaB activation." J. Biol. Chem. **281**(19): 13636-43.

Li, H., H. Zhu, et al. (1998). "Cleavage of BID by caspase 8 mediates the mitochondrial damage in the Fas pathway of apoptosis." Cell **94**(4): 491-501.

Li, Y., X. Yang, et al. (2007). "Requirement of N-glycosylation for the secretion of recombinant extracellular domain of human Fas in HeLa cells." Int. J. Biochem. Cell. Biol. **39**(9): 1625-1636.

Lowe, J. B. and J. D. Marth (2003). "A genetic approach to Mammalian glycan function." Annu. Rev. Biochem. **72**: 643-91.

Luo, X., I. Budihardjo, et al. (1998). "Bid, a Bcl2 interacting protein, mediates cytochrome c release from mitochondria in response to activation of cell surface death receptors." Cell **94**(4): 481-90.

Marsters, S. A., J. P. Sheridan, et al. (1996). "Apo-3, a new member of the tumor necrosis factor receptor family, contains a death domain and activates apoptosis and NF-kappa B." Curr. Biol. **6**(12): 1669-76.

Marsters, S. A., J. P. Sheridan, et al. (1998). "Identification of a ligand for the death-domain-containing receptor Apo3." Curr. Biol. **8**(9): 525-8.

Martin, D. A., L. Zheng, et al. (1999). "Defective CD95/APO-1/Fas signal complex formation in the human autoimmune lymphoproliferative syndrome, type Ia." Proc. Natl. Acad. Sci. USA **96**(8): 4552-7.

Medema, J. P., C. Scaffidi, et al. (1997). "FLICE is activated by association with the CD95 death-inducing signaling complex (DISC)." EMBO J. **16**(10): 2794-804.

Merino, D., N. Lalaoui, et al. (2006). "Differential inhibition of TRAIL-mediated DR5-DISC formation by decoy receptors 1 and 2." Mol. Cell. Biol. **26**(19): 7046-55.

Micheau, O., M. Thome, et al. (2002). "The long form of FLIP is an activator of caspase-8 at the Fas death-inducing signaling complex." J Biol Chem **277**(47): 45162-71.

Micheau, O. and J. Tschopp (2003). "Induction of TNF receptor I-mediated apoptosis via two sequential signaling complexes." Cell **114**(2): 181-90.

Mohr, A., R. M. Zwacka, et al. (2005). "Caspase-8L expression protects CD34+ hematopoietic progenitor cells and leukemic cells from CD95-mediated apoptosis." Oncogene **24**(14): 2421-9.

Mongkolsapaya, J., J. M. Grimes, et al. (1999). "Structure of the TRAIL-DR5 complex reveals mechanisms conferring specificity in apoptotic initiation." Nat. Struct. Biol. **6**(11): 1048-53.

Muppidi, J. R. and R. M. Siegel (2004). "Ligand-independent redistribution of Fas (CD95) into lipid rafts mediates clonotypic T cell death." Nat. Immunol. **5**(2): 182-9.

Muzio, M., A. M. Chinnaiyan, et al. (1996). "FLICE, a novel FADD-homologous ICE/CED-3-like protease, is recruited to the CD95 (Fas/APO-1) death--inducing signaling complex." Cell **85**(6): 817-827.

Muzio, M., B. R. Stockwell, et al. (1998). "An induced proximity model for caspase-8 activation." J. Biol. Chem. **273**(5): 2926-30.

Nagata, S. (1999). "Fas ligand-induced apoptosis." Annu. Rev. Genet. **33**: 29-55.

Naismith, J. H., T. Q. Devine, et al. (1996). "Structures of the extracellular domain of the type I tumor necrosis factor receptor." Structure **4**(11): 1251-62.

Nikolaev, A., T. McLaughlin, et al. (2009). "APP binds DR6 to trigger axon pruning and neuron death via distinct caspases." Nature **457**(7232): 981-9.

Oehm, A., I. Behrmann, et al. (1992). "Purification and molecular cloning of the APO-1 cell surface antigen, a member of the tumor necrosis factor/nerve growth factor receptor superfamily. Sequence identity with the Fas antigen." J. Biol. Chem. **267**(15): 10709-10715.

Okura, T., L. Gong, et al. (1996). "Protection against Fas/APO-1- and tumor necrosis factor-mediated cell death by a novel protein, sentrin." J. Immunol. **157**(10): 4277-81.

Pan, G., J. Ni, et al. (1997). "An antagonist decoy receptor and a death domain-containing receptor for TRAIL." Science **277**(5327): 815-8.

Pan, G., K. O'Rourke, et al. (1997). "The receptor for the cytotoxic ligand TRAIL." Science **276**(5309): 111-3.

Papoff, G., P. Hausler, et al. (1999). "Identification and characterization of a ligand-independent oligomerization domain in the extracellular region of the CD95 death receptor." J. Biol. Chem. **274**(53): 38241-50.

Parlato, S., A. M. Giammarioli, et al. (2000). "CD95 (APO-1/Fas) linkage to the actin cytoskeleton through ezrin in human T lymphocytes: a novel regulatory mechanism of the CD95 apoptotic pathway." EMBO J. **19**(19): 5123-34.

Parodi, A. J. (2000). "Protein glucosylation and its role in protein folding." Annu Rev Biochem **69**: 69-93.

Parodi, A. J. (2000). "Role of N-oligosaccharide endoplasmic reticulum processing reactions in glycoprotein folding and degradation." Biochem. J. **348 Pt 1**: 1-13.

Parodi, A. J. (2002). "Protein sweetener." Nature **415**(6870): 382-3.

Peter, M. E., S. Hellbardt, et al. (1995). "Cell surface sialylation plays a role in modulating sensitivity towards APO-1-mediated apoptotic cell death." Cell Death Differ. **2**(3): 163-171.

Peter, M. E. and P. H. Krammer (1998). "Mechanisms of CD95 (APO-1/Fas)-mediated apoptosis." Curr Opin Immunol **10**(5): 545-51.

Peter, M. E. and P. H. Krammer (2003). "The CD95(APO-1/Fas) DISC and beyond." Cell Death Differ. **10**(1): 26-35.

Peter, M. E., C. Scaffidi, et al. (1999). "The death receptors." Results Probl Cell Differ **23**: 25-63.

Pfeffer, K., T. Matsuyama, et al. (1993). "Mice deficient for the 55 kd tumor necrosis factor receptor are resistant to endotoxic shock, yet succumb to L. monocytogenes infection." Cell **73**(3): 457-67.

Reed, J. C., K. Doctor, et al. (2003). "Comparative analysis of apoptosis and inflammation genes of mice and humans." Genome Res. **13**(6B): 1376-88.

Ren, J., L. Wen, et al. (2008). "CSS-Palm 2.0: an updated software for palmitoylation sites prediction." Protein Eng. Des. Sel. **21**(11): 639-44.

Rieux-Laucat, F., F. Le Deist, et al. (1995). "Mutations in Fas associated with human lymphoproliferative syndrome and autoimmunity." Science **268**(5215): 1347-9.

Rodriguez, J. and Y. Lazebnik (1999). "Caspase-9 and APAF-1 form an active holoenzyme." Genes Dev **13**(24): 3179-84.

Salvesen, G. S. (2002). "Caspases and apoptosis." Essays Biochem **38**: 9-19.

Sato, T., S. Irie, et al. (1995). "FAP-1: a protein tyrosine phosphatase that associates with Fas." Science **268**(5209): 411-5.

Scaffidi, C., S. Fulda, et al. (1998). "Two CD95 (APO-1/Fas) signaling pathways." EMBO J. **17**(6): 1675-1687.

Scaffidi, C., J. P. Medema, et al. (1997). "FLICE is predominantly expressed as two functionally active isoforms, caspase-8/a and caspase-8/b." J. Biol. Chem. **272**(43): 26953-26958.

Scaffidi, C., I. Schmitz, et al. (1999). "The role of c-FLIP in modulation of CD95-induced apoptosis." J. Biol. Chem. **274**(3): 1541-1548.

Scaffidi, C., J. Volkland, et al. (2000). "Phosphorylation of FADD/ MORT1 at serine 194 and association with a 70-kDa cell cycle-regulated protein kinase." J. Immunol. **164**(3): 1236-1242.

Schabacker, D. S., I. Stefanovska, et al. (2006). "Protein array staining methods for undefined protein content, manufacturing quality control, and performance validation." Anal. Biochem. **359**(1): 84-93.

Schmidt, C. S., J. Liu, et al. (2003). "Enhanced B cell expansion, survival, and humoral responses by targeting death receptor 6." J. Exp. Med. **197**(1): 51-62.

Schmitz, I., A. Krueger, et al. (2002). "Specificity of anti-human CD95 (APO-1/Fas) antibodies." Biochem. Biophys. Res. Commun. **297**(3): 459-462.

Schmitz, I., H. Walczak, et al. (1999). "Differences between CD95 type I and II cells detected with the CD95 ligand." Cell Death Differ. **6**(9): 821-822.

Schneider-Brachert, W., V. Tchikov, et al. (2006). "Inhibition of TNF receptor 1 internalization by adenovirus 14.7K as a novel immune escape mechanism." J. Clin. Invest. **116**(11): 2901-13.

Schneider-Brachert, W., V. Tchikov, et al. (2004). "Compartmentalization of TNF receptor 1 signaling: internalized TNF receptosomes as death signaling vesicles." Immunity **21**(3): 415-28.

Scott, F. L., B. Stec, et al. (2009). "The Fas-FADD death domain complex structure unravels signalling by receptor clustering." Nature **457**(7232): 1019-1022.

Screaton, G. R., X. N. Xu, et al. (1997). "LARD: a new lymphoid-specific death domain containing receptor regulated by alternative pre-mRNA splicing." Proc. Natl. Acad. Sci. USA **94**(9): 4615-9.

Secchiero, P., A. Gonelli, et al. (2004). "Evidence for a proangiogenic activity of TNF-related apoptosis-inducing ligand." Neoplasia **6**(4): 364-73.

Senft, J., B. Helfer, et al. (2007). "Caspase-8 interacts with the p85 subunit of phosphatidylinositol 3-kinase to regulate cell adhesion and motility." Cancer Res. **67**(24): 11505-9.

Shapiro, L. and P. E. Scherer (1998). "The crystal structure of a complement-1q family protein suggests an evolutionary link to tumor necrosis factor." Curr. Biol. **8**(6): 335-8.

Shiozaki, E. N. and Y. Shi (2004). "Caspases, IAPs and Smac/DIABLO: mechanisms from structural biology." Trends Biochem. Sci. **29**(9): 486-94.

Siegel, R. M., F. K. Chan, et al. (2000). "The multifaceted role of Fas signaling in immune cell homeostasis and autoimmunity." Nat. Immunol. **1**(6): 469-74.

Siegel, R. M., J. K. Frederiksen, et al. (2000). "Fas preassociation required for apoptosis signaling and dominant inhibition by pathogenic mutations." Science **288**(5475): 2354-7.

Siegelin, M. D., L. S. Kossatz, et al. (2005). "Regulation of XIAP and Smac/DIABLO in the rat hippocampus following transient forebrain ischemia." Neurochem. Int. **46**(1): 41-51.

Sprick, M. R., E. Rieser, et al. (2002). "Caspase-10 is recruited to and activated at the native TRAIL and CD95 death-inducing signalling complexes in a FADD-dependent manner but can not functionally substitute caspase-8." EMBO J. **21**(17): 4520-4530.

Sprick, M. R., M. A. Weigand, et al. (2000). "FADD/MORT1 and caspase-8 are recruited to TRAIL receptors 1 and 2 and are essential for apoptosis mediated by TRAIL receptor 2." Immunity **12**(6): 599-609.

Srinivasula, S. M., M. Ahmad, et al. (1998). "Autoactivation of procaspase-9 by Apaf-1-mediated oligomerization." Mol. Cell **1**(7): 949-57.

Stanger, B. Z., P. Leder, et al. (1995). "RIP: a novel protein containing a death domain that interacts with Fas/APO-1 (CD95) in yeast and causes cell death." Cell **81**(4): 513-23.

Strand, S., P. Vollmer, et al. (2004). "Cleavage of CD95 by matrix metalloproteinase-7 induces apoptosis resistance in tumour cells." Oncogene **23**(20): 3732-3736.

Strasser, A. (1995). "Life and death during lymphocyte development and function: evidence for two distinct killing mechanisms." Curr Opin Immunol **7**(2): 228-34.

Sukits, S. F., L. L. Lin, et al. (2001). "Solution structure of the tumor necrosis factor receptor-1 death domain." J. Mol. Biol. **310**(4): 895-906.

Syntichaki, P. and N. Tavernarakis (2003). "The biochemistry of neuronal necrosis: rogue biology?" Nat Rev Neurosci **4**(8): 672-84.

Tang, G., Y. Minemoto, et al. (2001). "Inhibition of JNK activation through NF-kappaB target genes." Nature **414**(6861): 313-7.

Thompson, C. B. (1995). "Apoptosis in the pathogenesis and treatment of disease." Science **267**(5203): 1456-62.

Tibbetts, M. D., L. Zheng, et al. (2003). "The death effector domain protein family: regulators of cellular homeostasis." Nat. Immunol. **4**(5): 404-9.

Trauth, B. C., C. Klas, et al. (1989). "Monoclonal antibody-mediated tumor regression by induction of apoptosis." Science **245**(4915): 301-305.

Varfolomeev, E. E., M. Schuchmann, et al. (1998). "Targeted disruption of the mouse Caspase 8 gene ablates cell death induction by the TNF receptors, Fas/Apo1, and DR3 and is lethal prenatally." Immunity **9**(2): 267-76.

Varki, A., R. Cummings, et al. (2009). Essentials of Glycobiology, Cold Spring Harbor Laboratory Press.

Vexler, Z. S., T. P. Roberts, et al. (1997). "Transient cerebral ischemia. Association of apoptosis induction with hypoperfusion." J Clin Invest **99**(6): 1453-9.

Vocadlo, D. J. and G. J. Davies (2008). "Mechanistic insights into glycosidase chemistry." Curr. Opin. Chem. Biol. **12**(5): 539-55.

Wagner, K. W., E. A. Punnoose, et al. (2007). "Death-receptor O-glycosylation controls tumor-cell sensitivity to the proapoptotic ligand Apo2L/TRAIL." Nat. Med. **13**(9): 1070-1077.

Wajant, H. (2003). "Death receptors." Essays Biochem. **39**: 53-71.

Wajant, H., F. Henkler, et al. (2001). "The TNF-receptor-associated factor family: scaffold molecules for cytokine receptors, kinases and their regulators." Cell Signal. **13**(6): 389-400.

Wajant, H., K. Pfizenmaier, et al. (2003). "Tumor necrosis factor signaling." Cell Death Differ. **10**(1): 45-65.

Walkinshaw, G. and C. M. Waters (1995). "Induction of apoptosis in catecholaminergic PC12 cells by L-DOPA. Implications for the treatment of Parkinson's disease." J. Clin. Invest. **95**(6): 2458-64.

Wallach, D., E. E. Varfolomeev, et al. (1999). "Tumor necrosis factor receptor and Fas signaling mechanisms." Annu. Rev. Immunol. **17**: 331-67.

Walsh, C. M., B. G. Wen, et al. (1998). "A role for FADD in T cell activation and development." Immunity **8**(4): 439-49.

Wang, H., P. Wang, et al. (2007). "Cloning and characterization of a novel caspase-10 isoform that activates NF-kappa B activity." Biochim. Biophys. Acta **1770**(11): 1528-37.

Wang, J., H. J. Chun, et al. (2001). "Caspase-10 is an initiator caspase in death receptor signaling." Proc. Natl. Acad. Sci. USA **98**(24): 13884-8.

Wright, D. A., B. Futcher, et al. (1996). "Association of human fas (CD95) with a ubiquitin-conjugating enzyme (UBC-FAP)." J. Biol. Chem. **271**(49): 31037-43.

Yarema, K. J. and C. R. Bertozzi (2001). "Characterizing glycosylation pathways." Genome Biol. **2**(5): REVIEWS0004.

Yeh, W. C., J. L. Pompa, et al. (1998). "FADD: essential for embryo development and signaling from some, but not all, inducers of apoptosis." Science **279**(5358): 1954-8.

Yu, J. W., P. D. Jeffrey, et al. (2009). "Mechanism of procaspase-8 activation by c-FLIPL." Proc. Natl. Acad. Sci. USA **106**(20): 8169-74.

Zhang, F., W. Yin, et al. (2004). "Apoptosis in cerebral ischemia: executional and regulatory signaling mechanisms." Neurol Res **26**(8): 835-45.

Zhang, J., N. H. Kabra, et al. (2001). "FADD-deficient T cells exhibit a disaccord in regulation of the cell cycle machinery." J Biol Chem **276**(32): 29815-8.

Zhao, Y. X., G. Lajoie, et al. (2000). "Tumor necrosis factor receptor p55-deficient mice respond to acute Yersinia enterocolitica infection with less apoptosis and more effective host resistance." Infect. Immun. **68**(3): 1243-51.

Zou, H., Y. Li, et al. (1999). "An APAF-1.cytochrome c multimeric complex is a functional apoptosome that activates procaspase-9." J. Biol. Chem. **274**(17): 11549-56.

6. LIST OF FIGURES AND TABLES

7. LIST OF PUBLICATIONS AND CONFERENCES

1. Goltsev A.N., Babenko N.N., Dubrava T.G., Ostankov M.V., Shatnyeva O.M. (2006). 'Modification of the state of bone marrow HSC after cryopreservation'. The International Journal of Refrigeration, 29:358-367

2. Matveeva G.S., Shatnyeva O.M., Zueva M.I. (2004) 'Genetic analysis of stomach ulcer'. The bulletin of problem of biology and medicine. 3:59-62.

3. Shatnyeva O. et al., The role of CD95/APO-1/Fas glycosylation in the sensitivity and resistance of cells towards death receptor-induced apoptosis Internationales Symposium „Signal Transduction and Disease '. Aachen, Germany, 2009.

4. Shatnyeva O. et al, The role of CD95 glycosylation in CD95 signaling, EMBO Workshop, Model Organisms in Cell Death Research, Obergurgl , Austria, 2009.

5. Shatnyeva O. et al, The role of CD95 glycosylation in CD95 signaling, 14th International Summer School on Immunology IMMUNE SYSTEM: GENES, RECEPTORS AND REGULATION, Hvar, Croatia, 2007

6. Shatnyeva O., P.H. Krammer and Lavrik I.N. XI. Graduate Seminar Weil der Stadt 2006. "Differential glycosylation might influence CD95signaling".

7. Shatnyeva O.M. Undergraduate and Postgraduate Student International Conference on Molecular Biology and Genetics, Kijw, 2003. "The contribution of genetic and environmental components in the development of ulcerative disease".

8. Shatnyeva O.M. Undergraduate and postgraduate Student Conference on Medicine, Kharkov, 2005. "C3H mice as a model to study mammary gland cancer" .

9. Shatneyva O.M. "Modulation of state of immune system in C3H mice". International conference "Young scientists and progress in Biology", Lviv 2005.

8. ACKNOWLEDGEMENTS

This was an exceptionally worthwhile and highly interesting period for me, and I would like to express words of gratitude to those who have helped me during my work.

I would like to thank Prof. Dr. Peter H. Krammer for his support during this time at the Division of Immunogenetics. I appreciate his vast knowledge in many fields and would like to thank him for his supervision and for giving me the opportunity to work under his supervision on such an interesting topic and for his precious remarks

. I also would like to thank Prof. Walter Nickel for supervising the thesis from the side of the Faculty of Biosciences of the Heidelberg University.

Advice and help of various kinds were willingly given by Dr. Inna Lavrik. I am deeply grateful for the guidance during the period of my doctoral studies. The knowledge, I have gained from her scientific expertise is of invaluable importance for my development as a scientist.

I would like to thank Dr. Reinhard Schwartz-Albiez, Dr. Dieter Kübler, Dr. Andriy Kubarenko and Dr. Alexander Weber for the fruitful discussion on protein modifications.

I am deeply grateful to Dr. Karsten Gulow, Dr. Michael Kiessling, Dr. Andrea Mahr, Carina Pforr, Nickolai Fricker, Dr. Alexander Weber and Dr. Andriy Kubarenko, who were critical readers of this thesis and gave me helpful advice.

I would like to thank Petra Richter and Tatjana Schmidt for their excellent technical assistance. I am also thankful to the whole lab for the good atmosphere. I had a great time in the lab with all kinds of discussions we had during work. I am grateful for the generous help of Claudia Calla with the confocal microscopy.

I want to mention the time outside the lab. I would also like to thank my friends in Heidelberg, most of them also PhD students coming from countries all over the world. You all really enriched my experience here in Germany.

I gratefully acknowledge the strong support of my family, my friend Anna Kovtun and my husband, Andriy Kubarenko, who has been my help and strength.

Once again, to everybody,

The most sincere

THANK YOU

Olga Shatnyeva